frontiers | Research Topics

Neuro-otology – case report collection 2022

Edited by
Michael Strupp

Published in
Frontiers in Neurology

ISSN 1664-8714
ISBN 978-2-8325-2996-6
DOI 10.3389/978-2-8325-2996-6

About Frontiers

Frontiers is more than just an open access publisher of scholarly articles: it is a pioneering approach to the world of academia, radically improving the way scholarly research is managed. The grand vision of Frontiers is a world where all people have an equal opportunity to seek, share and generate knowledge. Frontiers provides immediate and permanent online open access to all its publications, but this alone is not enough to realize our grand goals.

Frontiers journal series

The Frontiers journal series is a multi-tier and interdisciplinary set of open-access, online journals, promising a paradigm shift from the current review, selection and dissemination processes in academic publishing. All Frontiers journals are driven by researchers for researchers; therefore, they constitute a service to the scholarly community. At the same time, the *Frontiers journal series* operates on a revolutionary invention, the tiered publishing system, initially addressing specific communities of scholars, and gradually climbing up to broader public understanding, thus serving the interests of the lay society, too.

Dedication to quality

Each Frontiers article is a landmark of the highest quality, thanks to genuinely collaborative interactions between authors and review editors, who include some of the world's best academicians. Research must be certified by peers before entering a stream of knowledge that may eventually reach the public - and shape society; therefore, Frontiers only applies the most rigorous and unbiased reviews. Frontiers revolutionizes research publishing by freely delivering the most outstanding research, evaluated with no bias from both the academic and social point of view. By applying the most advanced information technologies, Frontiers is catapulting scholarly publishing into a new generation.

What are Frontiers Research Topics?

Frontiers Research Topics are very popular trademarks of the *Frontiers journals series*: they are collections of at least ten articles, all centered on a particular subject. With their unique mix of varied contributions from Original Research to Review Articles, Frontiers Research Topics unify the most influential researchers, the latest key findings and historical advances in a hot research area.

Find out more on how to host your own Frontiers Research Topic or contribute to one as an author by contacting the Frontiers editorial office: frontiersin.org/about/contact

Neuro-otology – case report collection 2022

Topic editor
Michael Strupp — Ludwig Maximilian University of Munich, Germany

Citation
Strupp, M., ed. (2023). *Neuro-otology – case report collection 2022*. Lausanne: Frontiers Media SA. doi: 10.3389/978-2-8325-2996-6

Table of contents

frontiers | Frontiers in Neurology

CASE REPORT
published: 07 April 2022
doi: 10.3389/fneur.2022.880312

Erdheim-Chester Disease Revealed by Central Positional Nystagmus: A Case Report

Alexandra Weckel[1], Yohann Gallois[1], Rachel Debs[2], Bernard Escude[3], Laurent Tremelet[4], Fanny Varenne[5], Damien Biotti[2,6], Dominique Chauveau[7] and Fabrice Bonneville[8]*

[1] ENT, Department of Neurotology and Pediatric ENT, Pierre Paul Riquet Hospital, University Hospital of Toulouse, Toulouse, France, [2] Department of Neurology, Pierre-Paul Riquet/Purpan University Hospital, Toulouse, France, [3] Service de Radiologie, Clinique Pasteur, Toulouse, France, [4] ENT, Clinique du Dr Honoré CAVE, Montauban, France, [5] Department of Ophthalmology, Pierre-Paul Riquet/Purpan University Hospital, Toulouse, France, [6] Institut Toulousain des Maladies Infectieuses et Inflammatoires (Infinity) INSERM UMR1291 - Université Toulouse III, Toulouse, France, [7] Department of Nephrology and Organ Transplantation and Referral Center for Rare Renal Diseases, CHU Rangueil, Toulouse, France, [8] Department of Neuroradiology, Pierre-Paul-Riquet/Purpan University Hospital, Toulouse, France

OPEN ACCESS

Edited by:
Michael Strupp, Ludwig Maximilian University of Munich, Germany

Reviewed by:
Jorge Kattah, University of Illinois at Chicago, United States
Jae-Hwan Choi, Pusan National University Yangsan Hospital, South Korea

***Correspondence:**
Alexandra Weckel
weckel.a@chu-toulouse.fr

Specialty section:
This article was submitted to Neuro-Otology, a section of the journal Frontiers in Neurology

Received: *21 February 2022*
Accepted: *17 March 2022*
Published: *07 April 2022*

Citation:
Weckel A, Gallois Y, Debs R, Escude B, Tremelet L, Varenne F, Biotti D, Chauveau D and Bonneville F (2022) Erdheim-Chester Disease Revealed by Central Positional Nystagmus: A Case Report. Front. Neurol. 13:880312. doi: 10.3389/fneur.2022.880312

Erdheim-Chester disease (ECD) is a rare histiocytic disorder, recently recognized to be neoplastic. The clinical phenotype of the disease is extremely heterogeneous, and depends on the affected organs, with the most frequently reported manifestations being bone pain, diabetes insipidus and neurological disorders including ataxia. In this article, we report on a case of a 48-year-old woman, whose initial symptom of gait instability was isolated. This was associated with positional nystagmus with central features: nystagmus occurring without latency, clinically present with only mild symptoms, and resistant to repositioning maneuvers. The cerebral MRI showed bilateral intra-orbital retro-ocular mass lesions surrounding the optic nerves and T2 hyperintensities in the pons and middle cerebellar peduncles. A subsequent CT scan of the chest abdomen and pelvis found a left "hairy kidney", while ^{18} F-FDG PET-CT imaging disclosed symmetric 18F-FDG avidity predominant at the diametaphyseal half of both femurs. Percutaneous US-guided biopsy of perinephric infiltrates and the kidney showed infiltration by CD68(+), CD1a(-), Langerin(-), PS100(-) foamy histiocytes with *BRAF*^{V600E} mutation. The combination of the different radiological abnormalities and the result of the biopsy confirmed the diagnosis of ECD. Many clinical and radiological descriptions are available in the literature, but few authors describe vestibulo-ocular abnormalities in patients with ECD. Here, we report on a case of ECD and provide a precise description of the instability related to central positional nystagmus, which led to the diagnosis of ECD.

Keywords: Erdheim-Chester disease, dizziness, gait, nystagmus, central positional nystagmus, case report

INTRODUCTION

Although Erdheim-Chester disease (ECD) is a rare non-Langerhans cell histiocytic disease, over the past decade more than 1,000 cases have been reported in the literature (1). The first reports on two patients date back to 1931 (William Chester and Jakob Erdheim), but it was not until 1972 that it was named by Jaffe after he had reported a similar case (1).

Until recently, it was considered an inflammatory, non-neoplastic disease of unknown origin. However, based on recent studies, it is now acknowledged that it is a clonal myeloid disorder due to mutations that activate MAPK (mitogen-activated protein kinase *RAS-RAF-MEK-ERK*) pathways (1). In most cases there are mutually exclusive activating ERK mutations, including $BRAF^{V600E}$ and MAP2K1 mutations (2).

The diagnosis of ECD is based on a combination of histopathological, clinical and radiological features. Classic solid lesions show an infiltration of typically foamy or spumous lipid-laden histiocytes with admixed or surrounding fibrosis (2). In ECD, tissues are infiltrated by foamy CD68(+), CD163(+), Factor XIIIa(+), CD1a(−), and Langerin(−) fibrotic histiocytes.

These histological impairments clinically result in systemic damage affecting the urinary tract, bone structures and central nervous system. In the latter case, dizziness is frequently reported by patients and examinations of the cerebellum are well described. However, the literature shows that adequate vestibular examination is frequently overlooked, the diagnosis of ECD being often based on extra-vestibular signs.

We are the first to describe the clinical presentation of a patient, whose only initial symptom was dizziness and isolated instability with clinical positional nystagmus.

CASE PRESENTATION

A 48-year-old woman presented with gait instability. Her only medical history was total thyroidectomy for hyperthyroidism due to a nodular goiter in 2002.

Starting in September 2020, she began to experience dizziness, which was never really rotatory. She described unsteadiness and visual blurring during horizontal or vertical movements, with an impression that this symptom worsened over time. Given the persistence of this complaint, she consulted a doctor in December 2020. An ENT specialist identified signs of a possible lateral canal BPPV and after the 1st maneuver referred the patient to physical therapists for repositioning maneuvers. Despite 10 repositioning maneuvers, her symptoms persisted.

She was therefore admitted for consultation in our ENT department in June 2021, for diagnostic and therapeutic advices. On clinical examination a discrete static cerebellar syndrome (isolated wide base) was detected. There was no distal hypopallesthesia, deep tendon reflexes were globally present and symmetrical, with signs of pyramidal involvement (bilateral Rossolimo's sign more marked on the left side, without Babinski sign). Abdominal reflexes were normally present on the right and absent on the left. The patient also had no vesico-sphincteral disorders. There was no dysarthria, no dysmetria or dysdiadochokinesia and no extrapyramidal syndrome. She reported mild dysarthria and transient aphasia that were undetectable.

There was no ocular instability, and no spontaneous nystagmus in the light or in the dark. There was no saccadic intrusion, normal smooth pursuit and no ocular misalignment. Head shaking caused intense instability, concomitant with nystagmus with a down beat component, which was low and transient (5 s). During the supine roll test, we noted very discrete geotropic horizontal nystagmus on the left side, without any concomitant vertigo, occurring without latency, and of 30 s' duration. During the right supine roll test, we noted geotropic nystagmus, occurring without latency, and of short duration (5 s), without any concomitant vertigo. The Dix-Hallpike test was negative. Bedside or video head impulse test was not performed. With this atypical positional nystagmus (PN), a central nervous system cause was suspected. Actually, the fact that vertical downbeat nystagmus was caused by head shaking and the roll maneuver immediately triggered pure horizontal nystagmus (without a torsional component), without latency or vertigo but only dizziness, which was persistent despite 10 repositioning maneuvers, were not in favor of PN of peripheral origin.

Subsequently, the patient had a brain MRI (**Figure 1**) which showed mild T2 hyperintensities in the pons and bilateral middle cerebellar peduncles. Incidentally, it also revealed bilateral intra-orbital retro-ocular mass lesions surrounding the optic nerves. The lesions were hypointense on T2-weighted images and were avidly enhanced after gadolinium injection.

The patient also reported that she had been experiencing blurring in the left eye for a few months, after she was informed of the presence of an intra-orbital mass. A complete ophthalmologic examination was performed and was normal (Fundus, Visual Field, Visual Acuity and RNFL-OCT [Optical coherence tomography]).

The presence of these lesions led us to consider the possibility of ECD. Therefore, we performed further tests, including whole body FDG-PET/CT, blood tests and cardiac MRI, as recommended (3). She was referred to the neurology and nephrology departments.

The whole body ^{18}F-DFG PET/CT found multifocal radiotracer uptake in the long bone marrow, predominantly on the distal half of the femurs (**Figure 2**) associated with moderate radiotracer uptake of left perinephric tissue. The CT scan showed dense infiltration in upper left quadrant of the kidney ("hairy kidney") (**Figure 3**). These findings confirmed the suspicion of ECD.

The cardiac MRI was free of abnormalities. Biological findings included normal renal function (S creatinine, 58 μmol/l), no diabetes insipidus, and normal CRP (C reactive protein), but thrombocytosis.

A left ultrasound-guided percutaneous renal biopsy of the upper and peri-renal tissue was performed. A pathological examination showed perirenal fat and kidney capsule infiltration by spumous macrophages and CD68(+), CD1a(-), Langerin(-), PS100(-) foamy histiocytes bearing the $BRAF^{V600E}$ mutation (**Figure 4**).

Based on established diagnostic recommendations (3), ECD was confirmed based on:

Abbreviations: BPPV, benign paroxysmal positional vertigo; CT, computed tomography; CPN, central positional nystagmus; MRI, magnetic resonance imaging; ECD, Erdheim Chester disease; ICP, inferior cerebellar peduncle; MAPK, mitogen-activated protein kinase; OCT, optical coherence tomography; PN, positional nystagmus; PET, positron emission tomography.

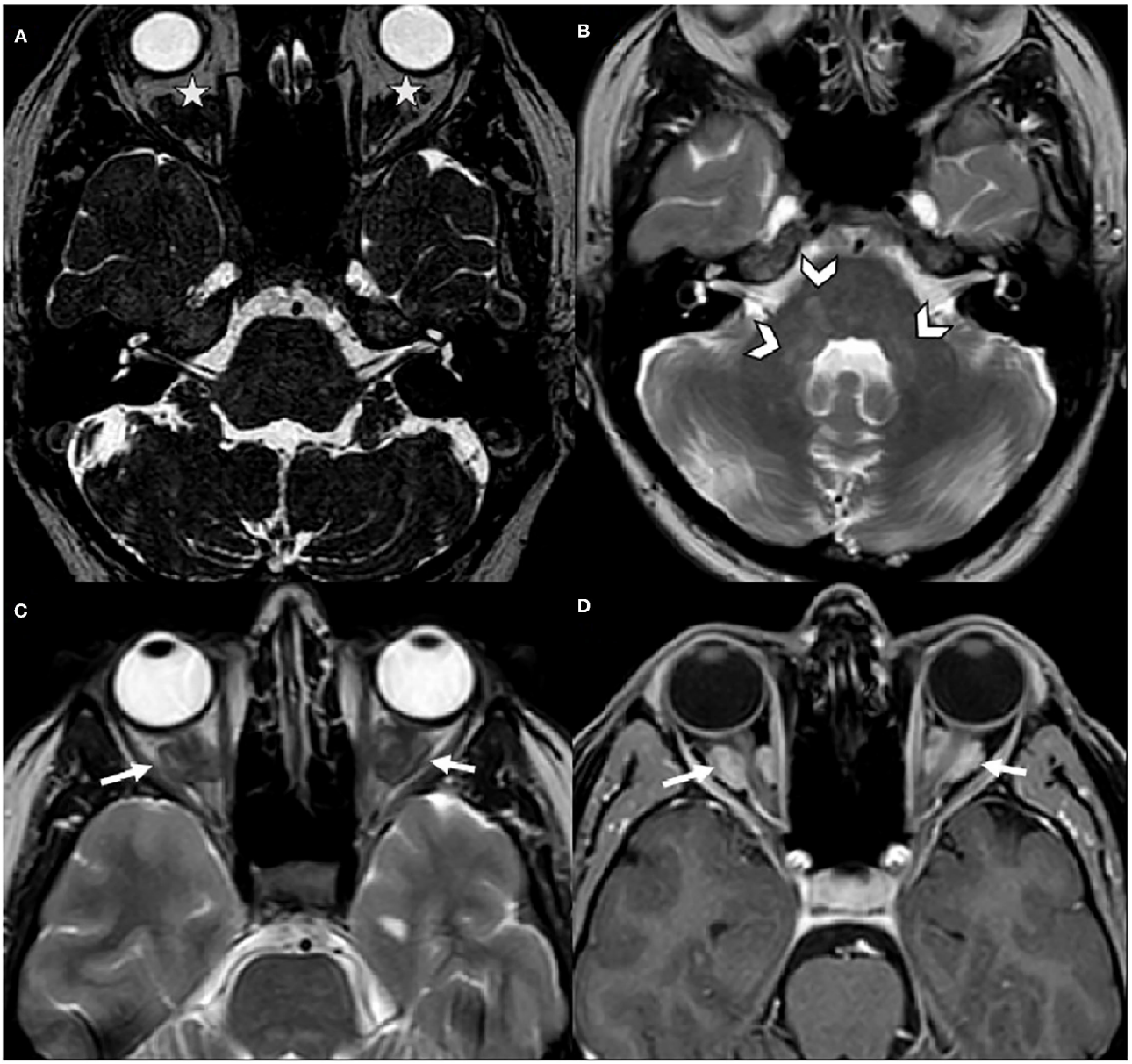

FIGURE 1 | Brain MRI. **(A)** Axial CISS was normal for internal auditory canals and cerebellopontine angles, but incidentally depicted bilateral intra-orbital mass lesions (stars). **(B,C)** Axial spin echo T2-weighted images revealed hyperintensities in the pons and the middle cerebellar peduncles (arrowheads) and demonstrated bilateral hypointense retro-ocular mass lesions (arrows). **(D)** Axial post-gadolinium T1-weighted image, these lesions surrounded the optic nerves sheaths and were avidly enhanced (arrows).

- progressive neurological disorders via the brainstem, with disorders of balance, and brain MRI images
- Bone ^{18}F DFG-avidity on PET/CT
- Unilateral left hairy kidney and perirenal infiltration with CD68(+), CD1a(-) foamy histiocytes bearing the *BRAF*^{V600E} mutation.

Our patient was treated as soon as the diagnostic was confirmed (end of September 2021) with vemurafenid (480 mg x 2 per day). In fact, the recommendations for first-line therapy is BRAF-inhibitor therapy with vemurafenib or dabrafenib (3). She developed numerous side effects, including severe loosening of the skin, diarrhea, red eyes, and weight loss. The treatment was first reduced (240 mg x 2 per day), then stopped after 2 months because of the persistence of these side effects. Treatment with dabrafenib was therefore initiated (75 mg x 2 per day). As of initiation, she presented iatrogenic bilateral anterior and intermediate uveitis predominantly on the right with contiguous papillitis on the right, which led to treatment cessation and

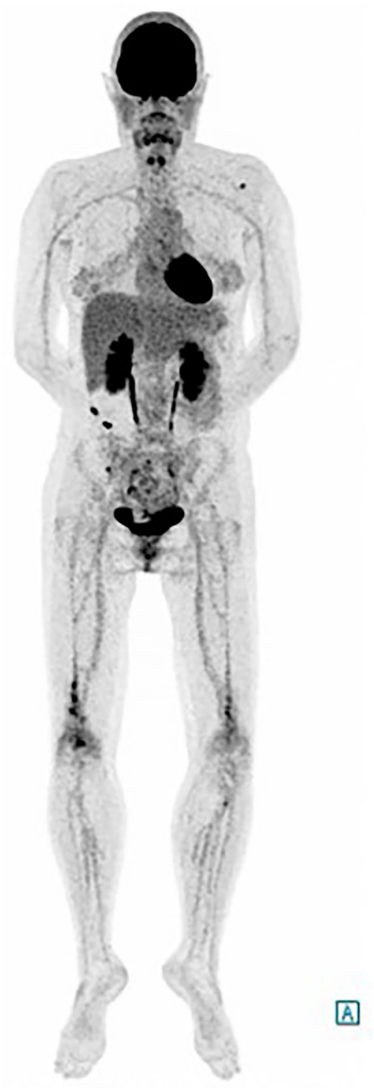

FIGURE 2 | FDG-PET/CT, showing multifocal radiotracer uptake in the long bone marrow predominantly on the distal half of the femurs.

reintroduction 10 days later, associated with trametinib (0.5mg x 2 per day). Besides uveitis, the ophthalmological examination remained normal.

Except for side effects, clinically the patient is perfectly stable. The patient continues to complain of isolated instability, with no other manifestations (except for those related to the reported secondary effects of the treatment). Wide base persist, and controlled MRI in February 2022 showed the same lesion as initial.

DISCUSSION

ECD

To our knowledge, this case of ECD is the first to present solely with gait disorder symptoms, with central positional nystagmus (CPN) that led to the discovery of a static cerebellar syndrome (isolated wide base).

ECD is a rare disease that usually appears in people aged 40 to 70 years, with a slight male predominance (1). The symptoms depend on the specific organ or system involved.

Symmetric osteosclerosis of femur, tibia, and fibula metadiaphysis is almost always discovered on radiographs in ECD (>95% of cases). This anomaly is best depicted by the absorption of a radiotracer in ^{99m}Tc bone scintigraphy or ^{18}F DFG-PET/CT scan (2). Bone pain is the most common presenting symptom of ECD, and occurs in 50% of the cases. It is mainly localized in the lower limbs (1). Our patient had no complaint of pain, but the PET identified multifocal bone radiotracer uptake, predominantly at the distal half of the femur.

ECD mass formations have been reported in various tissues, such as the retroperitoneum, neck, orbit and breast (4). Intra-orbital infiltration causing exophthalmos is observed in 25% of cases. For our patient (no clinical exophthalmos), there was an infiltrate around the two optic nerves, and the patient reported visual problems only after being informed of the presence of intra-orbital masses. The ophthalmological assessment found no impact on the optic nerves, nor any abnormalities in the visual field or OCT. Radiologists and ophthalmologists should be aware of this type of abnormality, because although this presentation is rare, it should be considered in the diagnosis of ECD (5, 6).

Dense infiltration of perinephric adipose tissue, described as "hairy kidney" is also common (68% of cases) (2), and was unilateral in our patient.

Neurological signs are reported at the time of diagnosis in 25% of cases and in 50% during progression. Pituitary impairment which causes diabetes insipidus (DI) is also common (22 to 47% of cases), as well as cerebellar or pyramidal impairment, found in 25% of cases. Neuropsychiatric symptoms are reported in up to 21% of cases, and cardiovascular manifestations in 22–36% of cases. Retroperitoneal fibroinflammatory lesions affects 30% of cases, ureteral obstruction being the most frequent complication. In addition, 10% of the patients have myeloid disease, in particular myelomonocytic leukemia (1).

Ataxia is found in 23% of patients and is associated with lesions involving retrobulbar fat or optic chiasma, and the cerebellum or the dentate area. Ataxic patients frequently have dysmetria, nystagmus, Babinski sign, and/or tendon hyperreflexia on physical examination (1). In a large series with 53 patients, Parks et al. described neurological symptoms found in 47% of the cases (25/53), with imbalance (n = 17), headache (n = 11), cognitive changes (n = 6), dysarthria (n = 6), diplopia (n = 5), dysphagia (n = 4), focal sensory deficit (n = 4) and focal motor deficit (n = 2) (7). Therefore, balance disorders are frequently found in patients with ECD. However, they are poorly described, including when there is a possibility of nystagmus, which is hardly described in the literature. The study by Batjia et al. on 30 patients, reported 63% of ataxia, but without details on physical examination and no description of possible nystagmus (8). Lauricella et al., described a case with gaze nystagmus, associated with other neurological signs, including hypermetria and dysarthria (9). Na

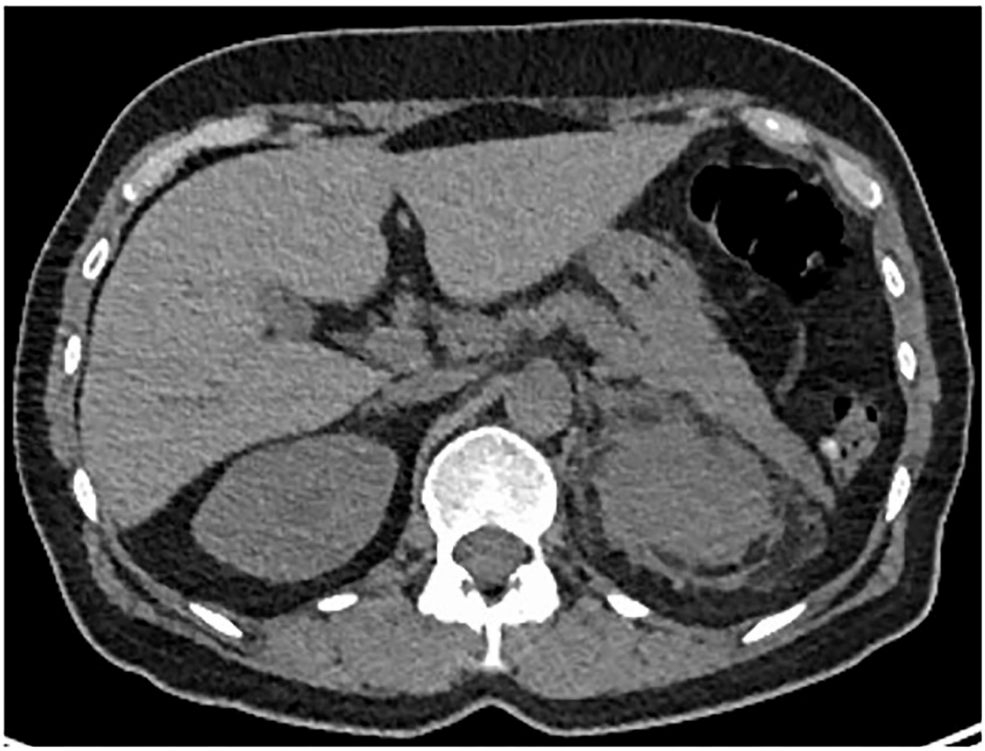

FIGURE 3 | Axial CT-Scan showing dense infiltration of left perinephric adipose tissue ("hairy kidney").

et al., reported the case of a patient with dysarthria, dysmetria and gaze nystagmus, associated with joint pain and painful axillary masses (4). Our patient presented with only CPN that was isolated and wide based. CPN has been associated with lesions involving the cerebellar vermis, nodulus and/or uvula, the dorsolateral region of the 4th ventricle, the tonsils, nucleus prepositus hypoglossi, and inferior, middle and superior cerebellar peduncles (10). The central positional nystagmus, either apogeotropic or geotropic, has been well described in inferior cerebellar peduncle (ICP) lesions damaging the fibers running from the nodulus/uvula onto the vestibular nucleus via ICP. Perverted head shaking nystagmus in this case also support an impairment of this connection or of the nodulus/uvula itself (11). ICP lesions are known to cause a distinct vestibular syndrome (12). However, on MRI, our patient had no visible lesion in the ICP. MRI showing T2 hyperintensities in the pons and middle cerebellar peduncles (MCPs), with no extension to the caudal dorsolateral portion of the 4th ventricle, which is the localization of the ICP. Our patient had lesions involving the middle cerebellar peduncles which could explain part of these presentation.

The Central Positional Nystagmus

Due to the non-specific clinical presentation, ECD is often difficult to diagnose, and a few cases involve isolated balance disorder as a mode of discovery. Our patient had very few clinical signs, but the presence of CPN led to encephalic imaging, and thus enabled the discovery of typical intra-orbital masses, associated with T2 hyperintensities of the pons and middle cerebellar peduncles, which led to a suspicion of ECD.

PN is defined as nystagmus caused by a change in position, with respect to gravity (13). It is then classified according to various characteristics and the site of the lesion as central or peripheral PN. There are multiple characteristics whereby a distinction can be made between a central and a peripheral PN, including whether it is paroxysmal or persistent, the latency, duration, fatigability, and the response to repositioning maneuvers. Many articles are available in the literature on CPN, and a 2017 meta-analysis analyzed the characteristics of nystagmus that led to the diagnosis of CPN. They show that although no rigorous study had evaluated the prevalence of CPN, it could be related to 11–12% of the positional nystagmus seen in oto-neurology consultation (14). Given the nature of the underlying impairment which is often serious, it is important to bear in mind the clinical elements that should evoke a central vs. peripheral etiology in this context. Some of the clinical features of a CPN origin are the pureness of the nystagmus (no torsional component), or a mix of horizontal and torsional nystagmus, as well as vertical components. For nystagmus triggered by canal stimulation, the atypical character of the nystagmus as well as the absence of improvement with repositioning maneuvers is a strong argument for CPN. The absence of latency is also a reliable and frequent indicator, as was the case in our patient. So there are many arguments, and it should be borne in mind that PN is not always peripheral (14). Once again, the example of our patient illustrates the value of rigorous analysis in the presence of PN.

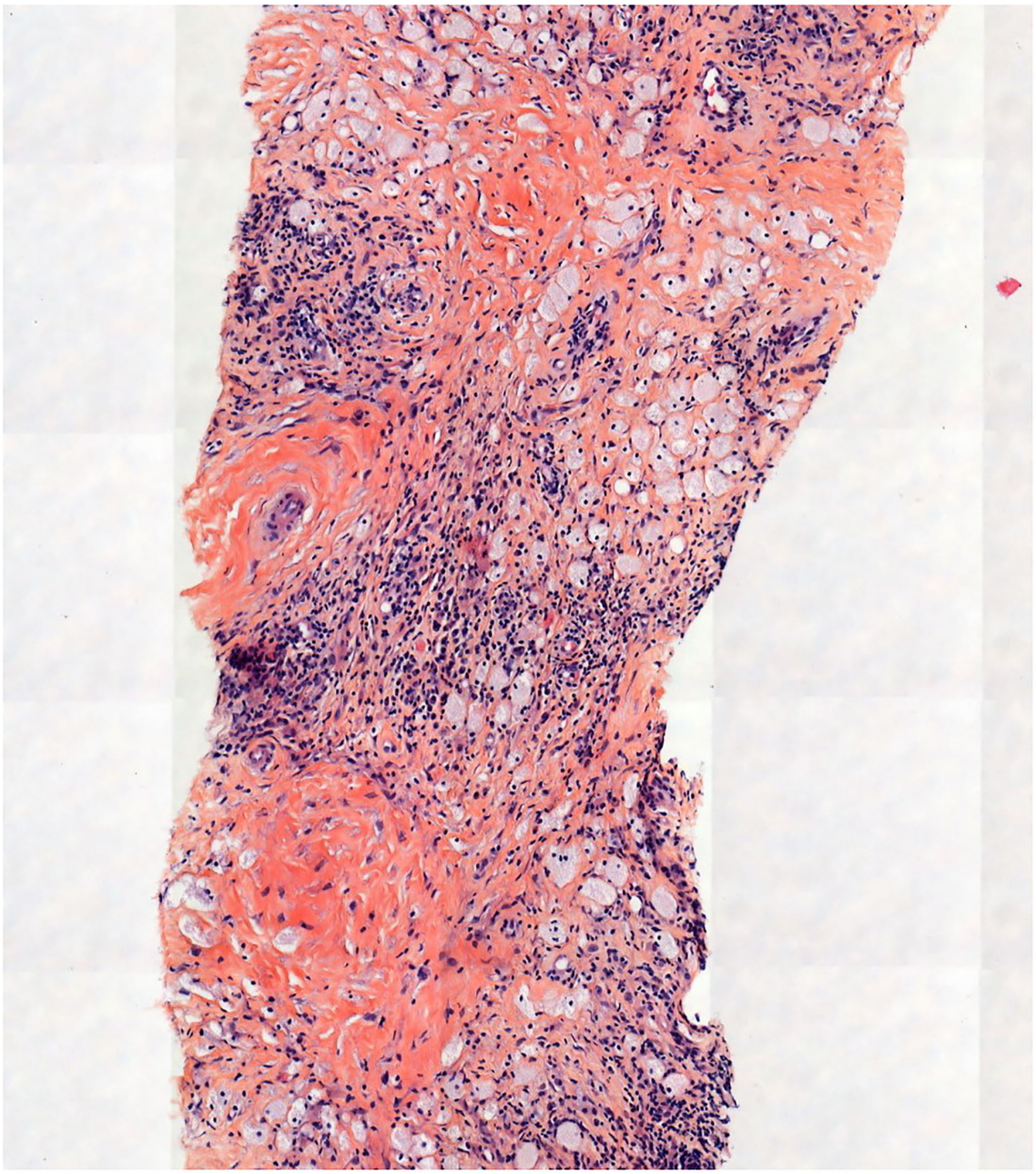

FIGURE 4 | Pathological examination showed perirenal fat and kidney capsule infiltrate made up of histiocytes, some of them with foamy cytoplasm (hematein-eosin-saffron, original magnification, x100).

CONCLUSION

Our case of ECD is the first that concerns a patient with only a complaint of instability, and offers a precise description of vestibulo-ocular abnormalities in this setting. A clinical examination identified CPN, and an associated static cerebellar syndrome. Together with suggestive imaging, these manifestations made it possible to diagnose ECD. Gait disturbance might be an underestimated entry sign of ECD. Therefore, the ability to differentiate CPN from peripheral PN might be crucial for early discovery of some complex neurological diseases.

DATA AVAILABILITY STATEMENT

The original contributions presented in the study are included in the article/supplementary material, further inquiries can be directed to the corresponding author.

ETHICS STATEMENT

The studies involving human participants were reviewed and approved by Toulouse University Hospital. The patients/participants provided their written informed consent to participate in this study.

AUTHOR CONTRIBUTIONS

AW had the idea of case reporting, analyzed the case, and drafted the manuscript to provide intellectual content. YG revised the figures and critically reviewed the manuscript. RD, BE, LT, FV, and DC critically reviewed the manuscript. DB prepared the MRI scans for figures and critically reviewed the manuscript. FB critically reviewed the manuscript and revised the MRI sequences for interpretation. All authors contributed to the article and approved the submitted version.

ACKNOWLEDGMENTS

We thank Ms. Delas Audrey, Ph.D. for helping us with the generation of the **Figure 4**.

REFERENCES

1. Starkebaum G, Hendrie P. Erdheim–Chester disease. *Best Pract Res Clin Rheumatol.* (2020) 34:101510. doi: 10.1016/j.berh.2020.101510
2. Diamond EL, Dagna L, Hyman DM, Cavalli G, Janku F, Estrada-Veras J, et al. Consensus guidelines for the diagnosis and clinical management of Erdheim-Chester disease. *Blood.* (2014) 124:483–92. doi: 10.1182/blood-2014-03-561381
3. Goyal G, Heaney ML, Collin M, Cohen-Aubart F, Vaglio A, Durham BH, et al. Erdheim-Chester disease: consensus recommendations for evaluation, diagnosis, and treatment in the molecular era. *Blood.* (2020) 135:1929–45. doi: 10.1182/blood.2019003507
4. Na S-J, Lee KO, Kim JE, Kim Y-D, A. Case of cerebral erdheim-chester disease with progressive cerebellar syndrome. *J Clin Neurol.* (2008) 4:45. doi: 10.3988/jcn.2008.4.1.45
5. Drier A, Haroche J, Savatovsky J, Godenèche G, Dormont D, Chiras J, et al. Cerebral, facial, and orbital involvement in erdheim-chester disease: ct and mr imaging findings. *Radiology.* (2010) 255:586–94. doi: 10.1148/radiol.10090320
6. Merritt H, Pfeiffer ML, Richani K, Phillips ME. Erdheim-Chester disease with orbital involvement: Case report and ophthalmic literature review. *Orbit.* (2016) 35:221–6. doi: 10.1080/01676830.2016.1176211
7. Parks NE, Goyal G, Go RS, Mandrekar J, Tobin WO. Neuroradiologic manifestations of Erdheim-Chester disease. *Neurol Clin Pract.* (2018) 8:15–20. doi: 10.1212/CPJ.0000000000000422
8. Bhatia A, Hatzoglou V, Ulaner G, Rampal R, Hyman DM, Abdel-Wahab O, et al. Neurologic and oncologic features of Erdheim–Chester disease: a 30-patient series. *Neuro-Oncol.* (2020) Jul 7;22(7):979–92. doi: 10.1093/neuonc/noaa008
9. Lauricella E. d'Amati A, Ingravallo G, Foresio M, Ribatti D, de Tommaso M, et al. Cerebellar ataxia and exercise intolerance in Erdheim-Chester disease. *Cerebellum Ataxias.* (2021) 8:3. doi: 10.1186/s40673-020-00125-x
10. Lemos J, Strupp M. Central positional nystagmus: an update. *J Neurol.* (2022) 269:1851–60. doi: 10.1007/s00415-021-10852-8
11. Lee S-U, Kim H-J, Lee E-S, Choi J-H, Choi J-Y, Kim J-S. Central positional nystagmus in inferior cerebellar peduncle lesions: a case series. *J Neurol.* (2021) 268:2851–7. doi: 10.1007/s00415-021-10435-7
12. Choi J-H, Seo J-D, Choi YR, Kim M-J, Kim H-J, Kim JS, et al. Inferior cerebellar peduncular lesion causes a distinct vestibular syndrome. *Eur J Neurol.* (2015) 22:1062–7. doi: 10.1111/ene.12705
13. von Brevern M, Bertholon P, Brandt T, Fife T, Imai T, Nuti D, et al. Benign paroxysmal positional vertigo: Diagnostic criteria: Consensus document of the Committee for the Classification of Vestibular Disorders of the Bárány Society. *J Vestib Res*. (2015) 25:105–17. doi: 10.3233/VES-150553
14. Macdonald NK, Kaski D, Saman Y, Al-Shaikh Sulaiman A, Anwer A, Bamiou D-E. Central positional nystagmus: a systematic literature review. *Front Neurol.* (2017) 8:141. doi: 10.3389/fneur.2017.00141

Conflict of Interest: The authors declare that the research was conducted in the absence of any commercial or financial relationships that could be construed as a potential conflict of interest.

frontiers | Frontiers in Neurology

CASE REPORT
published: 09 June 2022
doi: 10.3389/fneur.2022.892045

Case Report: Suppurative Labyrinthitis Induced by Chronic Suppurative Otitis Media

Qianwen Xiao[1,2,3], *Yuzhong Zhang*[1,2,3], *Jingrong Lv*[1,2,3], *Jun Yang*[1,2,3] *and Qing Zhang*[1,2,3]*

[1] Department of Otorhinolaryngology-Head and Neck Surgery, Xinhua Hospital, Shanghai Jiao Tong University School of Medicine, Shanghai, China, [2] Ear Institute, Shanghai Jiao Tong University School of Medicine, Shanghai, China, [3] Shanghai Key Laboratory of Translational Medicine on Ear and Nose Diseases, Shanghai, China

A discussion on suppurative labyrinthitis associated with chronic suppurative otitis media (CSOM) may seem to be an outdated issue due to the advent of antibiotics in the last century. In previous literature, limited cases of suppurative labyrinthitis have been reported. This case, therefore, is an excellent and rare opportunity to study its clinical symptoms, diagnoses, and treatments. This report described the case of a 39-year-old female with a history of CSOM for 20 years, and she often presented with otorrhea, vestibular disorder, and hearing impairment. CT of the temporal bone revealed fistulae in both the basal turn of the cochlea and the horizontal semicircular canal. Combined with the otolaryngology examination results, suppurative labyrinthitis was considered. During a three-month follow-up, her symptoms were improved significantly after surgery. In conclusion, suppurative labyrinthitis must not be overlooked and neglected; early diagnosis and treatments are of vital importance.

Keywords: suppurative labyrinthitis, hearing loss, vestibular disorder, semicircular canals, cochlea, fistulae

OPEN ACCESS

Edited by:
Michael Strupp, Ludwig Maximilian University of Munich, Germany

Reviewed by:
Leonardo Franz, University of Padua, Italy
Giuseppe Magliulo, Sapienza University of Rome, Italy

***Correspondence:**
Qing Zhang
zhangqing03@xinhuamed.com.cn

Specialty section:
This article was submitted to Neuro-Otology, a section of the journal Frontiers in Neurology

Received: *08 March 2022*
Accepted: *10 May 2022*
Published: *09 June 2022*

Citation:
Xiao Q, Zhang Y, Lv J, Yang J and Zhang Q (2022) Case Report: Suppurative Labyrinthitis Induced by Chronic Suppurative Otitis Media. Front. Neurol. 13:892045. doi: 10.3389/fneur.2022.892045

INTRODUCTION

Suppurative labyrinthitis is an inflammatory process involving bacterial invasion of the cochlea and vestibule (1). Bacteria can invade into the inner ear through oval window, round window, or pathologic fistula of the labyrinth leading to necrosis of membranous labyrinth, endolymphatic hydrops and so on. Symptoms of the disease are characterized by vertigo, tinnitus, nystagmus, and hearing impairment in the presence of a middle ear infection (2). Suppurative labyrinthitis, as one of the complications of chronic suppurative otitis media (CSOM), has been greatly reduced because of the widespread use of antibiotics (3, 4). However, this kind of disease still occur, especially in less favored communities in developing and developed countries, with significant morbidity (1, 4). Previous study had indicated suppurative labyrinthitis was identified as the most disabling among complications induced by CSOM, in that, affected individuals might experience complete hearing loss, seriously affecting their quality of life (5). Therefore, this disease should be valued. We present the case of a female patient with suppurative labyrinthitis aimed to gain a better understanding of its clinical symptoms, diagnoses, and therapies.

CASE DESCRIPTION

A generally healthy 39-year-old female with a history of CSOM for 20 years was seen at the otorhinolaryngology department of a local hospital. She presented with a 2-month history of

vertigo, tinnitus, hearing impairment, and perforation in her left tympanic membrane (TM) with foul-smelling purulent drainage. Each episode of vertigo lasted several seconds and worsened with activity and eased with inactivity. In severe cases of the vertigo, she had sometimes fallen to the floor, making it clear that the condition affected the quality of life of the patient. The local otolaryngologist prescribed ofloxacin ear drops, betahistine mesylate, gingko biloba extract, etc. The symptoms were relieved after treatments on nine consecutive days. However, these drugs treated the symptom, not the underlying problem. The perforation, drainage, and vertigo reoccurred once the treatments were stopped. Hence, those resolutions are temporary and it is necessary for the patient to search for a more effective therapy to treat the disease.

For further treatment, the patient was admitted to our hospital in February 2021. She underwent physical examinations and a detailed audiovestibular evaluation including pure tone audiometry (PTA), acoustic immittance testing, oscular (oVEMP) and cervical vestibular-evoked myogenic potentials (cVEMP), and head-impulse paradigm (HIMP). PTA was performed to evaluate the level of hearing loss. Acoustic immittance testing was performed to evaluate sound transmission function in the middle ear. The oVEMP was used to evaluate the functions of utricular and superior vestibular pathways, and the cVEMP was performed to evaluate the saccular and inferior vestibular pathway functions (6). For HIMP, it was performed to evaluate the functions of three semicircular canals (7). She also had CT of the

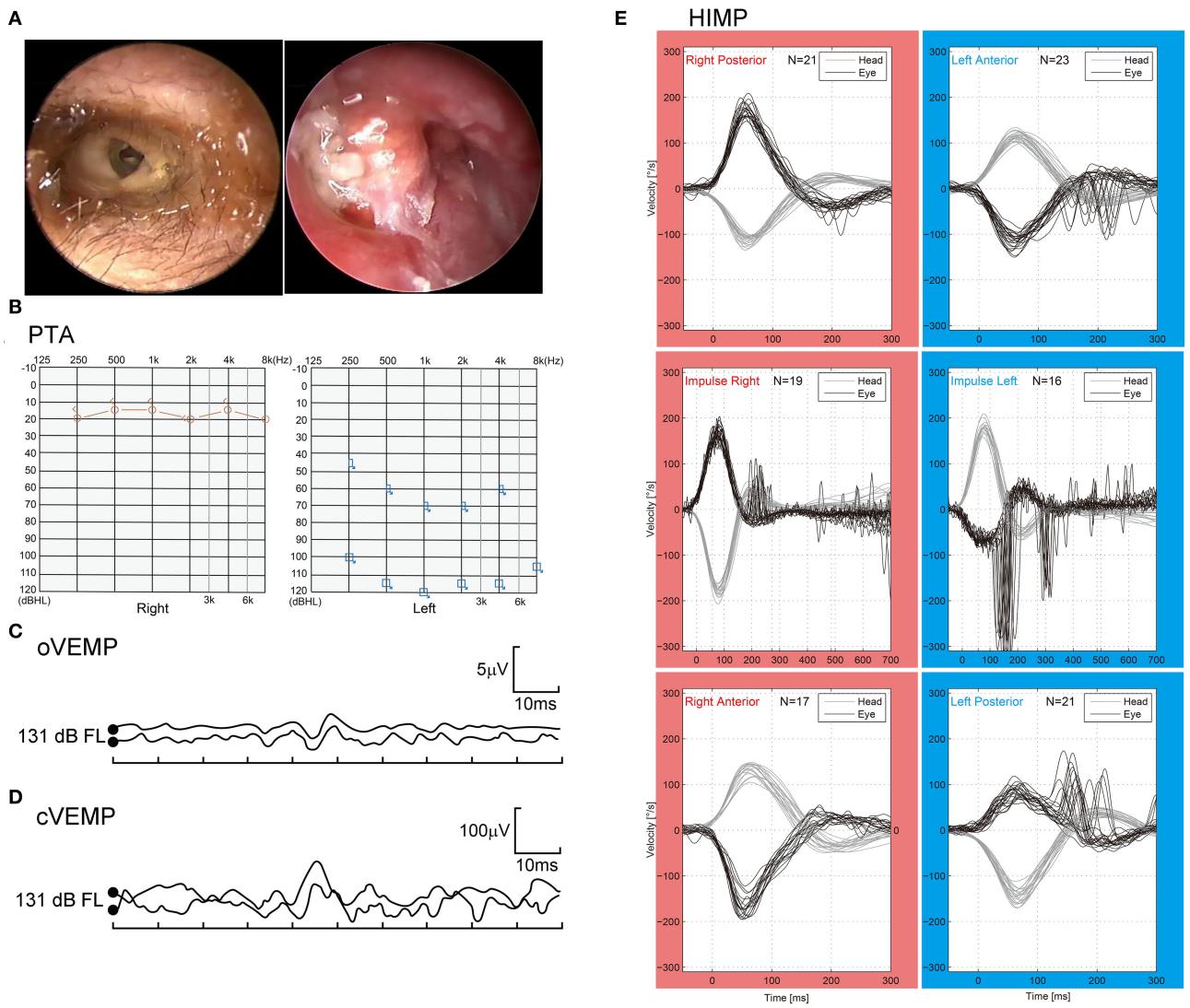

FIGURE 1 | (A) Oto-endoscope showed perforation in the left tympanic membrane with formation of granulation tissue and cholesteatoma. **(B)** There was no response to air and bone conductions in the left ear. PTA, pure tone audiometry. **(C,D)** The VEMPs could not be elicited in the left ear. VEMP, vestibular evoked myogenic potentials; oVEMP: ocular VEMP; cVEMP: cervical VEMP. **(E)** The HIMP revealed reduced VOR gains of the lateral, superior, and posterior semicircular canals in the left ear. HIMP, head-impulse paradigm; VOR, vestibulo-ocular reflex.

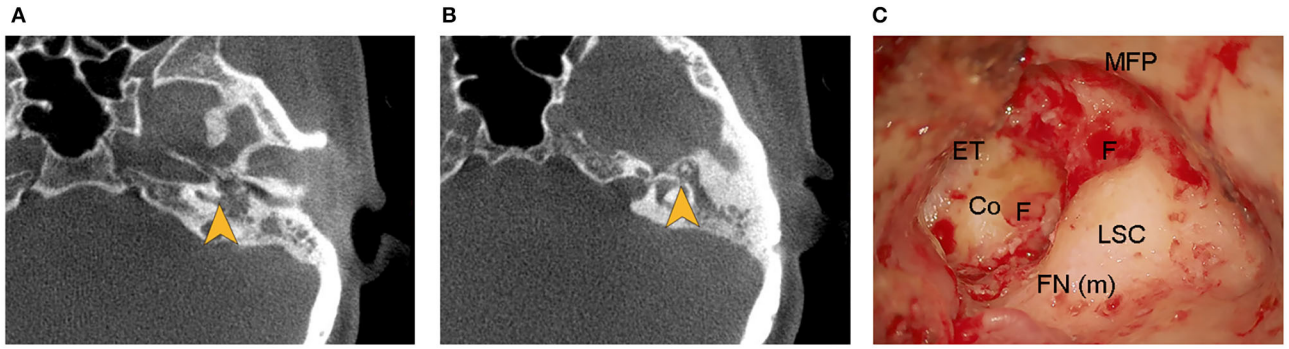

FIGURE 2 | (A,B) Computed tomographic images of the temporal bone showed fistulae (yellow arrows) in both the basal turn of the cochlea and the horizontal semicircular canal. **(C)** Fistulae in both the basal turn of the cochlea and the horizontal semicircular canal were evident during the operation. Co, cochlea; ET, epitympanum; F, fistula; FN (m), mastoid segment of facial nerve; LSC, lateral semicircular canal; MFP, middle fossa plate.

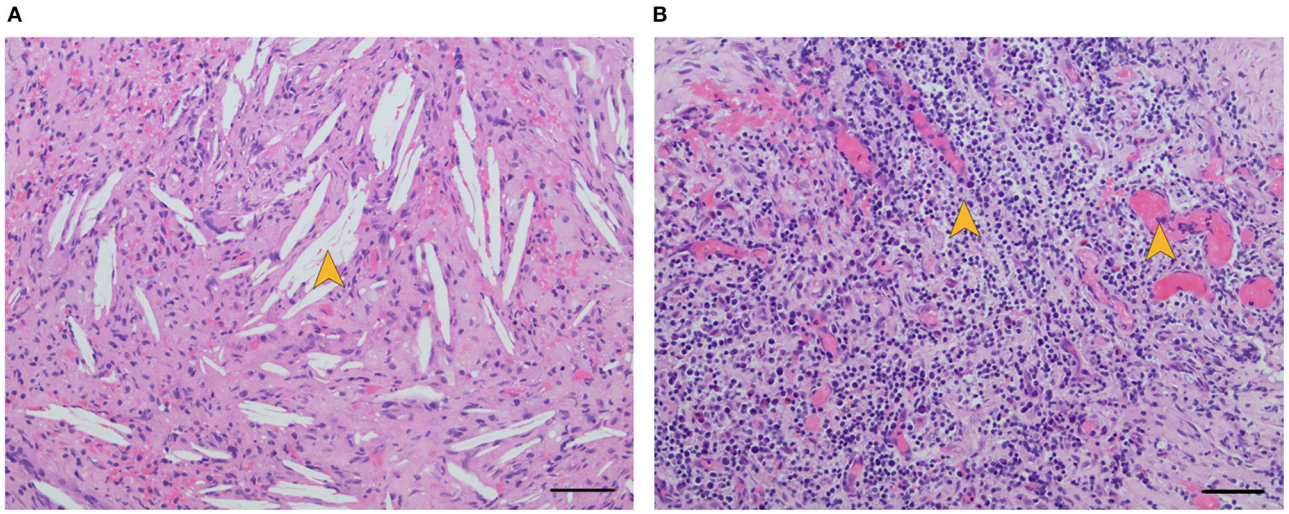

FIGURE 3 | H&E staining of biopsy specimen showed cholesterol clefts [**(A)**, yellow arrow] and inflammatory granulation tissue formation [**(B)**, yellow arrows] around fistulae. Scale bar, 50μm (×20).

temporal bone and MRI of the inner ear to find lesion sites intuitively.

On her physical examinations, Romberg's test was positive since the patient was unable to maintain an upright stance and her body leaned to the left side with eyes closed. Hennebert's sign was positive for the elicitation of pressure-induced nystagmus. The patient did not exhibit eye movements induced by sound, indicating the Tullio's phenomenon was negative. Oto-endoscope revealed an intact and clear right TM, and bloody and purulent secretions filling the left external auditory canal. Evacuation of the purulence showed perforation in her left TM with formation of granulation tissue and cholesteatoma (**Figure 1A**). Tympanometry examination showed a "B" type flat curve, indicating there was perforation in the tympanic membrane or blockage of the auditory canal (**Supplementary Figure 1, Supplementary Video 1**). The PTA illustrated there were no response to air and bone conductions in the left ear, but normal hearing in the right ear (**Figure 1B**). The patient showed absence of both oVEMP and cVEMP on the left side in bone-conducted vibration mode, with 500 Hz tone-burst stimulation delivered at 131 dB FL (**Figures 1C,D**). The VEMPs results elicited by air-conducted sound (ACS-VEMPs) and galvanic vestibular stimulation (GVS-VEMPs) are shown in **Supplementary Figure 2**. The HIMP displayed reduced vestibulo-ocular reflex (VOR) gains of the lateral, superior, and posterior semicircular canals during head impulses to the left side (**Figure 1E**). The CT scans of the temporal bone detected fistulae in both the basal turn of the cochlea and the horizontal semicircular canal (**Figures 2A,B**). Our MRI showed the vestibule and the cochlea were presented as nearly isointense on T1-weighted imaging (**Supplementary Figures 3A,B**). After contrast administration, the portion of lesion was slightly enhanced (**Supplementary Figures 3C,D**). Eventually, a clear

diagnosis of suppurative labyrinthitis was made after combining with speciality test results.

The patient underwent tympanoplasty after significant reduction of otorrhea. Intraoperative exploration revealed the entrance of the tympanum was obstructed by large amounts of cholesteatoma and granulation tissue, and there was a large amount of granulation tissue with cholesteatoma epithelium in the posterior tympanum. The surgical procedure was complicated by the intraoperative finding of fistulae in both the basal turn of the cochlea and the horizontal semicircular canal during surgery (**Figure 2C**). Interestingly, we found the granulation tissue gushed out of the horizontal semicircular fistula when the cochlear fistula was pushed, indicating formation of granulation tissue in the labyrinth (**Supplementary Video 2**). The horizontal semicircular canal was packed with temporalis myofascial flap after clearing up granulation tissue and necrotic tissue. H&E staining of the biopsy specimen showed cholesterol clefts and inflammatory granulation tissue formation around the fistulae **(Figure 3)**. The diagnosis of suppurative labyrinthitis was made again. The patient was discharged when antibiotic therapy was completed for 1 week after surgery. We provided important issues regarding maintaining a healthy lifestyle, including keeping the ears dry, avoiding scratching the ears, and persisting in vestibular rehabilitation training. During 3 months of follow-up, the patient was released from vertigo and otorrhea, and she expressed that surgery was a right choice. However, her hearing loss did not improve.

DISCUSSION

During the last 20th century, the introduction of antibiotics and immunizations led to a notable reduction in morbidity from complications related to otitis media (8). Intratemporal complications associated with otitis media mainly include labyrinthine fistula, mastoiditis, peripheral facial palsy, and labyrinthitis. Labyrinthitis is the least frequent complication with an annual incidence rate of 0.1% (4). Labyrinthitis usually consists of circumscribed labyrinthitis, serous labyrinthitis, and suppurative labyrinthitis. The identification of suppurative labyrinthitis is usually apparent through the observation of typical symptoms, which include hypacusis, tinnitus, vertigo, and moderate to severe mixed hearing loss (2, 3). Vertigo and disequilibrium are usually the presenting symptoms and can cause grave mortality. Vestibular neuritis and sudden deafness may also present with severe impairment of vestibular function, indicating that the diagnosis of suppurative labyrinthitis is not to be made based only on clinical symptoms (1, 9, 10).

Imaging tests are important tools to better understand pathological features and play an important role in diagnosis. Previous research has shown gadolinium in MRI is essential to detect inner ear inflammatory lesions and the temporal bone CT scans can identify lesion extent and location (11, 12). In our case, we found fistulae in both the basal turn of the cochlea and the horizontal semicircular canal through the temporal bone CT scans. This provides an important basis for us to quickly find the lesion site during the operation. We did find fistulae in both the basal turn of the cochlea and the horizontal semicircular canal during the surgery. H&E staining results of biopsy specimen showed the fistulae were filled with inflammatory granulation tissue and cholesterol clefts, indicating the patient is in the fibrosis stage of suppurative labyrinthitis (13). It is assumed that close contact of the infected granulation tissue and the underlying perilymph play a crucial role in the occurrence of physiopathological process (14, 15). However, there is no concrete and direct evidence of inflammation occurring during the period of suppurative labyrinthitis, and the studies of inflammatory response kinetics within the human inner ear are still limited (11). If we better understand the inflammatory process and its course, we can provide personalized treatments through identifying the type and the location of lesions. On 3 months of follow-up, our patient was released from vertigo after the surgery. We assumed that her vestibular symptoms were ameliorated through the process of vestibular functional compensation. Indeed, there is a spontaneous functional recovery because of neuronal and behavioral plasticity. For this reason, the intrinsic plasticity of the nervous system to reorganize may overcome the damages of the peripheral vestibular system, leading to a mitigation of vestibular symptoms (16). However, we found there was no improvement in hearing after surgery, suggesting once the inflammatory process developed into the inner ear, it resulted into an inevitable cell damage process (3). Thus, the hearing loss was already established when the patient was diagnosed with suppurative labyrinthitis. Regrettably, the patient missed the best time for diagnosis and treatments.

Early diagnosis and treatments of suppurative labyrinthitis are crucial to minimize the morbidity and mortality, and the doctor should be suspicious of this kind of disease when there are typical symptoms at present (15, 17). The decrease in morbidity and mortality may be attributable to advances in critical care, further studies on the mechanisms of inflammation, improvements in surgical techniques, close operation among clinics, and early referral of patients to otolaryngology.

DATA AVAILABILITY STATEMENT

The original contributions presented in the study are included in the article/**Supplementary Material**, further inquiries can be directed to the corresponding author.

ETHICS STATEMENT

The studies involving human participants were reviewed and approved by Shanghai Jiaotong University. Written informed consent to participate in this study was provided by the participants' legal guardian/next of kin. The patients/participants provided their written informed consent to participate in this study. Written informed consent was obtained from the individual(s) for the publication of any potentially identifiable images or data included in this article.

AUTHOR CONTRIBUTIONS

QZ and JY were the surgeon in the case. QX and YZ contributed to the data collection and writing. QZ, JL,

and JY guided the completion of this article. All authors contributed to manuscript revision and approved the submitted version.

FUNDING

This study was supported by the National Natural Science Foundation of China (Nos. 81970891, 81970876, and 82171137).

ACKNOWLEDGMENTS

We thank the patient and her family for their collaboration.

SUPPLEMENTARY MATERIAL

The Supplementary Material for this article can be found online at: https://www.frontiersin.org/articles/10.3389/fneur.2022.892045/full#supplementary-material

REFERENCES

1. Kaya S, Schachern PA, Tsuprun V, Paparella MM, Cureoglu S. Deterioration of vestibular cells in Labyrinthitis. *Ann Otol Rhinol Laryngol.* (2017) 126:89–95. doi: 10.1177/0003489416675356
2. Taxak P, Ram C. Labyrinthitis and Labyrinthitis Ossificans: a case report and review of the literature. *J Radiol Case Rep.* (2020) 14:1–6. doi: 10.3941/jrcr.v14i5.3706
3. Maranhão AS, Godofredo VR, Penido Nde O. Suppurative labyrinthitis associated with otitis media: 26 years' experience. *Braz J Otorhinolaryngol.* (2016) 82:82–7. doi: 10.1016/j.bjorl.2014.12.012
4. Maranhão AS, Andrade JS, Godofredo VR, Matos RC, Penido Nde O. Intratemporal complications of otitis media. *Braz J Otorhinolaryngol.* (2013) 79:141–9. doi: 10.5935/1808-8694.20130026
5. Leskinen K, Jero J. Acute complications of otitis media in adults. *Clin Otolaryngol.* (2005) 30:511–6. doi: 10.1111/j.1749-4486.2005.01085.x
6. Tanyeri O, Akdogan MV, Hizal E, Büyüklü AF. Assessment of vestibular function in adults with prelingual hearing loss using c/oVEMP tests. *J Int Adv Otol.* (2020) 16:24–7. doi: 10.5152/iao.2019.7280
7. Chawla A, Abdurahiman R, Chokkalingam V. The video head impulse test: our experience in 45 cases. *Indian J Otolaryngol Head Neck Surg.* (2018) 70:498–504. doi: 10.1007/s12070-018-1487-0
8. Wanna GB, Dharamsi LM, Moss JR, Bennett ML, Thompson RC, Haynes DS. Contemporary management of intracranial complications of otitis media. *Otol Neurotol.* (2010) 31:111–7. doi: 10.1097/MAO.0b013e3181c2a0a8
9. Jeong SH, Kim HJ, Kim JS. Vestibular neuritis. *Semin Neurol.* (2013) 33:185–94. doi: 10.1055/s-0033-1354598
10. Lee JY, Lee YW, Chang SO, Kim MB. Vestibular function analysis of sudden sensorineural hearing loss with dizziness. *J Vestib Res.* (2020) 30:203–12. doi: 10.3233/VES-200703
11. Floc'h JL, Tan W, Telang RS, Vlajkovic SM, Nuttall A, Rooney WD, et al. Markers of cochlear inflammation using MRI. *J Magn Reson Imaging.* (2014) 39:150–61. doi: 10.1002/jmri.24144
12. Al-Juboori A, Al Hail AN. Gradenigo's Syndrome and Labyrinthitis: conservative versus surgical treatment. *Case Rep Otolaryngol.* (2018) 2018:6015385. doi: 10.1155/2018/6015385
13. Paparella MM, Sugiura S. The pathology of suppurative labyrinthitis. *Ann Otol Rhinol Laryngol.* (1967) 76:554–86. doi: 10.1177/000348946707600303
14. Dubey SP, Larawin V. Complications of chronic suppurative otitis media and their management. *Laryngoscope.* (2007) 117:264–7. doi: 10.1097/01.mlg.0000249728.48588.22
15. Osma U, Cureoglu S, Hosoglu S. The complications of chronic otitis media: report of 93 cases. *J Laryngol Otol.* (2000) 114:97–100. doi: 10.1258/0022215001905012
16. Lacour M, Helmchen C, Vidal PP. Vestibular compensation: the neuro-otologist's best friend. *J Neurol.* (2016) 263 Suppl 1:S54–64. doi: 10.1007/s00415-015-7903-4
17. Wu JF, Jin Z, Yang JM, Liu YH, Duan ML. Extracranial and intracranial complications of otitis media: 22-year clinical experience and analysis. *Acta Otolaryngol.* (2012) 132:261–5. doi: 10.3109/00016489.2011.643239

Conflict of Interest: The authors declare that the research was conducted in the absence of any commercial or financial relationships that could be construed as a potential conflict of interest.

Publisher's Note: All claims expressed in this article are solely those of the authors and do not necessarily represent those of their affiliated organizations, or those of the publisher, the editors and the reviewers. Any product that may be evaluated in this article, or claim that may be made by its manufacturer, is not guaranteed or endorsed by the publisher.

frontiers | Frontiers in Neurology

CASE REPORT
published: 10 June 2022
doi: 10.3389/fneur.2022.902758

Case Report: New Application of a Gufoni Maneuver Variation for Apogeotropic Lateral Semicircular Canal Benign Paroxysmal Positional Vertigo

Jiaoxuan Dong[1], *Ling Li*[1], *Songbin He*[1], *Haipeng Liu*[2]* *and Fangyu Dai*[1]*

[1] *Department of Neurology, Zhoushan Hospital, Wenzhou Medical University, Zhoushan, China,* [2] *Research Centre for Intelligent Healthcare, Coventry University, Coventry, United Kingdom*

Background: Several canalith repositioning procedures (CRPs) such as Gufoni maneuver have been proposed to treat the apogeotropic lateral semicircular canal variant of BPPV (LC-BPPV). The reported success rate varied widely in different studies. Research showed that there was a risk of treatment failure due to insufficient repositioning of the debris. So far, there is insufficient evidence to recommend a preferable CRP for apogeotropic LC-BPPV.

Case description: A 49-year-old woman and a 48-year-old man diagnosed with apogeotropic LC-BPPV relapse were treated with original Gufoni maneuver for apogeotropic variant but no satisfactory result was obtained. A variation of Gufoni maneuver originally proposed for the geotropic variant was applied to detach otoconia toward the utricle or the non-ampullary arm. Apogeotropic nystagmus was successfully transformed into the geotropic variant. The subsequent Gufoni maneuver was successful. On a 64-year-old male with untreated apogeotropic LC-BPPV, we performed the Gufoni maneuver variation and observed a change in nystagmus direction. In all the three cases, no relapse of vertigo was reported after 1 month.

Conclusion: The new application of Gufoni maneuver variation may improve the treatment of apogeotropic LC-BPPV. Treatment efficacy and patient-specific optimization such as head rotation angle deserve a large-scale validation and further investigation.

Keywords: canalith repositioning procedure, benign paroxysmal positional vertigo (BPPV), semicircular canals, Gufoni maneuver, case report, apogeotropic variant

OPEN ACCESS

Edited by:
Michael Strupp, Ludwig Maximilian University of Munich, Germany

Reviewed by:
Bernardo Faria Ramos, Universidade Federal Do Espírito Santo, Brazil
Michael C. Schubert, Johns Hopkins University, United States

***Correspondence:**
Haipeng Liu
haipeng.liu@coventry.ac.uk
Fangyu Dai
diligentdfy@hotmail.com

Specialty section:
This article was submitted to Neuro-Otology, a section of the journal Frontiers in Neurology

Received: *23 March 2022*
Accepted: *11 May 2022*
Published: *10 June 2022*

Citation:
Dong J, Li L, He S, Liu H and Dai F (2022) Case Report: New Application of a Gufoni Maneuver Variation for Apogeotropic Lateral Semicircular Canal Benign Paroxysmal Positional Vertigo. Front. Neurol. 13:902758. doi: 10.3389/fneur.2022.902758

INTRODUCTION

Benign paroxysmal positional vertigo (BPPV) is the most frequent peripheral vestibular disorder induced by changes in head position relative to the gravitational axis (1). Of all BPPV cases, LC-BPPV is the second commonest subtype after posterior semicircular canal BPPV (PC-BPPV) (2). The apogeotropic variant of LC-BPPV is attributed to otoliths attached to the cupula (cupulolithiasis) on the canal side (Cup-C) or the utricular side (Cup-U), or free-floating otoliths in the ampullary arm of the LC (3). Owing to the three different pathological types, the treatment

of this variant is difficult. Several canalith repositioning procedures (CRPs) have been proposed for the apogeotropic variant (4), such as a new variation of Gufoni maneuver, i.e., the Zuma maneuver (5, 6), and recently, the mastoid vibration maneuver (7).

As one of the commonest CRP for LC-BPPV, the Gufoni maneuver has two variations. The original variation proposed for the geotropic variant of LC-BPPV consists of a quick movement onto the unaffected side followed by a downward head rotation, i.e., the "Gufoni nose-down" variation (8). Ciniglio Appiani et al. described the details of this variation in a publication in English in 2001 (9). In contrast, the variation originally proposed for apogeotropic LC-BPPV consists of a quick movement onto the affected side followed by an upward head rotation, i.e., the "Gufoni nose-up" variation (10).

The Gufoni maneuver for the apogeotropic variant (Gufoni nose-up variation) was considered efficient in converting LC-BPPV from the apogeotropic to the geotropic form (10). A randomized clinical trial indicated that the Gufoni maneuver was more effective than the head-shaking maneuver, with a 73.1% success rate (11). However, the reported success rate varied widely in different studies, which could be considerably lower. Research showed that there was a risk of treatment failure due to insufficient repositioning of the debris when the Gufoni nose-up variation was applied in apogeotropic LC-BPPV (12). So far, there is insufficient evidence to recommend a preferable CRP for apogeotropic LC-BPPV (13).

Recently, we had observed three patients experiencing severe apogeotropic LC-BPPV. We first performed the Gufoni nose-up variation but failed to convert it into the geotropic variant. Thus, we adopted the Gufoni maneuver for the geotropic variant (Gufoni nose-down variation) to treat the apogeotropic variant and achieved good efficiency.

METHODS

In the Gufoni nose-up variation for the apogeotropic variant, the patient is quickly moved from the sitting position onto the affected side, followed by a rapid 45° upward head rotation before returning to the sitting position (14). In contrast, the Gufoni nose-down variation adopted in this study, which is based on the Gufoni maneuver presented by Ramos et al. (14), starts from the sitting position, from which the patient is moved quickly onto the unaffected side, followed by a quick 45° downward turn and holding for 2 min (**Figure 1**). If the transformation of the nystagmus direction is achieved, the Gufoni maneuver for the geotropic variant (Gufoni nose-down variation) will be further performed.

CASE PRESENTATION

Case 1

A 49-year-old female with no history of vertigo experienced her first vertigo attack 3 months ago without any symptoms of headache, tinnitus, or deafness. The vertigo episode was related to her head position with a short duration of ∼1–2 min. The patient had no previous history of other chronic diseases. She had been diagnosed with apogeotropic LC-BPPV in our neurology department and was repositioned with the Gufoni maneuver (Gufoni nose-up variation). The vertigo relapsed 1 day ago before her second admission. The neurophysical examination showed negative results. No spontaneous or gaze-evoked nystagmus was found. The Brain CT showed no structural lesions. The supine roll test was performed with the patient lying on the examination table. Her head was briskly rotated to the right side from the supine position. An apogeotropic nystagmus lasting over 1 min was observed. After the maximal head yaw movement to the right, the patient's head was brought to the supine position and then briskly rotated to her left, which elicited a stronger apogeotropic nystagmus lasting over 1 min. According to Ewald's second law, the right side was the affected side. We performed the Gufoni nose-up variation once a day for 1 week, but there was no transformation of nystagmus direction. Then, we performed the Gufoni nose-down variation. The patient was brought onto the left side from sitting position. A horizontal nystagmus beating toward the uppermost ear was evoked. After a few seconds, the patient's head was inclined 45° downward in the yaw plane and held for 2 min. During this, we observed the nystagmus transforming into the geotropic variant. Subsequent treatment with the Gufoni maneuver (Gufoni nose-down variation) was successful. At the 4-week follow-up, the patient reported no vertigo relapse.

Case 2

A 48-year-old male with no history of vertigo suffered from serious vertigo 1 month ago and remitted spontaneously, and had a relapse 2 days ago while getting up. The vertigo attack was associated with positional change of the head. The neurological examination revealed normal cranial nerve. Strength was grade 5/5 in all four limbs with normal deep tendon reflexes. No spontaneous or gaze-evoked nystagmus was found. Brain MRI scanning revealed no structural lesions. He was diagnosed with right apogeotropic LC-BPPV in the supine roll test by observing the intensity of the nystagmus as in case 1. The Gufoni nose-up variation was performed, but no satisfactory result was obtained. Then, we performed the Gufoni nose-down variation. When the patient was briskly turned to left side-lying position from the sitting position, an apogeotropic nystagmus was observed. After a 45-degree downward turn and 2 min holding, the nystagmus was transformed into the geotropic form. He was treated with the Gufoni maneuver (Gufoni nose-down variation) subsequently and reported no relapse after 1 month.

Case 3

A 64-year-old male had positional vertigo 3 days ago. He had no history of vertigo before. No positive result was found in brain MRI and neurophysical examination. He was diagnosed with left apogeotropic LC-BPPV in the supine roll test by observing the intensity of the nystagmus as in cases 1 and 2 (**Supplementary Video 1**). We performed the Gufoni nose-down variation. The patient's head was first taken to the right lateral recumbent position where an apogeotropic nystagmus was induced and subsequently quickly rotated 45° downward. In about a minute, we observed the translation of nystagmus

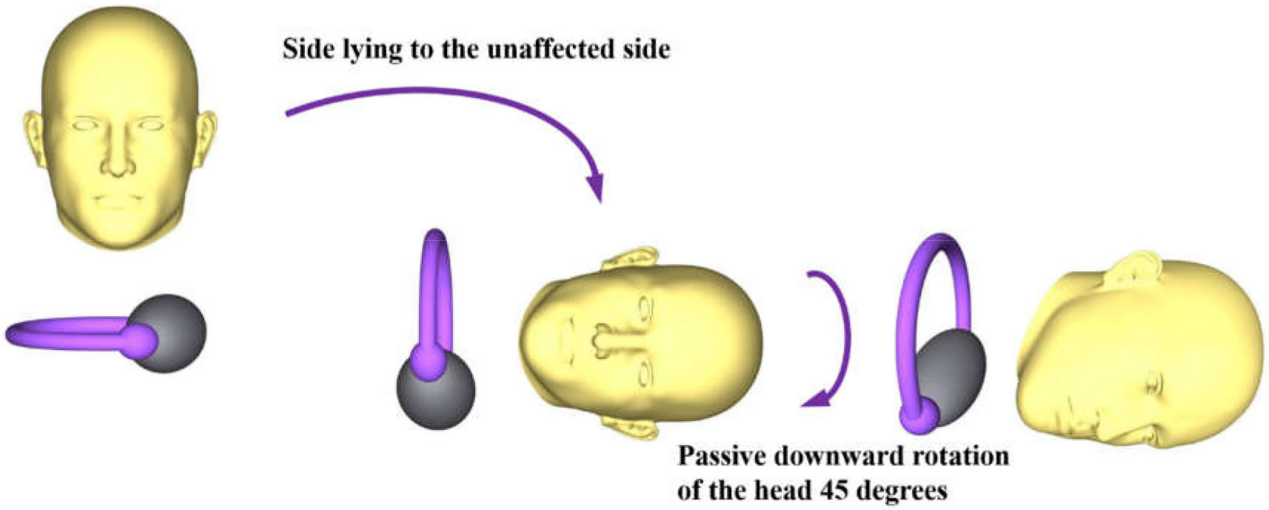

FIGURE 1 | New application of the Gufoni maneuver for apogeotropic LC-BPPV. The right side is the affected side.

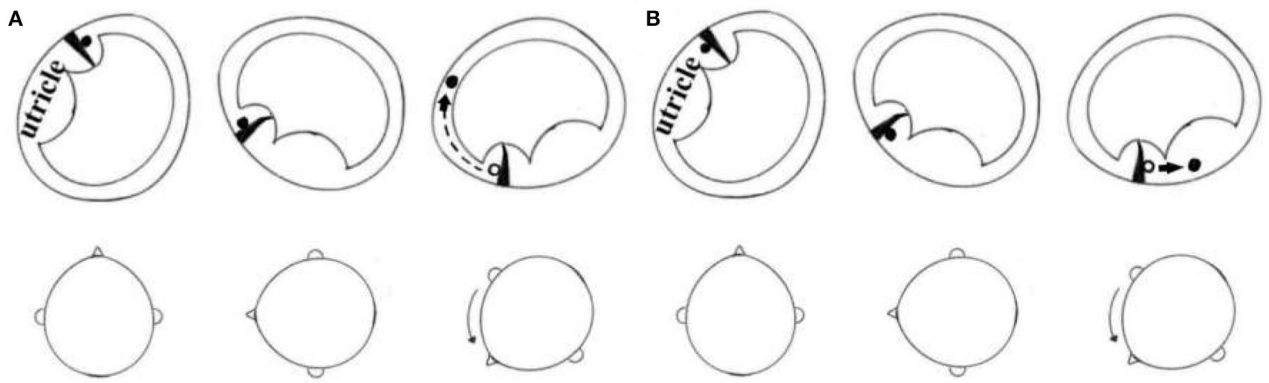

FIGURE 2 | New application of the Gufoni nose-down variation. **(A)** Debris on the canal side. **(B)** Debris on the utricular side. The right side is the affected side in both cases.

direction. Then, he was treated with the Gufoni maneuver (Gufoni nose-down variation), and the nystagmus disappeared. He reported no vertigo relapse at 1 month follow-up.

DISCUSSION

An apogeotropic nystagmus that never becomes geotropic is a sign of cupulolithiasis in peripheral vertigo (14). We assume two application scenarios of the proposed maneuver (**Figures 2A,B**). In the first situation, the otoconia are located on the canal side (**Figure 2A**). In our new application of the Gufoni maneuver (i.e., using Gufoni nose-down variation for apogeotropic LC-BPPV cases), as the three patients lied on the unaffected side from the sitting position, the lateral semicircular canal was on the earth-vertical plane. In this position, the otoconia are located above the cupula. Then, the head was suddenly rotated toward the ground. These two steps required rapid angular acceleration to detach the otoconia from the cupula. If separation had been achieved in the first step, the 45-degree downward turn could facilitate the movement of the detached otoconia toward the utricle or the non-ampullary arm. During our repositioning procedures, the nystagmus was transformed to the geotropic variant. The most likely explanation was that the otoconia moved to the non-ampullary arm. We considered that the most possible diagnosis of these patients was Cup-C. In the latter form (**Figure 2B**), the patient will be moved from the sitting position to the side-lying position on the healthy side, attaining the most gravity-dependent position after a brisk deceleration. Under the dual effects of gravity and inertia, the otoconia will be separated from the cupula. In the second step, which requires quick deceleration, the inertia favors the otoconial movement toward utricle. There is no need for another Gufoni maneuver (Gufoni nose-down variation) if repositioning is obtained.

According to the latest guidelines, there are two ways of Gufoni maneuver for treatment of two cupulolithiasis variants (13). However, the operator could not decide the proper maneuver at the first stage of treatment. This may cause clinical treatment failure. Inspired by existing studies, we adopted the Gufoni nose-down variation to separate otoconial debris from the cupula for apogeotropic LC-BPPV. Theoretically, the two subtypes of cupulolithiasis can be treated with this repositioning maneuver. This method might provide a reference for the development of a unified repositioning maneuver for both subtypes of cupololithasis using gravity and inertia (14). We believe that a single repositioning maneuver for all the variants of LC-BPPV could help the neurotological clinical practice.

However, there are some limitations in this study. We did not perform the bow and lean test and the seated supine positioning test (SSPT), which can fully confirm the diagnosis of LC-BPPV (6). The treatment efficacy requires further large-scale validation. Further investigation is needed regarding its patient-specific optimization such as head rotation angle. Video-Frenzel goggles are also needed to remove visual fixation.

DATA AVAILABILITY STATEMENT

The original contributions presented in the study are included in the article/**Supplementary Material**, further inquiries can be directed to the corresponding authors.

ETHICS STATEMENT

The studies involving human participants were reviewed and approved by Clinical Research Ethics Committee of Zhoushan Hospital. The patients/participants provided their written informed consent to participate in this study. Written informed consent was obtained from the individual(s) for the publication of any potentially identifiable images or data included in this article.

AUTHOR CONTRIBUTIONS

JD and FD: conception and study design. JD, HL, and FD: acquisition, analysis, and interpretation of data. JD: first draft of the manuscript. JD and HL: critical reading and manuscript revision. All the authors read and approved the submitted version.

FUNDING

This study was supported by the Medical Health Science and Technology Project of Zhejiang Provincial Health Commission and the Planned Projects of Bureau of Science and Technology of Zhoushan (2020ZH065 and 2020C31048).

ACKNOWLEDGMENTS

We would like to thank the patients for permitting the use of these data.

SUPPLEMENTARY MATERIAL

The Supplementary Material for this article can be found online at: https://www.frontiersin.org/articles/10.3389/fneur.2022.902758/full#supplementary-material

REFERENCES

1. Strupp M, Dlugaiczyk J, Ertl-Wagner BB, Rujescu D, Westhofen M, Dieterich M. Vestibular disorders. *DtschArztebl Int.* (2020) 117:300–10. doi: 10.3238/arztebl.2020.0300
2. Mandalà M, Salerni L, Nuti D. Benign positional paroxysmal vertigo treatment: a practical update. *Curr Treat Options Neurol.* (2019) 21:66. doi: 10.1007/s11940-019-0606-x
3. Ramos BF, Cal R, Brock CM, MangabeiraAlbernaz PL, Zuma e Maia F. Apogeotropic variant of horizontal semicircular canal benign paroxysmal positional vertigo: where are the particles? *Audiol Res.* (2019) 9:228. doi: 10.4081/audiores.2019.228
4. Zuma E, Maia F, Ramos BF, Cal R, Brock CM, Mangabeira Albernaz PL, et al. Management of lateral semicircular canal benign paroxysmal positional vertigo. *Front Neurol.* (2020) 11:1040. doi: 10.3389/fneur.2020.01040
5. Zuma E, Maia F. New treatment strategy for apogeotropic horizontal canal benign paroxysmal positional vertigo. *Audiol Res.* (2016) 6:163. doi: 10.4081/audiores.2016.163
6. Ramos BF, Cal R, MangabeiraAlbernaz PL, Zuma E, Maia F. The role of the reversed nystagmus during Zuma maneuver in patients treated for geotropic lateral canal benign paroxysmal positional vertigo. *J Neurol Sci.* (2022) 434:120160. doi: 10.1016/j.jns.2022.120160
7. Kim HA, Park SW, Kim J, Kang BG, Lee J, Han BI, et al. Efficacy of mastoid oscillation and the Gufoni maneuver for treating apogeotropic horizontal benign positional vertigo: a randomized controlled study. *J Neurol.* (2017) 264:848–55. doi: 10.1007/s00415-017-8422-2
8. Gufoni M, Mastrosimone L, Di Nasso F. Trattamento con manovra di riposizionamento per la canalolitiasi orizzontale [Repositioning maneuver in benign paroxysmal vertigo of horizontal semicircular canal]. *ActaOtorhinolaryngol Ital.* (1998) 18:363–7.
9. CiniglioAppiani G, Catania G, Gagliardi M. A liberatory maneuver for the treatment of horizontal canal paroxysmal positional vertigo. *OtolNeurotol.* (2001) 22:66–9. doi: 10.1097/00129492-200101000-00013
10. CiniglioAppiani G, Catania G, Gagliardi M, Cuiuli G. Repositioning maneuver for the treatment of the apogeotropic variant of horizontal canal benign paroxysmal positional vertigo. *OtolNeurotol.* (2005) 26:257–60. doi: 10.1097/00129492-200503000-00022
11. Kim JS, Oh SY, Lee SH, Kang JH, Kim DU, Jeong SH, et al. Randomized clinical trial for apogeotropic horizontal canal benign paroxysmal positional vertigo. *Neurology.* (2012) 78:159–66. doi: 10.1212/WNL.0b013e3182648b8b
12. Bhandari A, Bhandari R, Kingma H, Zuma E, Maia F, Strupp M. Three-dimensional simulations of six treatment maneuvers for horizontal canal benign paroxysmal positional vertigo canalithiasis. *Eur J Neurol.* (2021) 28:4178–83. doi: 10.1111/ene.15044
13. Bhattacharyya N, Gubbels SP, Schwartz SR, Edlow JA, El-Kashlan H, Fife T, et al. Clinical practice guideline: benign paroxysmal positional vertigo (update). *Otolaryngol Head Neck Surg.* (2017) 156(3_suppl):S1–47. doi: 10.1177/0194599816689667

14. Ramos BF, Cal R, MangabeiraAlbernaz PL, Zuma E, Maia F. Practical approach for lateral canal benign paroxysmal positional vertigo. *J Neurol Sci.* (2022) 434:120180. doi: 10.1016/j.jns.2022.120180

Conflict of Interest: The authors declare that the research was conducted in the absence of any commercial or financial relationships that could be construed as a potential conflict of interest.

Publisher's Note: All claims expressed in this article are solely those of the authors and do not necessarily represent those of their affiliated organizations, or those of the publisher, the editors and the reviewers. Any product that may be evaluated in this article, or claim that may be made by its manufacturer, is not guaranteed or endorsed by the publisher.

frontiers | Frontiers in Neurology

TYPE Case Report
PUBLISHED 06 October 2022
DOI 10.3389/fneur.2022.1028597

OPEN ACCESS

EDITED BY
Sun-Young Oh,
Jeonbuk National University,
South Korea

REVIEWED BY
Kwangdong Choi,
Pusan National University, South Korea
Jae-Hwan Choi,
Pusan National University Yangsan Hospital, South Korea

*CORRESPONDENCE
Nicolina Goldschagg
nicolina.goldschagg@med.uni-muenchen.de

SPECIALTY SECTION
This article was submitted to Neuro-Otology, a section of the journal Frontiers in Neurology

RECEIVED 26 August 2022
ACCEPTED 12 September 2022
PUBLISHED 06 October 2022

CITATION
Goldschagg N, Brem C and Strupp M (2022) Case report: Bitter vertigo. *Front. Neurol.* 13:1028597. doi: 10.3389/fneur.2022.1028597

Case report: Bitter vertigo

Nicolina Goldschagg[1]*, Christian Brem[2] and Michael Strupp[1]

[1]Department of Neurology and German Center for Vertigo and Balance Disorders, Ludwig Maximilians University, Munich, Germany, [2]Institute of Neuroradiology, University Hospital, Ludwig Maximilians University, Munich, Germany

Background: There are many causes of episodes of vertigo and very few causes of episodes of changes in taste, and the combination of the two is very rare. Here, we describe a patient with recurrent short episodes of vertigo in combination with simultaneous episodes of recurrent paroxysmal dysgeusia and altered feeling on the left side of face. The symptoms were caused by compression of the vestibulocochlear nerve and the facial nerve due to dolichoectasia of the basilar artery.

Methods: The patient was diagnosed in our routine clinical practice and underwent a complete neurological and neuro-otological examination, including video head impulse test, caloric irrigation, ocular and cervical vestibular evoked myogenic potentials, acoustic-evoked potentials, neuro-orthoptic examination, cranial MRI, and MR angiography. The patient was seen twice for follow-up.

Case: A 71-year-old patient primarily presented with a 2-year history of recurrent short episodes of spinning vertigo. Each of the episodes began with an altered feeling on the left side of the face, followed by a bitter taste on the left half of the tongue, and subsequently vertigo lasting for up to 15 s. The frequency of the attacks was high: up to 80 times per day. Laboratory tests revealed signs of a peripheral vestibular deficit on the left side. There were no signs of sensory or motor deficits or of altered taste between the episodes. An MRI of the brain showed an elongated basilar artery leading to an indentation of the facial and vestibulocochlear nerves on the left side.

Conclusion: We propose a neurovascular compression in the proximal part of two cranial nerves because of pulsatile compression by the elongated basilar artery with ephatic discharges as the cause of the recurrent episodes. Consistent with the theory of ephatic discharges, treatment with the sodium channel blocker lacosamide for over six months with a final dosage of 200 mg per day p.o. led to a significant reduction of the attack frequency and intensity. This treatment option with a sodium channel blocker should therefore not only be considered in vestibular paroxysmia but also in cases of paroxysmal dysgeusia.

KEYWORDS

vertigo, basilar artery aneurysm, vestibular paroxysmia, case report, dysgeusia, dolichoectasia

Introduction

There are a several common causes of changes in taste, including chemotherapy or infections, but paroxysmal dysgeusia has rarely been described (1). This case report describes a combination of vestibular, sensory, and gustatory symptoms due to compression of two cranial nerves because of dolichoectasia of the basilar artery. Recurrent short oligosymptomatic episodes of vertigo are also rare and are the leading symptom of vestibular paroxysmia (2), most often caused by neurovascular compression.

Case description

A 71-year-old patient presented with a 2-year history of recurrent very short episodes of spinning vertigo. Each of the episodes started with an altered feeling on the left side of the face, followed by a bitter taste on the left half of the tongue, and subsequently vertigo lasting for up to 10 to 15 s. He had a high frequency of attacks of up to 80 times per day.

The patient was seen in our routine clinical practice in the neurological outpatient clinic of LMU Munich. He underwent a complete neurological, neuro-otological, and neuro-ophthalmological examination, including video head impulse test, caloric irrigation, ocular- and vestibular-evoked myogenic potentials, acoustic-evoked potentials, neuro-orthoptic examination, cranial MRI, and MR angiography. The patient was seen twice for follow-up: after a treatment period of 6 months and after 4 years without medication.

Diagnostic assessment

The neurological examination revealed horizontal head-shaking nystagmus to the right. There were no signs of persisting sensory or motor deficits or of a taste deficit between the attacks. The video head impulse test showed a decreased gain of the VOR (gain on the left: 0.54, right: 0.83) and the caloric testing reduced excitability on the left side (mean peak slow phase velocity on the left with cold water 6.1°/s, with warm water 4.7°/s, on the right with cold water 13.2°/s, and with warm water 21.3°/s; side difference 52%). The amplitudes of the ocular vestibular-evoked myogenic potentials were reduced on the left side (p1-n1 amplitude: left 3.7μV, right 5.4 μV), as were the amplitudes of the cervical vestibular-evoked myogenic potentials (p1-n1 amplitude: left 74 μV, right 102 μV) (for details please refer to Supplementary Figure 1). The acoustic-evoked potentials were normal.

The MRI of the brain showed an elongated basilar artery leading to an indentation of the facial and vestibulocochlear nerves on the left side (Figure 1). On the MRI, no contact between the elongated basilar artery and the trigeminal and glossopharyngeal nerves was seen. There was also no evidence of brainstem edema, and no macroangiopathy or stenosis of the neck vessels was detectable on ultrasound.

The treatment with initially lacosamide 50 mg in the evening and later 200 mg per day p.o. led to a significant and stable reduction in the attack intensity and frequency from 80 to 1–2 attacks per day over nearly 5 months. The medication was stopped after the follow-up visit after 6 months at the request of the patient.

The follow-up visit after 4 years revealed 5–10 attacks per day without medication. The video head impulse test during the follow-up after 4 years still showed a decreased gain of the VOR (left: 0.71, right: 1.09) and caloric testing progressive reduced excitability on the left side (mean peak slow phase velocity on the left with cold water 2.8°/s, with warm water 2.3°/s, on the right with cold water 20.8°/s, and with warm water 9.2°/s; side difference 71%). The amplitudes of the ocular vestibular-evoked myogenic potentials were low on both sides (p1-n1 amplitude: left 1.1 μV, right 1.7 μV), and the cervical vestibular-evoked myogenic potentials were reduced on the left side (p1-n1 amplitude: left 70 μV, right 187 μV) (for details please refer to Supplementary Figure 2).

Discussion/Conclusion

Basilar artery dolichoectasia has a prevalence of about 0.8 to 4% (3), with higher values in older men, as in this case. Intracranial arterial dolichoectasia is well-known in patients with stroke, with an incidence of up to 17% in patients with posterior circulation stroke and over 45 years of age (4). A dolichoectatic artery can also lead to compression of cranial nerves with well documented case reports of hemifacial spasm (5), trigeminal neuralgia (6) or vestibular paroxysmia (7) or a combination of several symptoms. For instance, there are patients who have, in addition to recurrent episodes of vertigo, other neurological symptoms and signs such as facial hemispasm (8, 9) due to combined irritation of cranial nerves VIII and VII in the meatus acusticus internus where both nerves lie close to each other. There is also a description of the combination of trigeminal neuralgia and facial hemispasm (10).

Here, we describe an evidently very rare triad of unilateral facial sensory, gustatory, and vestibular symptoms due to compression of two cranial nerves: the facial and the vestibulocochlear nerves.

First, the unilaterally impaired sensation in the face is well-known in patients with prior isolated facial nerve dysfunction, as in Bell's palsy (11, 12); this is probably due to impairment of visceral efferent fibers of the facial nerve. Another possible explanation for the sensory symptoms in facial nerve palsy is impaired processing of the facial somatosensory information (11).

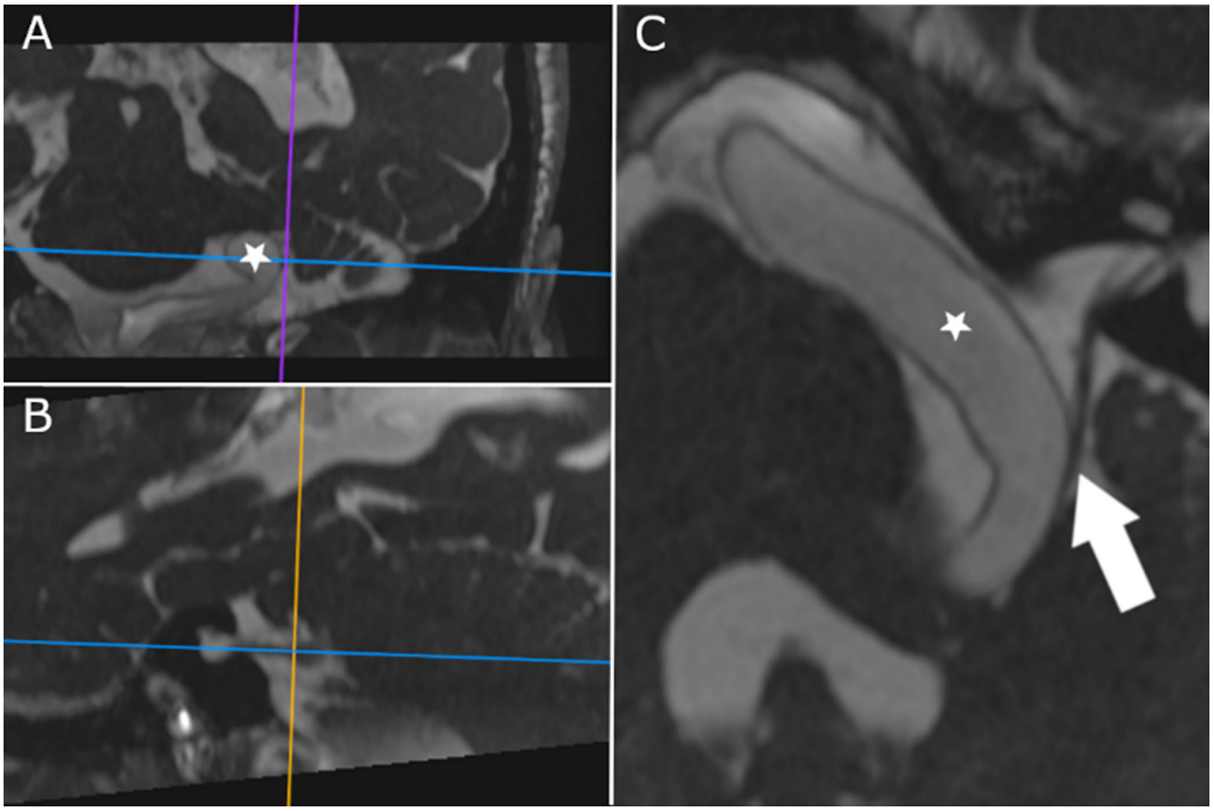

FIGURE 1
CISS-MRI in oblique axis reconstructed along the cisternal course of the vestibulocochlear and facial nerves (the horizontal line in **(A,B)** depicts the axis of **(C)**; vertical lines delineate the axis of the other planes, **(A,B)**, respectively; lines are centered on contact point of the vestibulocochlear nerve and the basilar artery). The dilated and elongated basilar artery (star) displaces the nerves, and direct contact is shown (arrow).

Second, the gustatory symptoms can be explained by an affection of the visceral afferent fibers of the facial nerve. These fibers rise from the ipsilateral nucleus tractus solitarius and reach the anterior two-thirds of the tongue via the chorda tympani and the lingual nerve. In this case, this leads to altered and bitter taste. Since these visceral fibers are un-myelinated and motor fibers are myelinated, this may explain why the patient had no facial hemispasm.

Third, the vestibular symptoms are similar to those of vestibular paroxysmia.

In our patient, the MRI showed no brainstem edema or compression of other cranial nerves as alternative explanations for the patient's symptoms.

Because of the short episodes with a duration of less than 1 min and a stereotypical phenomenology, we propose the ephatic discharges as the cause for the above-described symptoms, similar to other neurovascular compression syndromes of cranial nerves. Pulsatile compression of the nerves by an elongated basilar artery leads to pathological ephatic transmission between neighboring axons of the affected nerves.

Sodium channel blockers, and especially carbamazepine, are well-known treatment options for cranial neuralgias and may stabilize the cell membrane (13). For vestibular paroxysmia, a placebo-controlled trial showed a benefit of oxcarbazepine (14). Lacosamide is a third-generation antiepileptic drug and selectively enhances slow inactivation of voltage-gated sodium channels. Studies on patients with epilepsy showed that lacosamide is well-tolerated (15) and has a better tolerability profile than carbamazepine (16), leading to less withdrawal due to side effects. Consistent with the theory on ephatic discharges, treatment with the sodium-channel blocker lacosamide led to a significant reduction of the attack frequency and intensity in our patient. Lacosamide is therefore a well-tolerated treatment option for patients with cranial nerve compression syndromes, especially vestibular paroxysmia (17), trigeminal neuralgia, or their combination, as shown in this case.

Take-away lesson from the case

We present a patient with a unique triad of recurrent short episodes of vestibular, unilateral facial sensory, and gustatory symptoms due to compression of the facial and vestibulocochlear nerves by an elongated basilar artery. Consistent with the theory on ephatic discharges, treatment with lacosamide 200 mg per day p.o. led to a significant reduction of the attack frequency and intensity in our patient. Based on this case report, sodium channel blockers can also be a new treatment option for patients with paroxysmal dysgeusia.

Data availability statement

The raw data supporting the conclusions of this article will be made available by the authors, without undue reservation.

Ethics statement

Ethical review and approval was not required for the study on human participants in accordance with the local legislation and institutional requirements. The patients/participants provided their written informed consent to participate in this study. Written informed consent was obtained from the individual(s) for the publication of any potentially identifiable images or data included in this article.

Author contributions

NG: analysis and interpretation of the data and drafting/revision of the manuscript. CB: analysis and interpretation of the data, figure design, and critical revision of the manuscript for intellectual content. MS: examination, diagnosis and follow-up of the patient, concept, analysis and interpretation of the data, and critical revision of the manuscript for intellectual content. All authors contributed to the article and approved the submitted version.

Acknowledgments

We thank Katie Göttlinger for copyediting this manuscript.

Conflict of interest

Author MS is Joint Chief Editor of the Journal of Neurology, Editor in Chief of Frontiers of Neuro-otology, and Section Editor of F1000. He has received speaker's honoraria from Abbott, Auris Medical, Biogen, Eisai, Grünenthal, GSK, Henning Pharma, Interacoustics, J&J, MSD, NeuroUpdate, Otometrics, Pierre-Fabre, TEVA, UCB, and Viatris. He receives support for clinical studies from Decibel, USA, Cure within Reach, USA and Heel, Germany. He distributes "M-glasses" and "Positional vertigo App". He acts as a consultant for Abbott, Auris Medical, Heel, IntraBio, Sensorion, and Vertify.

The remaining authors declare that the research was conducted in the absence of any commercial or financial relationships that could be construed as a potential conflict of interest.

Publisher's note

Supplementary material

The Supplementary Material for this article can be found online at: https://www.frontiersin.org/articles/10.3389/fneur.2022.1028597/full#supplementary-material

SUPPLEMENTARY FIGURE 1
Examination results, first visit in 2018. **(A)** Caloric testing showed reduced excitability on the left side (mean peak slow phase velocity on the left with cold water 6.1°/s, with warm water 4.7°/s, on the right with cold water 13.2°/s, and with warm water 21.3°/s; side difference 52%). **(B)** Video head impulse test showed decreased gain of the VOR (gain on the left: 0.54, right: 0.83) **(C)** Amplitudes of the ocular vestibular-evoked myogenic potentials were reduced on the left side (p1-n1 amplitude: left 3.7 μV, right 5.4 μV). **(D)** Amplitudes of the cervical vestibular-evoked myogenic potentials were reduced on the left side (p1-n1 amplitude: left 74 μV, right 102 μV).

SUPPLEMENTARY FIGURE 2
Examination results, follow-up in 2022. **(A)** Caloric testing during the follow-up after 4 years showed progressive reduced excitability on the left side (mean peak slow phase velocity on the left with cold water 2.8°/s, with warm water 2.3°/s, on the right with cold water 20.8°/s, and with warm water 9.2°/s; side difference 71%). **(B)** Video head impulse test during the follow-up after 4 years still showed a decreased gain of the VOR (left:0.71, right: 1.09). **(C)** Amplitudes of the ocular vestibular-evoked myogenic potentials were low on both sides (p1-n1 amplitude: left 1.1 μV, right 1.7 μV). **(D)** Amplitudes of the cervical vestibular-evoked myogenic potentials were reduced on the left side (p1-n1 amplitude: left 70 μV, right 187 μV).

References

1. Jafari A, Alaee A, Ghods K. The etiologies and considerations of dysgeusia: A review of literature. *J Oral Biosci.* (2021) 63:319–26. doi: 10.1016/j.job.2021.08.006

2. Strupp M, Lopez-Escamez JA, Kim JS, Straumann D, Jen JC, Carey J, et al. Vestibular paroxysmia: Diagnostic criteria. *J Vestib Res.* (2016) 26:409–15. doi: 10.3233/VES-160589

3. Del Brutto VJ, Ortiz JG, Biller J. Intracranial arterial dolichoectasia. *Front Neurol.* (2017) 8:344. doi: 10.3389/fneur.2017.00344

4. Bogousslavsky J, Regli F, Maeder P, Meuli R, Nader J. The etiology of posterior circulation infarcts: a prospective study using magnetic resonance imaging and magnetic resonance angiography. *Neurology.* (1993) 43:1528–33. doi: 10.1212/WNL.43.8.1528

5. Munich SA, Morcos JJ. "Macrovascular" decompression of dolichoectatic vertebral artery causing hemifacial spasm using goretex sling: 2-dimensional operative video. *Operat Neurosurg.* (2019) 16:267–8. doi: 10.1093/ons/opy111

6. Honey CM, Kaufmann AM. Trigeminal Neuralgia due to Vertebrobasilar Artery Compression. *World Neurosurg.* (2018) 118:e155–e60. doi: 10.1016/j.wneu.2018.06.145

7. Pico F, Labreuche J, Amarenco P. Pathophysiology, presentation, prognosis, and management of intracranial arterial dolichoectasia. *Lancet Neurol.* (2015) 14:833–45. doi: 10.1016/S1474-4422(15)00089-7

8. Straube A, Büttner U, Brandt T. Recurrent attacks with skew deviation, torsional nystagmus, and contraction of the left frontalis muscle. *Neurology.* (1994) 44:177–8. doi: 10.1212/WNL.44.1.177

9. Silva-Hernández L, Silva-Hernández M, Gutiérrez-Viedma A, Yus M, Cuadrado ML. Hemifacial spasm and vestibular paroxysmia: Co-presence of two neurovascular compression syndromes in a patient. *Neurologia.* (2019) 34:131–3. doi: 10.1016/j.nrleng.2018.09.002

10. Han J, Wang T, Xie Y, Cao D, Kang Z, Song X. Successive occurrence of vertebrobasilar dolichectasia induced trigeminal neuralgia, vestibular paroxysmia and hemifacial spasm: A case report. *Medicine.* (2018) 97:e11192. doi: 10.1097/MD.0000000000011192

11. Cárdenas Palacio CA, Múnera Galarza FA. Cutaneous sensibility changes in bell's palsy patients. *Otolaryngol Head Neck Surg.* (2017) 156:828–33. doi: 10.1177/0194599817690107

12. Vanopdenbosch LJ, Verhoeven K, Casselman JW. Bell's palsy with ipsilateral numbness. *J Neurol Neurosurg Psychiatry.* (2005) 76:1017–8. doi: 10.1136/jnnp.2004.043059

13. Peterson-Houle GM, AbdelFattah MR, Padilla M, Enciso R. Efficacy of medications in adult patients with trigeminal neuralgia compared to placebo intervention: a systematic review with meta-analyses. *J Dental Anesthesia Pain Med.* (2021) 21:379–96. doi: 10.17245/jdapm.2021.21.5.379

14. Bayer O, Brémová T, Strupp M, Hüfner K. A randomized double-blind, placebo-controlled, cross-over trial (Vestparoxy) of the treatment of vestibular paroxysmia with oxcarbazepine. *J Neurol.* (2018) 265:291–8. doi: 10.1007/s00415-017-8682-x

15. Li J, Sun M, Wang X. The adverse-effect profile of lacosamide. *Expert Opin Drug Saf.* (2020) 19:131–8. doi: 10.1080/14740338.2020.1713089

16. Baulac M, Rosenow F, Toledo M, Terada K, Li T, De Backer M, et al. Efficacy, safety, and tolerability of lacosamide monotherapy versus controlled-release carbamazepine in patients with newly diagnosed epilepsy: a phase 3, randomised, double-blind, non-inferiority trial. *Lancet Neurol.* (2017) 16:43–54. doi: 10.1016/S1474-4422(16)30292-7

17. Strupp M, Elger C, Goldschagg N. Treatment of vestibular paroxysmia with lacosamide. *Neurol Clin Practice.* (2019) 9:539–41. doi: 10.1212/CPJ.0000000000000610

frontiers | Frontiers in Neurology

TYPE Case Report
PUBLISHED 10 October 2022
DOI 10.3389/fneur.2022.982191

OPEN ACCESS

EDITED BY
Michael Strupp,
Ludwig Maximilian University of Munich, Germany

REVIEWED BY
Anita Bhandari,
NeuroEquilibrium Diagnostic Systems Pvt Ltd, India
Giacinto Asprella Libonati,
Simple Departmental Operative Unit of Vestibology and Integrated Management of Otolaryngology Activities, Italy

*CORRESPONDENCE
Janet O. Helminski
janet.helminski@rosalindfranklin.edu

SPECIALTY SECTION
This article was submitted to Neuro-Otology, a section of the journal Frontiers in Neurology

RECEIVED 30 June 2022
ACCEPTED 26 July 2022
PUBLISHED 10 October 2022

CITATION
Helminski JO (2022) Case report: Atypical patterns of nystagmus suggest posterior canal cupulolithiasis and short-arm canalithiasis. *Front. Neurol.* 13:982191. doi: 10.3389/fneur.2022.982191

Case report: Atypical patterns of nystagmus suggest posterior canal cupulolithiasis and short-arm canalithiasis

Janet O. Helminski*

Department of Physical Therapy, Rosalind Franklin University, North Chicago, IL, United States

Background: Atypical posterior canal (PC) positional nystagmus may be due to the changes in cupular response dynamics from cupulolithiasis (cu), canalithiasis of the short arm (ca-sa), or a partial/complete obstruction—jam. Factors that change the dynamics are the position of the head in the pitch plane, individual variability in the location of the PC attachment to the utricle and the position of the cupula within the ampulla, and the location of debris within the short arm and on the cupula. The clinical presentation of PC-BPPV-cu is DBN with torsion towards the contralateral side in the DH positions and SHHP or no nystagmus in the ipsilateral DH position and no nystagmus upon return to sitting from each position. The clinical presentation of PC-BPPV-ca-sa is no nystagmus in the DH position and upbeat nystagmus (UBN) with torsion lateralized to the involved side upon return to sitting from each position.

Case description: A 68-year-old woman, diagnosed with BPPV, presented with DBN associated with vertigo in both DH positions and without nystagmus or symptoms on sitting up. In the straight head hanging position (SHHP), the findings of a transient burst of UBN with left torsion associated with vertigo suggested ipsicanal conversion from the left PC-BPPV-cu to canalithiasis. Treatment included a modified canalith repositioning procedure (CRP), which resulted in complete resolution. BPPV recurred 17 days later. Clinical presentation of BPPV included no nystagmus/symptoms in both the contralateral DH position and SHHP, DBN in the ipsilateral DH position without symptoms, and UBN with left torsion associated with severe truncal retropulsion and nausea on sitting up from provoking position. The findings suggested the left PC-BPPV-cu-sa and PC-BPPV-ca-sa. Treatment included neck extension, a modified CRP, and demi-Semont before complete resolution.

Conclusion: An understanding of the biomechanics of the vestibular system is necessary to differentially diagnose atypical PC-BPPV. DH test (DHT) findings suggest that PC-BPPV-cu presents with DBN or no nystagmus in one or two DH positions and sometimes SHHP and without nystagmus or no reversal/reversal of nystagmus on sitting up. The findings suggest PC-BPPV-ca-sa has no nystagmus in DH positions or DBN in the ipsilateral DH position and UBN with torsion lateralized to the involved side on sitting up.

KEYWORDS

benign paroxysmal positional vertigo, BPPV, posterior canal, downbeat nystagmus, case report, cupulolithiasis, short arm canalithiasis, positional nystagmus

Introduction

Benign paroxysmal positional vertigo (BPPV) presents as repeated episodes of positional vertigo that usually last <1 min. BPPV is the most common cause of vertigo and accounts for 17–42% of all cases of vertigo in adults (1–3). Of all cases of BPPV (n = 491), unilateral posterior canal (PC) BPPV and anterior canal (AC) BPPV have the highest and lowest frequency, respectively, accounting for 39 and 4% due to the canal position on the labyrinth (4, 5). BPPV is a mechanical disorder of the inner ear caused by otolithic debris that has separated from the utricular maculae and displaced into the canal–canalithiasis (6) or attached to the cupula–cupulolithiasis (7). With canalithiasis, debris may be located within the short or long arm of the canal (8) (Figure 1A). Debris may be adjacent or not adhere to the cupula in short-arm canalithiasis, changing cupular response dynamics (8–11). Debris may adhere to the cupula on the side of the utricle in cupulolithiasis—short-arm (11) or long-arm cupulolithiasis (10).

The diagnosis of BPPV is based on the history of positional vertigo (12) and the findings on both the Dix-Hallpike test (DHT) (12) and positional maneuvers. The DHT is used to examine the vertical canals. The pattern of nystagmus or no nystagmus in the initial position, in the provoking positions, and on return to the sitting position is crucial to hypothesize the location and direction of movement of the debris within the canal. In the initial sitting position, the clinician rotates the individual's head 45° to the side to be examined, the plane of the PC and AC being vertical. Next, the canal to be tested is rotated within the vertical plane to the provoking position of DHT (DH position). With the head turned 45°, the individual is brought to the supine recumbent position and the head is extended ∼20° (12) or 40° (13) below the earth horizontal for a total of ∼110–130° of movement in the pitch plane. In the provoking position, with PC-BPPV-ca-la, the otolithic debris settles in the lowest position within the canal, inducing the flow of endolymph in the direction of moving particles and causing nystagmus. If the flow of endolymph moves away from the ampulla (ampullofugal), the afferent is excited and moves towards the ampulla (ampullopetal) the afferent is inhibited. Upon excitation the observed peripheral positional nystagmus is upbeat nystagmus (UBN) towards the forehead) with torsion lateralized to the involved side (the superior pole of both eyes) in the head-referenced coordinate system. When the head is returned to upright, the debris settles toward the ampulla, reversing the flow of endolymph, inhibiting the afferent, and generating a peripheral positional downbeat nystagmus (DBN) (toward the chin) with torsion lateralized to the uninvolved side.

In DH positions and the straight head hanging position (SHHP), the clinician may observe a peripheral DBN, with or without torsion suggesting the activation of one of the vertical canals of the coplanar pair, either AC excitation of the dependent PC inhibition (14, 15). AC excitation is characterized by a DBN with or without torsion lateralized to the involved side that is always observed in the SHHP and sometimes in one or both DH positions due to the orientation of the initial ampullary segment relative to the utricle (16). On sitting up, the inhibition of the AC afferent should generate a reversal of nystagmus. However, there is no reversal of nystagmus or no nystagmus occurs (17). Cambi et al. (14) were the first to suggest that a peripheral and positional DBN may be due to PC inhibition. It was hypothesized that DBN was caused by limited movement of debris to the non-ampullary or distal segment of the PC, referred to as "apogeotropic PC-BPPV" (15, 18), or to the periampullary or proximal segment of the PC, referred to as "sitting up vertigo" (19) due to an obstruction of the PC lumen. "Sitting up vertigo" was associated with or without DBN with torsion lateralized toward the uninvolved side in the DH position or SHHP and UBN with torsion lateralized to the involved side upon return to upright. These obstructions were thought to be due to large fragments of otolithic debris or constriction of the PC lumen (15, 18, 19).

However, emerging evidence suggests that a peripheral DBN observed in the DH position and SHHP may be due to a change in the dynamics of the cupular response because of PC-BPPV cupulolithiasis (PC-BPPV-cu) (8, 9, 20) and PC-BPPV canalithiasis of the short arm (PC-BPPV-ca-sa) (11). It was originally postulated that PC-BPPV-cu, in the ipsilateral DH position (involved side), evoked a gradual-onset, low-amplitude, persistent [>1 min (21)] UBN with torsion toward the involved ear (7, 22). However, the degree of neck extension in the DH position (8, 10), the natural variability of the orientation of the cupula within the population (23, 24), and the location of the debris within the short arm and on the cupula were not considered. These factors influence the patterns of nystagmus and the success of treatment for PC-BPPV-cu (23). In the DH position, if the short arm is connected more superiorly or if the DH position is less pronounced, the head extends ∼20° below the earth horizontal, nystagmus may not be observed because the cupula axis is oriented in the earth vertical, and no cupula deflection occurs (Figures 1A,B) (8, 11, 22). In the DH position, if the short arm is connected more inferiorly and/or if the DH position is more pronounced, the head extends ∼30–40° below the earth horizontal, the afferent is inhibited and a constant, low-amplitude DBN with or without torsion toward the unaffected side will be observed (Figure 1C) (8, 11) in the contralateral DH position (uninvolved side) and sometimes in the ipsilateral DH position and SHHP (17).

There are no practical clinical guidelines for the management of PC-BPPV-cu, PC-BPPV-ca-sa, and AC-BPPV canalithiasis (12). The purpose of this case report is to describe the clinical presentation, diagnostic process, and particle repositioning maneuvers for an individual who presented with two atypical patterns of positional nystagmus, suggesting a change in PC cupular response dynamics. The first variant was primarily DBN in DH positions with no nystagmus

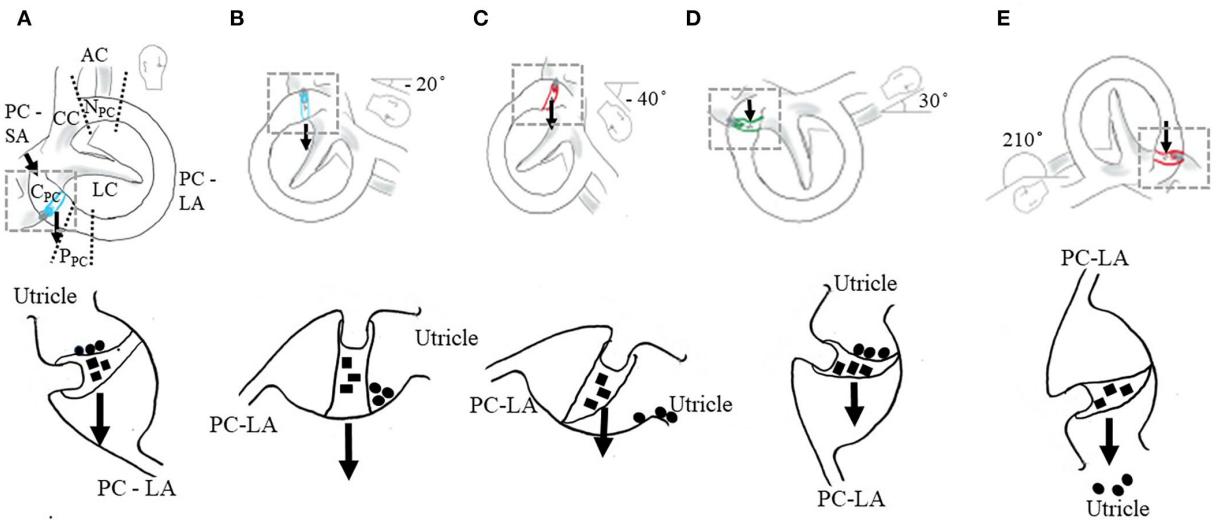

FIGURE 1
Positional testing (top row) and proposed mechanisms of atypical nystagmus from the PC. The location of debris within canal–cupulolithiasis (■) and canalithiasis of the short arm (•) (bottom row). Illustrated for the right membranous labyrinth. AC, anterior canal; LC, lateral canal; PC, posterior canal; CC, common crus; N_{PC}, non-ampullary segment of PC (distal); P_{PC}, periampullary segment of PC (proximal); and C_{PC}, cupula of PC. The area of the PC between the CC and ampulla is the long arm (LA) and between the ampulla and the utricle is the short arm (SA). The PC long arm has two regions, the periampullary segment—proximal segment near the ampulla and the non-ampullary segment—distal segment near the common crus. Arrow indicates the line of gravity. **(A–C)** Right PC cupulolithiasis. The amount of head extension and flexion in the provoking position will vary the orientation of the axis of the PC cupula relative to the earth horizontal varying the amount and direction of nystagmus. **(A)** Initial position of the Dix-Hallpike test (DHT). In the sitting position, 45° neck rotation toward right (top row). No deflection of cupula. No nystagmus or symptoms (bottom row). **(B)** Head right DH position—recumbent position with the neck rotated 45° toward right and extended 20° below the earth horizontal (top row). Neutral position of ipsilateral PC cupula, the axis of the cupula is oriented in the earth vertical resulting in no nystagmus (bottom row). **(C)** Head right DH position with the neck extended 40° from the earth horizontal (top row). In the pronounced provoking position, the weight of the cupula causes the deflection of the cupula toward the utricle, inhibiting the PC afferent generating a constant, low-amplitude downbeat nystagmus (DBN) with or without torsion lateralized to the uninvolved side (bottom row). **(D,E)** Two earth horizontal positions for the right PC cupula oriented 180° to each other. **(D)** The right half Hallpike (HH) position—recumbent position with the neck rotated 45° toward right and flexed 30° from the earth horizontal. The right PC cupula axis is in the earth horizontal (top row). A weighted cupula causes a maximum deflection of the cupula toward the long arm resulting in the excitation of PC afferent generating an upbeat nystagmus (UBN) with torsion lateralized to the involved side (bottom row). **(E)** Inverted release (IR) position for the right PC cupula. Left side-lying position with the neck flexed 20° and rotated 45° down (top row). A weighted cupula causes a maximum deflection of the cupula toward the utricle, resulting in the inhibition of PC afferent generating a DBN with or without torsion lateralized to the uninvolved side (bottom row).

on sitting, suggesting PC-BPPV-cu. Ipsilateral canal conversion from DBN to UBN during the SHHP suggested PC-BPPV-cu on the long-arm side. The second variant was slight DBN in the DH position due to PC-BPPV-cu on the short-arm side and primarily UBN on sitting, suggesting PC-BPPV-ca-sa. This case met all institutional health insurance, portability, and accountability act requirements, and the approval was obtained from Midwestern University's Institute Review Board.

Patient information

A woman aged 68 years experienced spontaneous episodic vertigo triggered with changes in the head position relative to gravity. She was referred for the management of BPPV by Midwestern University's Multispecialty Clinic and was evaluated 12 days after onset. Neurootologic history included intermittent sensation of pressure, tinnitus, and hyperacoustics of the left ear. She had no significant medical or family history.

Clinical findings

Clinical neurologic (25) and oculomotor examinations (26) were normal except for mild balance impairment. The clinician observed a slight spontaneous right beat nystagmus in all positions of gaze without fixation. The use of videonystagmography (VNG) (Chartr, Otometrics, Denmark) during positional testing and treatment prevented visual fixation and the suppression of nystagmus. Lab testing, vestibular function testing, and radiographic imaging were not performed. See the timeline for the first and second episodes of care (Table 1).

TABLE 1 Timeline for first and second episode of care including clinical findings, diagnostic assessment, and therapeutic intervention.

Timeline	First variant PC-BPPV-cu-la		Second variant PC-BPPV-cu-sa and PC-BPPV-ca-sa		
	Day 12	**Day 19**	**Day 32**	**Day 33**	**Day 34**
Positional testing					
DHT—head R					
• Direction	• **Persistent DBN**	• None	• None	• Persistent DBN	• None
• Symptoms	• **Vertigo**	• None	• None	• None	• None
Return to upright					
• Direction	• RBN	• None	• **Transient UBN, LT**	• None	• None
• Symptoms	• None	• None	• **Vertigo, truncal retropulsion**	• Imbalance, nausea	• None
DHT—head L					
• Direction	• **Persistent DBN**	• None	• DBN (8 s) to persistent LBN	• Persistent LBN	• None
• Symptoms	• **Vertigo**	• None	• None	• Slight imbalance	• None
Return to upright					
• Direction	• RBN	• None	• **Transient UBN, LT**	• Transient UBN	• None
• Symptoms	• None	• None	• **Vertigo, truncal retropulsion**	• Imbalance, nausea	• None
SHHP					
• Direction	• **Ipsicanal conversion, transient UBN, LT**	• None	• None	• Persistent DBN	• None
• Symptoms	• Vertigo	• None	• None	• None	• None
Return to upright					
• Direction	• Transient DBN, RT	• None	• **Transient UBN, LT**	• None	• None
• Symptoms	• Vertigo	• None	• **Vertigo, truncal retropulsion**	• Slight imbalance	• None
Diagnosis/mechanism	L PC-BPPV-cu-la Ipsicanal conversion to L PC-BPPV-ca-la	BPPV resolved	L PC-BPPV-ca-sa	L PC-BPPV-cu-sa and -ca-sa	BPPV resolved
Therapeutic intervention	• L CRP x3 • Activity restriction	• Activity restriction • Vitamin D levels	• Neck Extension x3 • CRP—x1 • Activity restriction	• Neck Extension x3. • CRP—x1 • Demi-semont x3 • Activity restriction	

PC-BPPV, posterior canal benign paroxysmal positional vertigo; ca, canalithiasis; cu, cupulolithiasis; la, long arm; sa, short arm; DBN, downbeat nystagmus; UBN, upbeat nystagmus; T, torsion; R, right; L, left; LBN, left beat nystagmus; RBN, right beat nystagmus; CRP, canalith repositioning procedure. Bold values key findings.

First variant: Peripheral DBN DH positions

Diagnostic assessment of the first variant: Peripheral DBN provoking positions

In the first episode of care, clinicians observed in both DH positions with the head positioned ∼40° below the earth horizontal (13) a DBN (no torsion) with a short latency of onset, long duration (>1 min), and crescendo–decrescendo velocity profile associated with symptoms of vertigo. On return to upright from both DH positions, the clinician observed a right beat nystagmus and the patient reported no symptoms. In the SHHP, there was a 60 s latency until the onset of a transient burst of UBN with left torsion, associated with an intense sensation of vertigo. On return to sitting, the clinician observed a burst of DBN with right torsion associated with vertigo (Supplementary Video S1).

Interpretation of the first variant: Peripheral DBN provoking positions

Central positional vertigo is associated with neurologic findings and, in most cases, impaired pursuit (27). In this case, the history and findings of DBN in both DH positions and the absence of associated neurologic signs suggested vertical canal involvement—either the inhibition of PC or the excitation of AC. Without fixation, the patient had a mild spontaneous right-beating nystagmus (RBN) that increased in intensity without symptoms on return to upright from DH positions. The patient had a history of left neurootologic involvement, which might

have resulted in a peripheral RBN or had a pseudo-spontaneous nystagmus. The persistence of DBN in DH positions and the absence of nystagmus in the SHHP suggests PC involvement. In the SHHP, DBN is always observed with AC-BPPV and sometimes with PC involvement (17). With canalithiasis of the AC, the duration of attacks is <1 min (21, 28). Initially, in the SHHP, the clinician did not observe any nystagmus, suggesting PC-BPPV. At 60 s, the transient burst of UBN with left torsion suggested the excitation of primary afferents to the left PC and an ipsicanal switch, conversion of PC-BPPV-cu-la to PC-BPPV-ca-la (8). The nystagmus changed the direction from a DBN in DH positions to an UBN in SHHP. Left torsion with UBN suggested left ear involvement. On sitting up, DBN with right torsion—suggested the inhibition of the left PC afferent associated with PC-BPPV-ca-la. Based on the history and the ipsicanal switch on positional testing, no further vestibular function testing or radiographic imaging was indicated. The patient's initial symptoms were consistent with those of atypical BPPV involving the PC (8). If she did not show any improvement in or the resolution of symptoms after two to three sessions of particle repositioning maneuver, she would be referred for further diagnostic testing to rule out central involvement (12).

Therapeutic intervention of the first variant: Peripheral DBN provoking positions

Typical left PC-BPPV was treated with three cycles of a modified canalith repositioning procedure (CRP) (29). In the first cycle, an orthotropic UBN with left torsion was observed in the first and second positions, mild DBN in the right side lying position and no positional nystagmus on return to upright. Activity restrictions were provided due to the complexity of BPPV (12) and were consistent with those provided to patients with intractable BPPV (30). Restrictions included sleeping with the head of the bed elevated to 40°, sleeping on the back or right side, and limiting up/down head movements for 1 week (30).

Follow-up and outcomes of the first variant: Peripheral DBN provoking positions

In a 1-week follow-up, the patient reported no symptoms of vertigo with daily routine. Positional testing was negative, suggesting that left PC-BPPV had resolved. The patient was relieved that BPPV was resolved and the concern was that it would recur. Activity restrictions were continued, and vitamin D levels were reviewed and found to be within the recommended range (31) to minimize the risk of recurrence of BPPV.

Second variant recurrence: UBN sitting up

Diagnostic assessment—second variant recurrence—first session UBN sitting up

Approximately 17 days following the resolution of atypical PC-BPPV, the patient rolled over in the bed and experienced the sensation of vertigo. Clinical examination findings 3 days following the recurrence suggested no associated neurologic signs. The primary complaint was imbalance and nausea on sitting up and with walking. She reported falling while ascending a riser without a rail. Positional testing was performed with VNG (without fixation). With the right DH position and SHHP, the clinician observed no nystagmus, and the patient reported no symptoms. With the left DH position, there was a mild DBN for 8 s followed by an LBN and no symptoms. On return to upright from each position, the clinician observed a transient burst of UBN with left torsion associated with a strong sitting up vertigo and truncal retropulsion (Supplementary Video S2).

Interpretation—recurrence of the second variant—first session UBN sitting up

The findings suggest PC-BPPV-cu-sa and PC-BPPV-ca-sa. Nystagmus or symptoms are absent in the contralateral DH position and SHHP, but there is a mild DBN in the ipsilateral (left) DH position, which suggests left PC-BPPV-cu-sa. Due to the orientation of the axis of the cupula relative to the earth horizontal, an inhibitory response was generated resulting in DBN. In 19% of patients, following successful particle repositioning maneuvers, a DBN in the ipsilateral DH position suggests the movement of otolithic debris from the long arm to the short arm during the maneuver (11). UBN associated with left torsion on return to upright from all positions and without other neurologic signs suggests vertical canal involvement. On sitting up, PC otolith debris moved from the utricle to the cupula, deflecting the cupula away from the utricle causing the excitation of the afferent generating an UBN with associated torsion (11). Left torsion suggests the excitation of the left PC. The findings do not suggest a periampullary jam in the PC lumen (19) [periampullary restricted canalolithiasis model (32)] based on the history of recent successful treatment of the left PC-BPPV and no nystagmus observed in the contralateral DH position. It is proposed that, with a periampullary jam, an increase in DBN with torsional nystagmus is observed in the contralateral DH position and no nystagmus in the ipsilateral DH position (19). In this case, no nystagmus was observed in the contralateral DH position and DBN was observed in the ipsilateral position. In the ipsilateral DH position following DBN, an LBN was observed,

which suggests possible debris settlement in the long arm of the LC.

Therapeutic intervention—recurrence of the second variant—first session UBN sitting up

Atypical left PC-BPPV was treated with three cycles of neck extension (33) and a modified CRP (29). The patient was provided with post maneuver activity restrictions. Following the maneuver, the patient reported less intense truncal retropulsion and nausea on sitting up and imbalance on walking. Symptoms gradually resolved over 4 h.

Diagnostic assessment—recurrence of the second variant—second session

The next day, the individual woke up with severe vertigo and imbalance. She was escorted by her husband to the clinic. On examination, the clinician observed a DBN in the contralateral DH position and SHHP and a LBN in the ipsilateral DH position. On return to upright from the contralateral provoking position and SHHP, there was no nystagmus but there was a slight UBN upon return to upright from the ipsilateral provoking position.

Interpretation—evolution of the second variant—second session

Positional test findings suggest the left PC-BPPV-cu-sa. The debris within the short arm may be adherent—PC cupulolithiasis of the short arm or adjacent to the cupula (nonadherent)—PC-ca-sa (11). An inverted release (IR) position (lying on the uninvolved side with the head flexed 20° and rotated 45° downward) would determine if the debris was attached to the cupula. In case of being adjacent to the cupula, no nystagmus would occur because the debris would move from the cupula to the utricle (10). LBN in the SHHP may be due to a pseudo-spontaneous nystagmus from the left lateral canal.

Therapeutic intervention—evolution of the second variant—second session

The patient was treated with neck extension (33) in an attempt to create ipsicanal conversion followed by demi-Semont (18), the final position the same as IR, to remove particles from the cupula on the side of the utricle. The patient were provided with post maneuver activity restrictions, and continued to complain of imbalance and nausea. In the evening, BPPV resolved spontaneously.

Follow-up and outcomes—evolution of the second variant—second session

At a 1-week follow-up, she had no vertigo or imbalance with her daily routine and positional testing was negative. She was grateful to have resolved BPPV but was concerned about its recurrence.

Discussion

This case report describes the clinical presentation of two variants of atypical nystagmus from PC-BPPV due to a change in cupular response dynamics, one from cupulolithiasis with debris on the long-arm side and the other from primarily short arm canalithiasis and cupulolithiasis. The clinical presentation of the first variant from PC-BPPV-cu-la was persistent DBN with torsion lateralized to the uninvolved side, associated with symptoms of vertigo in DH positions and no nystagmus or associated symptoms on return to upright. An ipsicanal conversion occurred from PC-BPPV-cu with debris on the long-arm side to canalithiasis in the long arm. This occurred when the patterns of nystagmus changed from an atypical persistent positional DBN in the DH position to a typical positional transient UBN with torsion lateralized toward the involved side (60 s delay to onset) in the SHHP. This ipsilateral canal conversion supported the mechanism of the first variant as PC-BPPV-cu-la. PC-BPPV was successfully treated with a modified CRP. BPPV recurred 17 days later. Her primary complaint was imbalance and nausea. The second variant was both PC-BPPV-cu-sa and PC-BPPV-ca-sa. The clinical presentation of PC-BPPV-cu-sa was no nystagmus or symptoms in the contralateral DH position and SHHP, and DBN with torsion lateralized to the uninvolved side (duration of 8 s) followed by an RBN in the ipsilateral DH position. A burst of UBN with torsion to the involved side associated with symptoms of imbalance and nausea on return to upright from all provoking positions suggested PC-BPPV-ca-sa. The patient was treated with neck extension and a modified CRP. Symptoms gradually resolved over 4 h. The next morning, the patient awoke with symptoms of imbalance and nausea. The clinical presentation was DBN with torsion away from the involved side in DH positions and SHHP, suggesting PC-BPPV-cu. There was a subtle UBN with torsion toward the involved side on return to upright from the ipsilateral DH position, suggesting PC-BPPV-ca-sa. She was successfully treated with neck extension and demi-Semont maneuver. Symptoms gradually resolved within 4 h.

Emerging evidence suggests that atypical positional DBN from the PC may be due to the changes in the cupular response from cupulolithiasis or short-arm canalithiasis (8, 11, 32). The following factors will change the orientation of the cupula axis with respect to the earth horizontal, influencing the patterns of nystagmus and the success of treatment, especially in the case

of PC-BPPV-cu and PC-BPPV-ca-sa. The ability to position the head in extension may be hindered by cervical or thoracic spine mobility limitations or pain, necessitating modifications to the positions. The examiner may choose to perform a DH position that has less or more pronounced head extension in the supine (Figure 1B) (12) or head extension more pronounced in the supine recumbent position (Figure 1C) (13). If less pronounced, the head is extended ∼20° below the earth horizontal, no nystagmus is observed if the axis of the cupula is oriented in the earth vertical and no cupula deflection occurs (Figures 1A,B) (8, 11, 22). If more pronounced, the head extends ∼30–40° below the earth horizontal, the afferent is inhibited and a constant, low-amplitude DBN with or without torsion towards the uninvolved side will be observed (Figure 1C) (11, 12). The patterns of nystagmus will also be influenced by the orientation of the cupula due to the natural individual variability in the location of PC attachment to the utricle (23) and the position of the cupula within the ampulla (24). In the DH position, if the short arm is connected more superiorly, nystagmus may not be observed because the axis of the cupula is oriented in the earth vertical and no deflection of the cupula occurs (Figures 1A,B) (8, 11). If the short arm is connected more inferiorly, the afferent is inhibited and a constant, low-amplitude DBN with or without torsion toward the unaffected side will be observed (Figure 1C) (8, 11). Lastly, the location of the debris within the short arm (11), the adherence of debris to the cupula on the side of the utricle or long arm, and the proximity of debris to the cupula (adjacent) (11) will influence the patterns of nystagmus and the particle repositioning maneuver performed to successfully treat PC involvement.

When atypical nystagmus from the PC is suspected, additional positional testing should be performed to identify the location of the debris within the canal. The half Hallpike (HH) position and IR position may be used to differentiate between PC-BPPV-cu and PC-BPPV-ca-sa and to also differentiate PC-BPPV-cu from AC-BPPV canalithiasis (10, 21). The cupula is deflected maximally by the gravitational force when the axis of the affected cupula is oriented in the earth horizontal. Two earth horizontal positions oriented at 180° to each other: the HH (recumbent supine position with the head rotated 45° toward the involved side, flexed 30°) (10, 22) and the IR position (lying on the uninvolved side with the neck flexed 20°, rotated 45° downward) (10) (Figures 1D,E). If the vertical canals are involved, in the HH, the direction of nystagmus is UBN with torsion lateralized to the involved side. With the IR, the direction of nystagmus reverses the direction relative to the HH position. If nystagmus is stronger in the HH position, it is generated by the posterior cupula due to the inhibition of the PC and if stronger in the inverse position it is generated by the contralateral anterior cupula due to the excitation of the PC (10). If no nystagmus is observed in the IR, otolithic debris may be adjacent to the cupula within the short arm of the PC—PC-BPPV-ca-sa. Persistent positional DBN in the ipsilateral DH position following a successful particle repositioning maneuver for PC-BPPV may be due to ipsilateral PC-BPPV-cu-sa (11). As a result of the maneuver, debris is repositioned from the long arm to the utricle, then to the short arm, and finally settles adjacent to the cupula (11).

PC-BPPV-cu and PC-BPPV-ca-sa have also been implicated as a mechanism of type 2 BPPV (11). The proposed diagnostic criteria for type 2 BPPV are symptoms suggestive of BPPV without nystagmus during the DHT or supine roll test and a short episode of vertigo with truncal retropulsion during and immediately after sitting up from the ipsilesional side (34). Recently, Harmat et al. (11) hypothesized two possible mechanisms of type 2 BPPV, PC-BPPV-ca-sa with debris located inferiorly at the base of the PC cupula incapable of deflecting the cupula or PC-BPPV-cu-sa with debris attached to the surface of the cupula on the side of the utricle loading the cupula but not changing its position. This further supports the role of the cupula in atypical PC-BPPV.

It is recognized that atypical nystagmus from the PC may be generated by limited movement of the debris within the lumen caused by a partial or complete obstruction from an innate stenosis of the canal and/or large fragments of utricular otolithic debris in a normal canal (35). The location of the obstruction determines the presentation of atypical PC-BPPV (Figure 1A). Vannucchi et al. (15) suggested that an obstruction of the lumen of the PC located in the distal or non-ampullary segment of the long arm of the PC near the common crus (Figure 1A) would generate a DBN associated with torsion lateralized to the uninvolved ear or without torsion due to the inhibition of the PC afferent. On return to sitting, there would be no nystagmus because the non-ampullary segment would be oriented in the earth horizontal (Figure 1A). This pattern of nystagmus was referred to as "apogeotropic PC-BPPV" (15, 18) and was further described by Cambi et al. (14) and Califano et al. (17). Scocco et al. (19) later suggested that an obstruction may occur in the periampullary segment (proximal segment) of the long arm of the PC (Figure 1) resulting in "sitting up vertigo." The pattern of nystagmus suggestive of a periampullary obstruction is no nystagmus in the ipsilateral DH position, and it is either no nystagmus or persistent DBN with or without torsion lateralized to the uninvolved side in the contralateral DH or SHHP (19). Upon return to upright from the DH position and SHHP, an UBN with torsion lateralized to the involved side may be observed (19). Differentiation between non-ampullary and periampullary obstructions is based on the findings from the head yaw test (the supine recumbent position with the head turned 90° to the ipsilateral (involved) and contralateral (uninvolved) sides). UBN in contralateral yaw and DBN in ipsilateral yaw suggest non-ampullary involvement while DBN in contralateral yaw and UBN in ipsilateral yaw suggest periampullary involvement (19).

Partial or complete obstruction to the lumen of the canal would modify the direction of endolymph displacement and

cause a transient high-frequency VOR deficit in the involved vertical canal (36, 37). In individuals with persistent positional DBN, with or without torsion in the DH positions and SHHP and without nystagmus on return to upright, the video head impulse test (vHIT) was able to detect the involved vertical canal of the coplanar pair, either PC-BPPV canal obstruction or AC-BPPV (36, 37). However, in typical acute PC-BPPV, the vHIT was unable to identify the involved canal (38). In this case, the vHIT was not used to identify the involved canal.

In this case, in the SHHP, the 60-s latency before the onset of a transient burst of UBN with left torsion (lateralized to the involved side) suggested an ipsicanal switch from PC-BPPV-cu-la to PC-BPPV-ca-la, implying left PC involvement (14). Computer simulations of the Yarcovino maneuver demonstrate a canal switch from AC-BPPV to PC-BPPV (39). The degree of head extension relative to the earth horizontal in the Yarcovino maneuver and SHHP are similar. A canal switch would result in DBN and possibly a reversal in the direction of torsion. In this case, only UBN with torsion lateralized to the involved side was observed in the SHHP. Therefore, an ipsicanal switch rather than a canal switch occurred. It is hypothesized that the longer latency may reflect the time taken for otolithic debris to move through the ampulla into the long arm of the canal (40), the slow sedimentation velocity caused by small particles (29, 40), silent debris defined as the movement of otolithic debris along the canal wall (29), or neutral head position—an axis of the affected posterior cupula oriented in the earth vertical (22).

Limitations of this case are the need for further positional testing to confirm the left PC-BPPV-cu, neuroimaging to rule out CNS involvement, and vHIT to rule out canal jam or obstruction. Ipsicanal conversion occurred during the SHHP, so no HH or IR was performed. Neuroimaging was not performed. The most common pattern of central positional nystagmus evoked with positional testing is positional DBN (41, 42). When the clinician observes DBN in the provoking position, CNS involvement should be considered. An individual should be referred for a thorough neurologic examination, additional CNS testing, and/or magnetic resonance imaging (MRI) of the brain and posterior fossa if associated auditory or neurological symptoms are present. If symptoms are consistent with BPPV and show no improvement or resolution after two to three sessions of particle repositioning maneuvers (12), a referral should be made for further testing. No associated neurologic signs were not observed in this individual, and the history was not suggestive of CNS involvement. No vHIT was performed to rule out complete or partial occlusion. The location of the obstruction determines the presentation of atypical PC-BPPV, the non-ampullary segment (distal) (18) or the descending periampullary segment (proximal) (19) (Figure 1A). The vHIT has only identified obstructions within the non-ampullary segment of the PC.

The strategy for resolving PC-BPPV-cu is to use the provocative positions that achieve the release of the otolithic debris from the cupula, depending on which side of the cupula the debris is located (10). The SHHP may be used to cause an ipsicanal switch from PC-BPPV-cu to PC-BPPV-ca-la. Once converted to canalithiasis, typical PC-BPPV may be treated with a modified CRP (29) or liberatory maneuver (43). If the debris is located on the side of the cupula near the utricle, the release position can be obtained by having the patient lie on the uninvolved side with the neck flexed 20° and rotated 45° downward (10) (Figure 1E). This is the same position as the side lying position of the CRP, the 180° inverted position of the liberatory maneuver, demi-Semont (lying on the uninvolved side with the neck rotated 45° downward) and 45° forced prolonged positioning (lying on the uninvolved side with the neck rotated 45°downward) (18). If the debris is located on the side of the long arm, a modified CRP or liberatory maneuver may be performed.

Data availability statement

The raw data supporting the conclusions of this article will be made available by the authors, without undue reservation.

Ethics statement

The studies involving human participants were reviewed and approved by Institutional Review Board, Midwestern University, Downers Grove, IL, USA. Written informed consent for participation was not required for this study in accordance with the national legislation and the institutional requirements. Written informed consent was obtained from the individual(s) for the publication of any potentially identifiable images or data included in this article.

Author contributions

JH: conception, study design, acquisition, analysis, interpretation of data, draft of the manuscript, critical reading, and manuscript revision. Author read and approved the submitted version.

Acknowledgments

Thanks to the individual for permitting the use of these data, reviewers, Teri Elliot-Burke, PT, DPT, MHS, and Midwestern University Multi-Specialty Clinic, Physical Therapy Institute.

Conflict of interest

The author declares that the research was conducted in the absence of any commercial or financial relationships

that could be construed as a potential conflict of interest.

Publisher's note

All claims expressed in this article are solely those of the authors and do not necessarily represent those of their affiliated organizations, or those of the publisher, the editors and the reviewers. Any product that may be evaluated in this article, or claim that may be made by its manufacturer, is not guaranteed or endorsed by the publisher.

Supplementary material

The Supplementary Material for this article can be found online at: https://www.frontiersin.org/articles/10.3389/fneur.2022.982191/full#supplementary-material

SUPPLEMENTARY VIDEO S1
Video, Supplemental Digital Content S1, which illustrates the first variant of the left PC-BPPV—downbeat nystagmus (DBN) in both DH positions and no positional nystagmus upon return to upright from both positions. Upon return to upright, right-beating nystagmus (RBN) is observed. Ipsicanal switch from cupulolithiasis to canalithiasis of the left PC-BPPV during the straight head hang position (SHHP). Digital recordings of ocular nystagmus during positional testing. Digital recordings were edited to reduce the size of files. Digital recordings begin at the point where the individual assumes the provoking position or sitting up except for the SHHP. The SHHP begins at 60 s latency before onset. For each position, digital recordings were reduced from 2 min to 30 s.

SUPPLEMENTARY VIDEO S2
Video, Supplemental Digital Content S2, which illustrates the second variant of the left PC-BPPV—no nystagmus in provoking positions and upbeat nystagmus (UBN) upon return to upright. SHHP were repeated two times. DBN was developed in SHHP. Digital recordings of ocular nystagmus during positional testing. Digital recordings were edited to reduce the size of files. Digital recordings begin at the point where the individual assumes the provoking position or sitting up. For each position, digital recordings were reduced from 2 min to 30 s. Upon sitting up, the individual was provided with light to suppress nystagmus and reduce nausea.

References

1. Hanley K, O'Dowd T, Considine N. A systematic review of vertigo in primary care. *Br J Gen Pract.* (2001) 51:666–71.

2. Katsarkas A. Benign paroxysmal positional vertigo (BPPV): idiopathic vs. post-traumatic. *Acta Otolaryngol.* (1999) 119:745–9.

3. Schappert SM. National ambulatory medical care survey: 1989 summary. *Vital Health Stat.* (1992) 13:1–80.

4. Ling X, Zhao DH, Shen B, Si LH, Li KZ, Hong Y, et al. Clinical characteristics of patients with benign paroxysmal positional vertigo diagnosed based on the diagnostic criteria of the barany society. *Front Neurol.* (2020) 11:602. doi: 10.3389/fneur.2020.00602

5. Kim JS, Zee DS. Clinical practice. Benign paroxysmal positional vertigo. *N Engl J Med.* (2014) 370:1138–47. doi: 10.1056/NEJMcp1309481

6. Hall SF, Ruby RR, McClure JA. The mechanics of benign paroxysmal vertigo. *J Otolaryngol.* (1979) 8:151–8.

7. Schuknecht HF. Cupulolithiasis. *Arch Otolaryngol.* (1969) 90:765–78.

8. Buki B, Mandala M, Nuti D. Typical and atypical benign paroxysmal positional vertigo: literature review and new theoretical considerations. *J Vestib Res.* (2014) 24:415–23. doi: 10.3233/VES-140535

9. Buki B. Benign paroxysmal positional vertigo: toward new definitions. *Otol Neurotol.* (2014) 35:323–8. doi: 10.1097/MAO.0000000000000197

10. Epley JM. Human experience with canalith repositioning maneuvers. *Ann N Y Acad Sci.* (2001) 942:179–91. doi: 10.1111/j.1749-6632.2001.tb03744.x

11. Harmat K, Tamas LT, Schubert MC, Gerlinger I, Komoly S, Buki B. Prevalence of and theoretical explanation for type 2 benign paroxysmal positional vertigo. *J Neurol Phys Ther.* (2022) 46:88–95. doi: 10.1097/NPT.0000000000000383

12. Bhattacharyya N, Gubbels SP, Schwartz SR, Edlow JA, El-Kashlan H, Fife T, et al. Clinical practice guideline: benign paroxysmal positional vertigo (update). *Otolaryngol Head Neck Surg.* (2017) 156(3_suppl):S1–S47. doi: 10.1177/0194599816689667

13. Aw ST, Todd MJ, Aw GE, McGarvie LA, Halmagyi GM. Benign positional nystagmus: a study of its three-dimensional spatio-temporal characteristics. *Neurology.* (2005) 64:1897–905. doi: 10.1212/01.WNL.0000163545.57134.3D

14. Cambi J, Astore S, Mandala M, Trabalzini F, Nuti D. Natural course of positional down-beating nystagmus of peripheral origin. *J Neurol.* (2013) 260:1489–96. doi: 10.1007/s00415-012-6815-9

15. Vannucchi P, Pecci R, Giannoni B. Posterior semicircular canal benign paroxysmal positional vertigo presenting with torsional downbeating nystagmus: an apogeotropic variant. *Int J Otolaryngol.* (2012) 2012:413603. doi: 10.1155/2012/413603

16. Bertholon P, Bronstein AM, Davies RA, Rudge P, Thilo KV. Positional down beating nystagmus in 50 patients: cerebellar disorders and possible anterior semicircular canalithiasis. *J Neurol Neurosurg Psychiatry.* (2002) 72:366–72. doi: 10.1136/jnnp.72.3.366

17. Califano L, Salafia F, Mazzone S, Melillo MG, Califano M. Anterior canal BPPV and apogeotropic posterior canal BPPV: two rare forms of vertical canalolithiasis. *Acta Otorhinolaryngol Ital.* (2014) 34:189–97.

18. Vannucchi P, Pecci R, Giannoni B, Di Giustino F, Santimone R, Mengucci A. Apogeotropic posterior semicircular canal benign paroxysmal positional vertigo: some clinical and therapeutic considerations. *Audiol Res.* (2015) 5:130. doi: 10.4081/audiores.2015.130

19. Scocco DH, Garcia IE, Barreiro MA. Sitting up vertigo. Proposed variant of posterior canal benign paroxysmal positional vertigo. *Otol Neurotol.* (2019) 40:497–503. doi: 10.1097/MAO.0000000000002157

20. Nuti D, Zee DS, Mandala M. Benign paroxysmal positional vertigo: what we do and do not know. *Semin Neurol.* (2020) 40:49–58. doi: 10.1055/s-0039-3402733

21. von Brevern M, Bertholon P, Brandt T, Fife T, Imai T, Nuti D, et al. Benign paroxysmal positional vertigo: diagnostic criteria. *J Vestib Res.* (2015) 25:105–17. doi: 10.3233/VES-150553

22. Imai T, Takeda N, Ito M, Sekine K, Sato G, Midoh Y, et al. 3D analysis of benign positional nystagmus due to cupulolithiasis in posterior semicircular canal. *Acta Otolaryngol.* (2009) 129:1044–9. doi: 10.1080/00016480802566303

23. Bradshaw AP, Curthoys IS, Todd MJ, Magnussen JS, Taubman DS, Aw ST, et al. A mathematical model of human semicircular canal geometry: a new basis for interpreting vestibular physiology. *J Assoc Res Otolaryngol.* (2010) 11:145–59. doi: 10.1007/s10162-009-0195-6

24. Rabbitt RD, Breneman KD, King C, Yamauchi AM, Boyle R, Highstein SM. Dynamic displacement of normal and detached semicircular canal cupula. *J Assoc Res Otolaryngol.* (2009) 10:497–509. doi: 10.1007/s10162-009-0174-y

25. Greenberg D, Aminoff M, Simon P. *Clinical Neurology, 11 Edn.* New York: McGraw-Hill Professional Publishing Lange (2021). p. 1–429.

26. Strupp M, Kremmyda O, Adamczyk C, Bottcher N, Muth C, Yip CW, et al. Central ocular motor disorders, including gaze palsy and nystagmus. *J Neurol.* (2014) 261:S542–58. doi: 10.1007/s00415-014-7385-9

27. Choi SY, Jang JY, Oh EH, Choi JH, Park JY, Lee SH, et al. Persistent geotropic positional nystagmus in unilateral cerebellar lesions. *Neurology.* (2018) 91:e1053–e7. doi: 10.1212/WNL.0000000000006167

28. Bertholon P, Antoine JC, Martin C, Michel D. Simultaneous occurrence of a central and a peripheral positional nystagmus during the Dix-Hallpike manoeuvre. *Eur Neurol.* (2003) 50:249–50. doi: 10.1159/000073868

29. Rajguru SM, Ifediba MA, Rabbitt RD. Three-dimensional biomechanical model of benign paroxysmal positional vertigo. *Ann Biomed Eng.* (2004) 32:831–46. doi: 10.1023/B:ABME.0000030259.41143.30

30. Horinaka A, Kitahara T, Shiozaki T, Ito T, Wada Y, Yamanaka T, et al. Head-up sleep may cure patients with intractable benign paroxysmal positional vertigo: a 6-month randomized trial. *Laryngoscope Investig Otolaryngol.* (2019) 4:353–8. doi: 10.1002/lio2.270

31. Jeong SH, Kim JS, Shin JW, Kim S, Lee H, Lee AY, et al. Decreased serum vitamin D in idiopathic benign paroxysmal positional vertigo. *J Neurol.* (2013) 260:832–8. doi: 10.1007/s00415-012-6712-2

32. Scocco DH, Barreiro MA, Garcia IE. Sitting-up vertigo as an expression of posterior semicircular canal heavy cupula and posterior semicircular canal short arm canalolithiasis. *J Otology.* (2022) 17:101–6. doi: 10.1016/j.joto.2022.02.001

33. Helminski J, Hain T. Evaluation and treatment of benign paroxysmal positional vertigo. *Ann Long-Term Care Clin Care Aging.* (2007) 15:33–9.

34. Buki B, Simon L, Garab S, Lundberg YW, Junger H, Straumann D. Sitting-up vertigo and trunk retropulsion in patients with benign positional vertigo but without positional nystagmus. *J Neurol Neurosurg Psychiatry.* (2011) 82:98–104. doi: 10.1136/jnnp.2009.199208

35. Horii A, Kitahara T, Osaki Y, Imai T, Fukuda K, Sakagami M, et al. Intractable benign paroxysmal positioning vertigo: long-term follow-up and inner ear abnormality detected by three-dimensional magnetic resonance imaging. *Otol Neurotol.* (2010) 31:250–5. doi: 10.1097/MAO.0b013e3181cabd77

36. Castellucci A, Malara P, Delmonte S, Ghidini A. A possible role of video-head impulse test in detecting canal involvement in benign paroxysmal positional vertigo presenting with positional downbeat nystagmus. *Otol Neurotol.* (2019) 41:386–91. doi: 10.1097/MAO.0000000000002500

37. Castellucci A, Malara P, Martellucci S, Botti C, Delmonte S, Quaglieri S, et al. Feasibility of using the video-head impulse test to detect the involved canal in benign paroxysmal positional vertigo presenting with positional downbeat nystagmus. *Front Neurol.* (2020) 11:578588. doi: 10.3389/fneur.2020.578588

38. Califano L, Iannella R, Mazzone S, Salafia F, Melillo MG. The video head impulse test in the acute stage of posterior canal benign paroxysmal positional vertigo. *Acta Otorhinolaryngol Ital.* (2021) 41:69–76. doi: 10.14639/0392-100X-N1033

39. Bhandari A, Bhandari R, Kingma H, Strupp M. Diagnostic and therapeutic maneuvers for anterior canal BPPV canalithiasis: three-dimensional simulations. *Front Neurol.* (2021) 12:740599. doi: 10.3389/fneur.2021.740599

40. Squires TM, Weidman MS, Hain TC, Stone HA. A mathematical model for top-shelf vertigo: the role of sedimenting otoconia in BPPV. *J Biomech.* (2004) 37:1137–46. doi: 10.1016/j.jbiomech.2003.12.014

41. Choi JY, Kim JH, Kim HJ, Glasauer S, Kim JS. Central paroxysmal positional nystagmus: characteristics and possible mechanisms. *Neurology.* (2015) 84:2238–46. doi: 10.1212/WNL.0000000000001640

42. De Schutter E, Adham ZO, Kattah JC. Central positional vertigo: a clinical-imaging study. *Prog Brain Res.* (2019) 249:345–60. doi: 10.1016/bs.pbr.2019.04.022

43. Semont A, Freyss G, Vitte E. Curing the BPPV with a liberatory maneuver. *Adv Otorhinolaryngol.* (1988) 42:290–3.

frontiers | Frontiers in Neurology

TYPE Case Report
PUBLISHED 09 November 2022
DOI 10.3389/fneur.2022.1043452

OPEN ACCESS

EDITED BY
Michael Strupp,
Ludwig Maximilian University of Munich, Germany

REVIEWED BY
Jeremy Hornibrook,
University of Canterbury, New Zealand
Franco Trabalzini,
University of Florence, Italy

*CORRESPONDENCE
Koji Nishimura
k_nishimura@ent.kuhp.kyoto-u.ac.jp

SPECIALTY SECTION
This article was submitted to Neuro-Otology, a section of the journal Frontiers in Neurology

RECEIVED 13 September 2022
ACCEPTED 06 October 2022
PUBLISHED 09 November 2022

CITATION
Nishimura K, Murofushi T and Hakuba N (2022) Case report: Concurrent intravestibular schwannoma mimicking Ménière's disease and cochlear hydrops detected *via* delayed three-dimensional fluid-attenuated inversion recovery magnetic resonance imaging. *Front. Neurol.* 13:1043452. doi: 10.3389/fneur.2022.1043452

Case report: Concurrent intravestibular schwannoma mimicking Ménière's disease and cochlear hydrops detected *via* delayed three-dimensional fluid-attenuated inversion recovery magnetic resonance imaging

Koji Nishimura*, Toshihisa Murofushi and Nobuhiro Hakuba

Department of Otolaryngology, Teikyo University School of Medicine, Mizonokuchi Hospital, Kawasaki, Japan

Objective: To present a case of intralabyrinthine schwannoma (ILS) presenting as Ménière's disease diagnosed *via* 4-h delayed gadolinium-enhanced three-dimensional fluid-attenuated inversion recovery magnetic resonance imaging (3D-FLAIR MRI) and treated successfully using the translabyrinthine approach.

Patient: A patient who was diagnosed with intravestibular ILS.

Interventions: The patient underwent comprehensive preoperative neurological examinations and MRI. The tumor was resected using the translabyrinthine approach and was pathologically confirmed as schwannoma based on the surgical specimen.

Main outcome measures: Preoperative audiogram and vestibular test findings and MRI images.

Results: Preoperatively, pure-tone audiogram showed progressive sensorineural hearing loss only on the affected side. The video head impulse test and vestibular evoked myogenic potential test showed vestibular dysfunction on the affected ear. Immediate gadolinium-enhanced T1-weighted MRI revealed an enhanced region in the vestibule. Meanwhile, magnetic resonance cisternography showed a filling defect. Delayed 3D-FLAIR MRI revealed a signal void in the scala media of the cochlea indicative of cochlear hydrops, and a strong signal in the perilymph at the basal cochlea suggestive of impaired blood–labyrinthine barrier.

Conclusion: Delayed 3D-FLAIR MRI is useful in diagnosing concurrent ILSs and endolymphatic hydrops.

KEYWORDS

delayed 3D-FLAIR MR imaging, endolymphatic hydrops (EH), intralabyrinthine schwannomas (ILSs), intravestibular schwannoma, vestibular evoked myogenic potential (VEMP), video head impulse test (vHIT), Ménière's disease

Introduction

Vestibular schwannomas (VSs) are benign neoplasms commonly arising from the Schwann cells of the vestibular division of the vestibulocochlear nerve. Intralabyrinthine schwannomas (ILSs) are a rare clinical entity, and they arise from the distal branches of the vestibular and cochlear nerves within the membranous labyrinth (1, 2). The common symptoms of ILSs are unilateral hearing loss, tinnitus, imbalance/dizziness and occasionally episodes of vertigo, which are similar to those of Ménière's disease (MD) (3, 4). Endolymphatic hydrops is a characteristic of MD and other inner ear diseases, such as endolymphatic tumors. Moreover, VSs can cause endolymphatic hydrops (5–9). Naganawa et al. developed magnetic resonance imaging (MRI) methods to facilitate the visualization of endolymphatic hydrops in living humans using intravenous gadolinium-based contrast media (10, 11). Herein, we report a case of concurrent ILS mimicking MD and cochlear hydrops diagnosed *via* gadolinium-enhanced MRI.

Case report

A woman in her 30's visited our department due to hyperacusis in the right ear. Audiogram showed almost normal hearing level (Figure 1A). The patient did not present with spontaneous or positional nystagmus. However, she occasionally experienced vertigo in the morning 4 years prior to her initial visit to our department. Four years after the first visit, she presented with vertigo, tinnitus, and hearing loss in the right ear. Audiogram revealed moderate right sensorineural hearing loss particularly at low frequencies (Figure 1B). Magnetic resonance (MR) cisternography showed no VS in the cerebellopontine angle. However, a filling defect of fluid intensity was detected in the vestibule of the right ear, and this finding was overlooked by an otolaryngologist and a radiologist (Figure 2A asterisk). Corticosteroid was prescribed for 7 days for acute sensorineural hearing loss in the right ear. Thereafter, partial hearing improvement was observed (Figure 1C). Nevertheless, the patient continually presented with tinnitus in the right ear and dizziness. Thus, her hearing function was evaluated

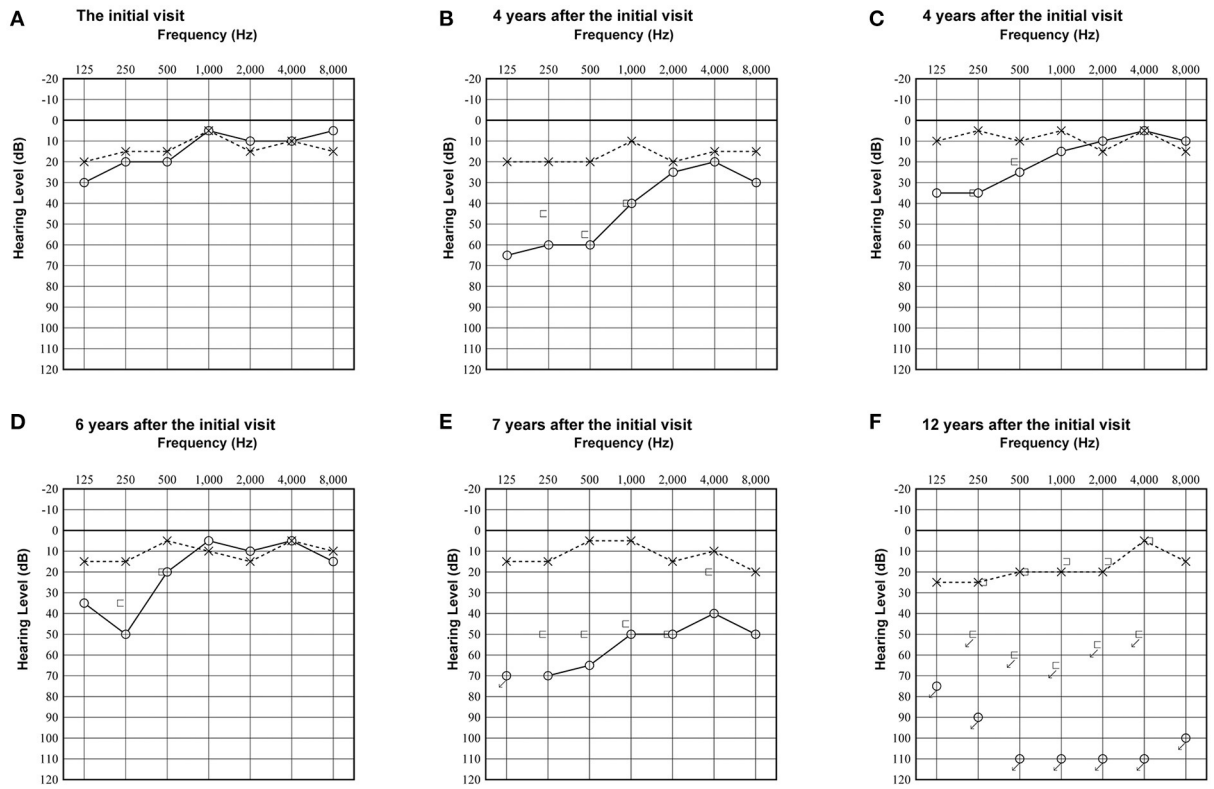

FIGURE 1
Pure-tone audiogram at the initial visit showed almost normal hearing threshold on both sides **(A)**. Audiogram 4 years after the initial visit revealed moderate sensorineural hearing loss in the right ear at low and middle frequencies **(B)**. Audiogram after treatment with corticosteroid with partial hearing improvement **(C)**. Audiogram 6 years after the initial visit showed mild hearing loss in the right ear only at low frequencies **(D)**. Audiogram 7 years after the initial visit revealed severe hearing loss in the right ear at all frequencies **(E)**. Audiogram 12 years after the initial visit showed profound sensorineural hearing loss in the right ear **(F)**.

regularly. Results showed moderate hearing loss in the right ear at low frequencies (Figure 1D). Seven years after the initial visit, she complained of worsening hearing loss in the right ear. Audiogram revealed moderate sensorineural hearing loss at all frequencies in the right ear (Figure 1E). She was again treated with corticosteroid. However, there was no hearing improvement. Twelve years after the initial visit, her hearing function deteriorated. Audiogram revealed profound sensorineural hearing loss in the right ear (Figure 1F). Both cervical and ocular vestibular evoked myogenic potential (cVEMP and oVEMP) were not detected upon right ear stimulation (Figure 3A). The video head impulse test (vHIT) showed decreased vestibulo-ocular reflex (VOR) gains in both the anterior and posterior canals on the affected and unaffected sides. Covert catch-up saccades were observed during eye movement elicited by right lateral semicircular canal stimulation. This result indicated decreased right lateral semicircular canal function (Figure 3B). Due to episodes of recurring vertigo and fluctuating hearing loss, endolymphatic hydrops, possibly correlated with MD, was considered as the preliminary diagnosis (12). Thus, delayed 3D-FLAIR MRI was performed to confirm endolymphatic hydrops (10, 11) or identify other conditions. MR cisternography showed a filling defect of fluid intensity in the vestibule of the right ear (Figure 2B asterisk). Gadolinium-enhanced T1-weighted imaging revealed a moderately enhanced region in the right vestibule, which indicated a hypervascular mass in the right vestibule (Figure 2C asterisk). Delayed 3D-FLAIR MRI showed endolymphatic hydrops in the right cochlea (Figure 2D arrows) with a stronger signal intensity in the scala tympani in the basal portion of the cochlea (Figure 2D arrowhead) than in the contralateral ear. The patient wanted to undergo intralabyrinthine tumor resection. Thus, surgery using the translabyrinthine approach was performed (Figure 4). Wide mastoidectomy was performed, followed by transmastoid labyrinthectomy. Then, a pink irregular shaped mass was found to fill the vestibule. After tumor resection, residual tumor was not observed microscopically and endoscopically. An 8-mm mass was completely resected. The whorls of spindle-shaped cells and the palisading structure of cells were consistent with schwannoma. The patient did not present with complications nor vertigo after the surgery. Further, she was followed-up every month, and she underwent clinical vestibular evaluations.

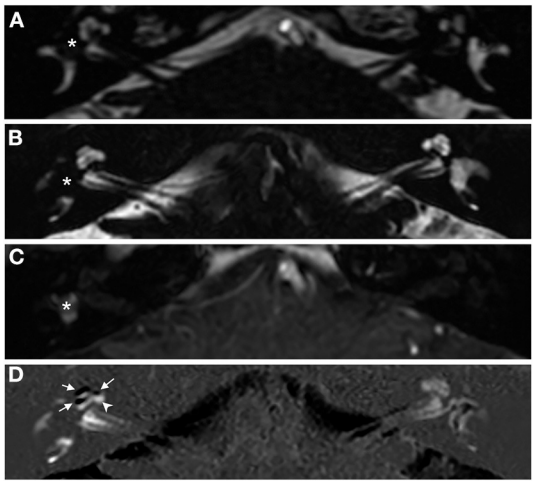

FIGURE 2
Axial magnetic resonance (MR) images obtained from a patient with concurrent right intravestibular schwannoma and endolymphatic hydrops in the right cochlea. **(A)** MR cisternography images obtained 4 years after the patient's initial visit to our department. **(B–D)** MR images obtained 12 years after the patient's initial visit to our department. **(A,B)** MR cisternography revealed a filling defect in the right vestibule (asterisks). **(C)** Gadolinium-enhanced T1-weighted imaging showed an enhanced region in the right vestibule indicating the presence of a hypervascular mass (asterisk). **(D)** Delayed 3D-FLAIR image, subtraction of the positive endolymphatic image from the positive perilymphatic image revealed black areas (arrowheads) representing the right cochlear hydrops and diffuse perilymphatic hyperintense area (arrowhead) indicative of blood–labyrinth barrier impairment.

Discussion

Herein, we present a case of concurrent endolymphatic hydrops diagnosed *via* 3D-FLAIR MRI and ILS diagnosed *via* pathological examination of surgical specimen. To the best of our knowledge, there are only two studies describing endolymphatic hydrops diagnosed *via* delayed 3D-FLAIR MRI in patients with ILS (7, 13). One possible mechanism underlying endolymphatic hydrops is the presence of a tumor obstructing the ductus reuniens, which connects the cochlear duct and the saccule. Endolymphatic hydrops is also detected *via* delayed 3D-FLAIR MRI (14) and non-contrast-enhanced 3D-FLAIR MRI (6) in some VS cases. Hence, other than mechanical stenosis of the ductus reuniens, a common mechanism associated with this condition may exist between VSs and ILSs.

ILSs commonly cause unilateral hearing loss, tinnitus, vertigo, and aural fullness, which fairly overlap with MD symptoms. In accordance with this finding, 39% of patients with ILS were previously diagnosed with MD (15). If a patient is diagnosed with MD, the diagnosis is more challenging to reconsider. Our patient was also misdiagnosed with MD. However, she underwent gadolinium-enhanced T1-weighted MRI, which revealed a vestibular tumor. Prior to the initial series of ILSs diagnosed *via* MRI (16), ILS was diagnosed incidentally during surgery (17, 18), or autopsy (19, 20). Currently, MRI is the gold standard for diagnosing ILSs (1, 2). ILSs are characterized a low signal intensity within the membranous labyrinth, which appears as filling defects, on thin-section T2-weighted images. On post-gadolinium T1-weighted images, ILSs appear as enhanced masses. The

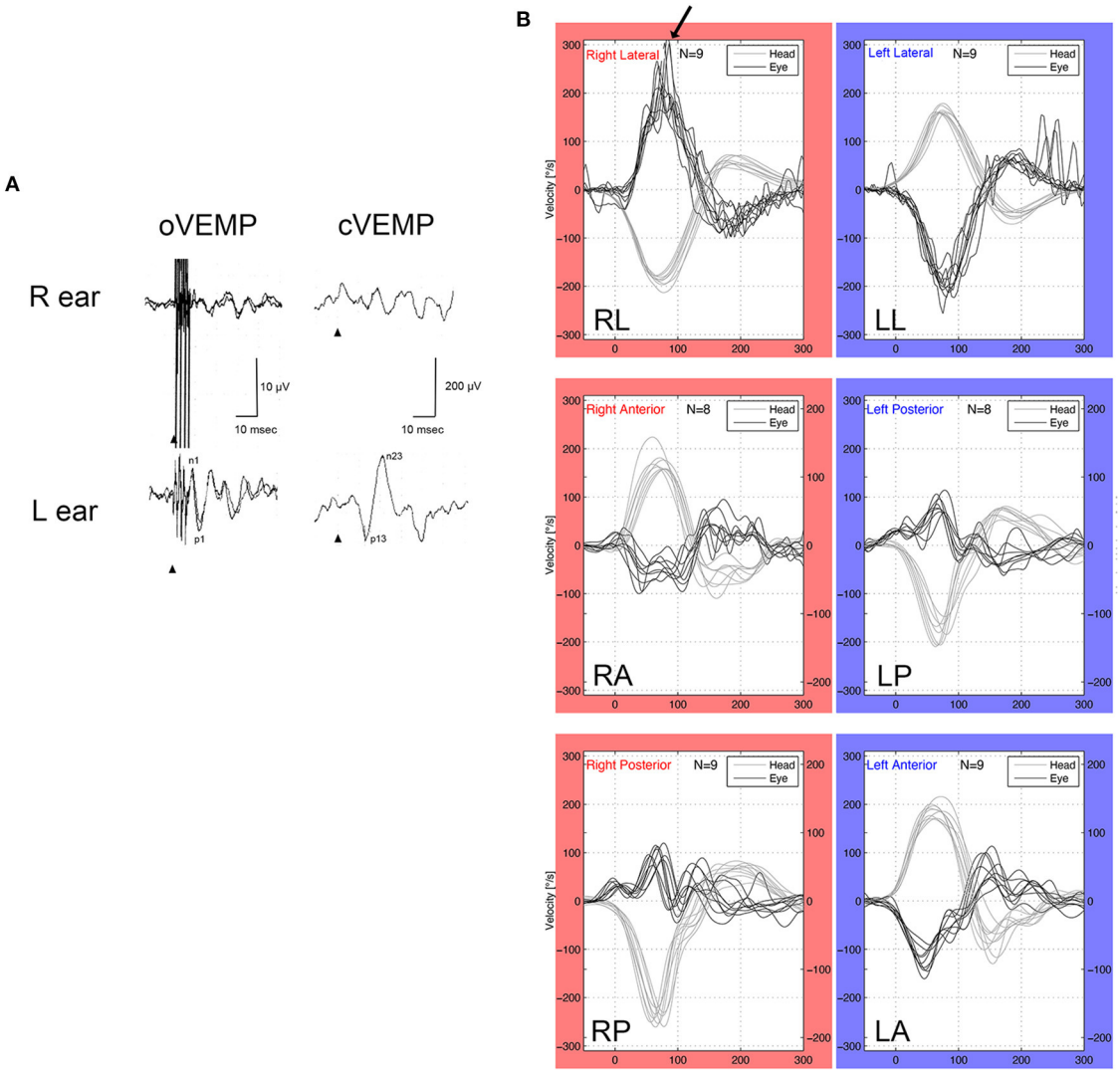

FIGURE 3
VEMP and vHIT. **(A)** oVEMP (500-Hz bone conduction) and cVEMP (500-Hz air condition). The patient had normal oVEMP and cVEMP on the unaffected side (left ear), and she presented with abnormal oVEMP and cVEMP in the affected side (right ear). **(B)** vHIT showed hyporeflexia in the anterior and posterior semicircular canals of both ears. Meanwhile, vHIT of the left lateral semicircular canal was normal, and vHIT of the right lateral semicircular canal had covert saccades (arrow), which indicated that the right lateral semicircular canal had decreased function.

imaging characteristics of our patient were in accordance with those of ILSs. Delayed 3D-FLAIR MRI was initially performed to visualize endolymphatic hydrops in patients with MD (10, 11, 21). A few studies have reported the characteristics of ILSs on delayed 3D-FLAIR MRI (7, 13, 22). The strong enhancement in the ipsilateral cochlear basal on delayed 3D-FLAIR MRI in the current case was in accordance with that of two previous reports on perilymphatic hyperintense areas surrounding the tumor (13, 22). Perilymphatic enhancement on delayed 3D-FLAIR MRI was also detected in patients with intracanalicular or cerebellopontine angle VSs, which might be caused by leakage of gadolinium into the cochlear perilymphatic space *via* the impaired blood–labyrinth barrier (14). Thus, sensorineural hearing loss in a subset of patients with VSs and ILSs is caused by alterations in blood–labyrinth barrier permeability. In addition, hearing loss was the most common presenting symptom in patients with ILSs regardless of tumor location (2). Homann et al. first detected endolymphatic hydrops *via* delayed 3D-FLAIR MRI in a patient with ILS (7). In similar studies investigating ILSs *via* delayed 3D-FLAIR MRI, endolymphatic hydrops was detected in 11.1% (3/27) (13), and 0% (0/3) of patients (22), respectively. However, in studies about ILSs detected *via* non-contrast-enhanced 3D-FLAIR MRI, endolymphatic hydrops was observed in

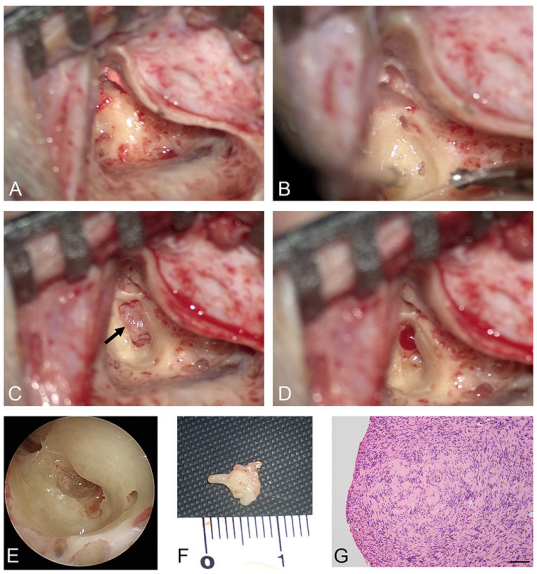

FIGURE 4
Intraoperative findings. After cortical mastoidectomy **(A)** and labyrinthectomy **(B)**, a pink mass was observed in the right vestibule (arrow) **(C)**. After tumor resection, the intravestibular region was evaluated both microscopically **(D)** and endoscopically **(E)**. An 8-mm mass was excised **(F)**. **(G)** High-power microphotograph showed a nuclear palisading pattern. Scale bar = 100 μm.

46.7% (14/30) of patients (23). Delayed 3D-FLAIR MRI is more effective in diagnosing endolymphatic hydrops than non-contrast-enhanced 3D-T2-weighted gradient-echo steady-state sequences (FIESTA-c) particularly in cases without ILSs (24). Of note, delayed 3D-FLAIR MRI in cases of ILSs might underestimate endolymphatic hydrops since gadolinium might leak in the endolymph due to impairment of the inner ear microenvironment caused by the tumor. Thus, different modalities can affect the assessment of endolymphatic hydrops in ILSs. In our case, concurrent endolymphatic hydrops and intravestibular ILS were detected *via* delayed 3D-FLAIR MRI. Endolymphatic hydrops may exist with ILSs. However, it cannot be clearly identified *via* delayed 3D-FLAIR MRI.

In the current case, the asymmetric ratios of cVEMP and oVEMP were 100%, which indicated severe otolith dysfunction on the affected side. Approximately 75% of patients with intravestibular ILS and 55.6% of patients with intracochlear ILS present with an abnormal cVEMP (25). Hence, unlike auditory functional differences, intralabyrinthine localizations could affect vestibular functional differences. Our patient presented with decreased VOR gains in both sides of the anterior and posterior semicircular canals, and covert catch-up saccades in the lateral semicircular canal on the affected side. The long duration of unilateral vestibular dysfunction (16 years in the current case) might help achieve good dynamic visual performance. Lee et al. presented a case of ILS mimicking MD based on a positive vHIT result in all semicircular canals on the affected side (26). The causes of decreased VOR gains on the left anterior and posterior semicircular canals remain unknown. However, the risk of ILS should be considered.

Hearing function cannot be preserved with surgical resection of ILSs. Thus, in patients with serviceable hearing or tolerable symptoms, the wait-and-see strategy is recommended (1, 8). Surgery is indicated if ILS extends toward the cerebellopontine angle or into the middle ear, or if a patient presents with intractable vestibular symptoms (1). In cases in which surgery can be performed, tumor localization is important in surgical planning. In the current case, the tumor was located in the vestibule and did not extend to other regions. Hence, according to the classification of Kennedy (1) or Salzman (2), it was considered an intravestibular type.

Conclusion

Combined fluctuating hearing loss and episodic vertigo attacks can be observed in ILS and MD. Therefore, delayed 3D-FLAIR MRI is useful in the diagnosis of concurrent ILSs and endolymphatic hydrops.

Data availability statement

The raw data supporting the conclusions of this article will be made available by the authors, without undue reservation.

Ethics statement

Ethical review and approval was not required for the study on human participants in accordance with the local legislation and institutional requirements. The patients/participants provided their written informed consent to participate in this study. Written informed consent was obtained from the individual(s) for the publication of any potentially identifiable images or data included in this article.

Author contributions

KN conceived the idea of the study and drafted the original manuscript. All authors reviewed the manuscript draft, revised its intellectual content critically and approved the final version of the manuscript for publication.

Funding

The study was supported by JSPS KAKENHI Grant Number 22H03239.

Acknowledgments

We thank Tatsuya Aso for pathological examinations.

Conflict of interest

The authors declare that the research was conducted in the absence of any commercial or financial relationships that could be construed as a potential conflict of interest.

Publisher's note

References

1. Kennedy RJ, Shelton C, Salzman KL, Davidson HC, Harnsberger HR. Intralabyrinthine schwannomas: diagnosis, management, and a new classification system. *Otol Neurotol.* (2004) 25:160–7. doi: 10.1097/00129492-200403000-00014

2. Salzman KL, Childs AM, Davidson HC, Kennedy RJ, Shelton C, Harnsberger HR. Intralabyrinthine schwannomas: imaging diagnosis and classification. *Am J Neuroradiol.* (2012) 33:104–9. doi: 10.3174/ajnr.A2712

3. Lee SU, Bae YJ, Kim HJ, Choi JY, Song JJ, Choi BY, et al. Intralabyrinthine schwannoma: distinct features for differential diagnosis. *Front Neurol.* (2019) 10:750. doi: 10.3389/fneur.2019.00750

4. Marinelli JP, Lohse CM, Carlson ML. Incidence of intralabyrinthine schwannoma: a population-based study within the United States. *Otol Neurotol.* (2018) 39:1191–4. doi: 10.1097/MAO.0000000000001875

5. Butman JA, Nduom E, Kim HJ, Lonser RR. Imaging detection of endolymphatic sac tumor-associated hydrops. *J Neurosurg.* (2013) 119:406–11. doi: 10.3171/2013.2.JNS12608

6. Naganawa S, Kawai H, Sone M, Nakashima T, Ikeda M. Endolympathic hydrops in patients with vestibular schwannoma: visualization by non-contrast-enhanced 3D FLAIR. *Neuroradiology.* (2011) 53:1009–15. doi: 10.1007/s00234-010-0834-y

7. Homann G, Fahrendorf D, Niederstadt T, Nagelmann N, Heindel W, Lutkenhoner B, et al. HR 3 Tesla MRI for the diagnosis of endolymphatic hydrops and differential diagnosis of inner ear tumors–demonstrated by two cases with similar symptoms. *Rofo.* (2014) 186:225–9. doi: 10.1055/s-0033-1356221

8. Zhang Y, Li F, Dai C, Wang W. Endolymphatic hydrops in patients with intralabyrinthine schwannomas. *Front Surg.* (2020) 7:623078. doi: 10.3389/fsurg.2020.623078

9. Eliezer M, Poillon G, Maquet C, Gillibert A, Horion J, Marie JP, et al. Sensorineural hearing loss in patients with vestibular schwannoma correlates with the presence of utricular hydrops as diagnosed on heavily T2-weighted MRI. *Diagn Interv Imaging.* (2019) 100:259–68. doi: 10.1016/j.diii.2019.01.006

10. Naganawa S, Nakashima T. Visualization of endolymphatic hydrops with MR imaging in patients with Meniere's disease and related pathologies: current status of its methods and clinical significance. *Jpn J Radiol.* (2014) 32:191–204. doi: 10.1007/s11604-014-0290-4

11. Naganawa S, Yamazaki M, Kawai H, Bokura K, Sone M, Nakashima T. Visualization of endolymphatic hydrops in Meniere's disease with single-dose intravenous gadolinium-based contrast media using heavily T(2)-weighted 3D-FLAIR. *Magn Reson Med Sci.* (2010) 9:237–42. doi: 10.2463/mrms.9.237

12. Lopez-Escamez JA, Carey J, Chung WH, Goebel JA, Magnusson M, Mandala M, et al. Diagnostic criteria for Meniere's disease. *J Vestib Res.* (2015) 25:1–7. doi: 10.3233/VES-150549

13. Poillon G, Horion J, Daval M, Bouccara D, Hautefort C, Housset J, et al. MRI characteristics of intralabyrinthine schwannoma on post-contrast 4 h-delayed 3D-FLAIR imaging. *Diagn Interv Imaging.* (2022) 103:171–6. doi: 10.1016/j.diii.2021.09.011

14. Bowen AJ, Carlson ML, Lane JI. Inner ear enhancement with delayed 3D-FLAIR MRI imaging in vestibular schwannoma. *Otol Neurotol.* (2020) 41:1274–9. doi: 10.1097/MAO.0000000000002768

15. Van Abel KM, Carlson ML, Link MJ, Neff BA, Beatty CW, Lohse CM, et al. Primary inner ear schwannomas: a case series and systematic review of the literature. *Laryngoscope.* (2013) 123:1957–66. doi: 10.1002/lary.23928

16. Doyle KJ, Brackmann DE. Intralabyrinthine schwannomas. *Otolaryngol Head Neck Surg.* (1994) 110:517–23. doi: 10.1177/019459989411000608

17. Miyamoto RT, Isenberg SF, Culp WM, Tubergen LB. Isolated intralabyrinthine schwannoma. *Am J Otol.* (1980) 1:215–7.

18. Vernick DM, Graham MD, McClatchey KD. Intralabyrinthine schwannoma. *Laryngoscope.* (1984) 94:1241–3. doi: 10.1288/00005537-198409000-00020

19. Mayer O. Ein Fall von multiplen Tumoren in den Endausbreitungen des Akustikas. *Z Ohrenheilkd.* (1917) 1917:95–113.

20. Hoshino T, Ishii D. Intralabyrinthine neurilemmoma. A histopathological report. *J Otorhinolaryngol Relat Spec.* (1972) 34:117–23. doi: 10.1159/000275037

21. Nakashima T, Naganawa S, Teranishi M, Tagaya M, Nakata S, Sone M, et al. Endolymphatic hydrops revealed by intravenous gadolinium injection in patients with Meniere's disease. *Acta Otolaryngol.* (2010) 130:338–43. doi: 10.3109/00016480903143986

22. Kurata N, Kawashima Y, Ito T, Ooka T, Tsutsumi T. Four-hour delayed gadolinium-enhanced 3D-FLAIR MR imaging highlights intralabyrinthine micro-schwannomas. *Otol Neurotol.* (2021) 42:e1444–e8. doi: 10.1097/MAO.0000000000003310

23. Venkatasamy A, Bretz P, Karol A, Karch-Georges A, Charpiot A, Veillon F, et al. of endolymphatic hydrops in patients with intralabyrinthine schwannomas: a case-controlled study using non-enhanced T2-weighted images at 3 T. *Eur Arch Otorhinolaryngol.* (2021) 278:1821–7. doi: 10.1007/s00405-020-06271-6

24. Eliezer M, Poillon G, Horion J, Lelion P, Gerardin E, Magne N, et al. MRI diagnosis of saccular hydrops: comparison of heavily-T2 FIESTA-C and 3D-FLAIR sequences with delayed acquisition. *J Neuroradiol.* (2021) 48:446–52. doi: 10.1016/j.neurad.2019.04.005

25. Dubernard X, Somers T, Veros K, Vincent C, Franco-Vidal V, Deguine O, et al. Clinical presentation of intralabyrinthine schwannomas: a multicenter study of 110 cases. *Otol Neurotol.* (2014) 35:1641–9. doi: 10.1097/MAO.0000000000000415

26. Lee SU, Kim HJ, Choi JY, Song JJ, Choi BS, Kim JS. Teaching video neuroimages: intralabyrinthine schwannoma masquerading as Meniere disease. *Neurology.* (2020) 94:e1227–e8. doi: 10.1212/WNL.0000000000009095

frontiers | Frontiers in Neurology

TYPE Original Research
PUBLISHED 23 November 2022
DOI 10.3389/fneur.2022.1048218

OPEN ACCESS

EDITED BY
Michael Strupp,
Ludwig Maximilian University of Munich, Germany

REVIEWED BY
Andrés Soto-Varela,
Complejo Hospitalario Universitario de Santiago, Spain
Jorge Rey-Martinez,
Donostia University Hospital, Spain

*CORRESPONDENCE
Jun Yang
yangjun@xinhuamed.com.cn
Lianhua Sun
sunlianhua@xinhuamed.com.cn

†These authors have contributed equally to this work

SPECIALTY SECTION
This article was submitted to Neuro-Otology, a section of the journal Frontiers in Neurology

RECEIVED 19 September 2022
ACCEPTED 24 October 2022
PUBLISHED 23 November 2022

CITATION
Sun L, Lin Z, Wang X, Shen J, Li Y, Huang Y and Yang J (2022) Molecular etiology study of hearing loss in 13 Chinese Han families.
Front. Neurol. 13:1048218.
doi: 10.3389/fneur.2022.1048218

Molecular etiology study of hearing loss in 13 Chinese Han families

Lianhua Sun[1,2,3*†], Zhengyu Lin[1,2,3†], Xiaowen Wang[1,2,3], Jiali Shen[1,2,3], Yue Li[1,2,3], Yuyu Huang[1,2,3] and Jun Yang[1,2,3*]

[1]Department of Otorhinolaryngology-Head and Neck Surgery, Xinhua Hospital, Shanghai Jiaotong University School of Medicine, Shanghai, China, [2]Shanghai Jiaotong University School of Medicine Ear Institute, Shanghai, China, [3]Shanghai Key Laboratory of Translational Medicine on Ear and Nose Diseases, Shanghai, China

Hearing loss affecting about 2/1000 newborns is the most common congenital disease. Genetic defects caused approximately 70% of patients who have non-syndromic hearing loss. We recruited 13 Chinese Han deafness families who tested negative for *GJB2*, *SLC26A4*, and mitochondrial 12S rRNA. The probands of each family were performed whole-exome sequencing (WES) or targeted next-generation sequencing (NGS) for known deafness genes to study for pathogenic causes. We found four novel mutations of *CDH23*, one novel mutation of *MYO15A*, one novel mutation of *TMC1*, one novel mutation of *PAX3*, and one novel mutation of *ADGRV1*, one novel CNV of *ADGRV1*, and one novel CNV of *STRC*. Hearing loss is a highly hereditary and heterogeneous disease. The results in the limited samples of this study show that Usher and Waardenburg syndrome-related genes account for a major proportion are strongly associated with Chinese Han hearing loss patients negative for *GJB2*, *SLC26A4*, and mitochondrial 12S rRNA, followed by *STRC* resulting in mild to moderate deafness.

KEYWORDS

deafness, targeted sequencing, whole-exome sequencing, gene mutation, etiological analysis

Introduction

Hearing loss is the most common congenital disease affecting about 2/1,000 newborns (1). Approximately 70% of non-syndromic hearing loss is caused by genetic defects (2). Autosomal recessive non-syndromic deafness, the most common form of hearing loss, is usually pre-lingual and accounts for 80% of non-syndromic hereditary deafness. Autosomal dominant non-syndromic deafness, which is often post-lingual, accounts for the remaining 20% (3). Mitochondria and X-linked inheritance account for only 1–2% of non-syndromic deafness. About 30% of genetic deafness is associated with about 700 symptoms described to date, leading to syndromic deafness (4). To date, more than 44 syndromic deafness genes and 100 non-syndromic deafness genes have been mapped (http://hereditaryhearingloss.org).

Currently, next-generation sequencing (NGS) is increasingly applied in clinics to enable accurate diagnosis. In this study, we recruited 13 Chinese Han deafness families negative for *GJB2*, *SLC26A4* and mitochondrial 12S rRNA. The probands of each family

were performed targeted NGS for known hearing loss genes or whole-exome sequencing (WES) to study for pathogenic causes.

Subjects and methods

Subjects collection and audiological evaluations

Thirteen patients (HL1∼13) were recruited from the Department of Otorhinolaryngology-Head and Neck Surgery of Xinhua Hospital affiliated with Shanghai Jiaotong University School of Medicine. Informed consent was approved from all subjects to participate in this study from October 1, 2018 to December 31, 2020. For child participants, written consent will be sought from their parents or guardians. All patients had a detailed medical history and a thorough examination to rule out noise, trauma, pregnancy infection, and other non-genetic factors. All affected subjects were evaluated by audiological examinations, including otoscopy, pure-tone audiometry (PTA), distortion product otoacoustic emissions (DPOAEs), and auditory brainstem response (ABR). Magnetic resonance imaging (MRI) was performed on the HL13 proband. The research was approved by the Ethics Committee of Xinhua Hospital affiliated to Shanghai Jiaotong University School of Medicine (No. XHEC-D-2021-060).

Targeted NGS

Genomic DNA of all family members was extracted from whole peripheral blood leukocytes. Using polymerase chain reaction (PCR) amplification, *GJB2*, *SLC26A4*, and the mitochondrial 12S rRNA exon were directly sequenced first in 13 probands. A panel of 415 hearing loss–related genes was performed by targeted NGS in 12 probands excluding HL6 (Supplementary Table 1). Data processing including targeted gene capturing, filtering of multiple databases for variations, and bioinformation analysis was previously reported in detail (5). Potential causative mutations, which were detected by targeted NGS, were identified for each proband using Sanger sequencing. Where possible, a co-segregation analysis of all family members was also conducted.

Whole exome sequencing

The whole exome sequence of the HL6 proband was sequenced in the Illumina platform by the NextSeq500 sequencer, and the obtained reads by whole exome sequence were mapped to the human genome reference sequence hg19.

SNP arrays

We used SNP arrays to detect the chromosomal regions of CNV identified by targeted NGS in the HL5. SNP arrays were performed as previously reported in detail (5).

Multiplex ligation-dependent probe amplification

The SALSA® MLPA® probe mixes P461-A1 DIS (MRC-Holland, Amsterdam, The Netherlands) was used to identify deletion/duplication of *STRC-CATSPER2* in HL6 and HL7 family members, according to the manufacturer's instructions. The PCR amplification products were analyzed on ABI 3500 Genetic Analyzer (Life-Technologies, Carlsbad, CA) using Gene Marker 1.91 software (Soft Genetics, State College, PA).

Results

Clinical manifestations

There are eight female and five male probands. Those affected individuals ranged in age from 14 months to 49 years. Patients from 13 Chinese families all had congenital, bilateral, and sensorineural hearing loss. They all come to the doctor because they have failed newborn hearing screening or were diagnosed with hearing abnormalities in infancy. Their hearing loss was relatively stable, with the exception of a mild progression of HL5 proband. Hearing loss was defined as varying degrees, including moderate, severe, and profound hearing loss. Click on the auditory brainstem response thresholds was 60–70 dBs for HL5, 40 dBs for HL6, 60–70 dBs for HL7, 40 dBs for the left ear, and 90 dBs for the right ear of HL11 proband. The other probands had profound hearing loss. The HL5 proband was diagnosed with retinitis pigmentosa by an ophthalmologist as a teenager including symptoms of small vision, night blindness, and amblyopia. The HL10 proband had a heterochromia iridis, and her father had a heterochromia iridis but no hearing loss. The HL11 proband had excessive freckles, and his father had excessive freckles but no hearing loss. The HL12 proband had hydronephrosis. Ear malformation was observed in the HL13 proband by MRI, including abnormal enlargement of inner ear canal, bone defect of cochlear apex and skull base, and cerebrospinal fluid.

Genetic findings

To detect possible causative variations by target NGS or WES, nonsynonymous variants were filtered, with minor allele frequencies greater than 0.005 for autosomal recessive, and

TABLE 1 The gene mutation of HL1-13.

Gene	Mutation type	Nucleotide change (transcript version)	Amino acid change	InterAcmg	Mutationtaster	Pathogenic grade	SIFT (score)	Allele frequency in controls	References
Autosomal recessive									
USH2A	Missense	c.9611A>G (NM_206933)	p.H3204R	PM3_Strong, BP4	Polymorphism (1)	Uncertain	Tolerated (0.052)	0/1000	25649381
	Missense	c.7068T>G (NM_206933)	p.N2356K	PM1, BP4	Disease_causing (0.937)	Uncertain	Damaging (0.005)	0/1000	30245029
CDH23	Stop coden	c.2333G>A (NM_022124)	p.W778*	PVS1, PM2	Disease_causing_automatic (1)	Likely_pathogenic	-	0/1000	Novel
	Stop coden	c.6409C>T (NM_022124)	p.Q2137*	PVS1, PM2	Disease_causing_automatic (1)	Likely_pathogenic	-	0/1000	Novel
CDH23	Splicing	c.3579+5G>A (NM_022124.5)	-	PM2	-	Uncertain	-	0/1000	Novel
	Splicing	c.7051_7054+1dup (NM_022124.5)	-	PVS1, PM2	-	Likely pathogenic	-	0/1000	Novel
MYO15A	Missense	c.5693G>A (NM_016239.3)	p.R1898Q	PM2, PP3	Disease_causing (1)	Uncertain	Damaging (0.011)	0/1000	Novel
	Frameshift	c.10258_10260del TTC(NM_016239.3)	p.F3420 fs*	PM3_Strong, PM2, PM4	-	Likely pathogenic	-	0/1000	31250571
ADGRV1	Frameshift	c.12177_12181delGGTTG (NM_032119)	p.V4060 fs*12	PVS1,PM2	-	Likely pathogenic	-	0/1000	Novel
	CNV (whole)	chr5: 89887683 - 90431463	-	-	-	-	-	-	Novel
STRC	CNV (whole)	chr15:43888567-43988112	-	-	-	-	-	-	Novel
STRC	CNV (E15-29)	chr15:43891839-43902647	-	-	-	-	-	-	26969326
TMC1	Splicing	c.16+1C>T (NM_138691)	-	PVS1,PM3_Strong,PM2	Disease_causing (1)	Pathogenic	-	0/1000	25525159
	Splicing	c.535+5G>A (NM_138691)	-	PM2	-	Uncertain	-	0/1000	Novel
Autosomal dominant									

(Continued)

10.3389/fneur.2022.1048218

TABLE 1 (Continued)

Gene	Mutation type	Nucleotide change (transcript version)	Amino acid change	InterAcmg	Mutationtaster	Pathogenic grade	SIFT (score)	Allele frequency in controls	References
PAX3	Frameshift	c.534_535insGGAGGCAGAGGAA (NM_001127366)	p.Q178 fs*29	PVS1,PM2	-	Likely pathogenic	-	0/1000	Novel
PAX3	Splicing	c.1174-2A>T (NM_181457)	-	PVS1, PM3_Strong, PM2	Disease_causing (1)	Pathogenic	-	0/1000	27759048
MITF		c.909G>A (NM_000248)	p.T303T	PM3_Strong,PM2	-	Likely pathogenic	-	0/1000	29986705
PROKR2	Missense	c.337T>C (NM_144773)	p.Y113H	BS1, BS2	Disease_causing (1)	Benign	Damaging (0)	0/1000	30576231
X-linked recessive									
POU3F4	whole deletion	-	-	-	-	-	-	-	27577114

-, No information; *, stop coden.

minor allele frequencies greater than 0.0005 for autosomal dominant. Candidate causative mutations are summarized in Table 1. In 8 recessive families, bi-allelic mutations were found in known deafness genes, part of which were identified by parental genotyping including p.H3204R and p.N2356K in *USH2A* (OMIM 608400), p.Q2137X and p.W778X in *CDH23* (OMIM 605516), c.3795 + 5 G>A and c.7051_7054 + 1dup in *CDH23* (OMIM 605516), p.R1898Q and c.10258_10260 del in *MYO15A* (OMIM 602666), c.12177_12181delGGTTG and a duplication in *ADGRV1* (OMIM 602851), partial or whole gene deletion in *STRC* (OMIM 606440), c.16 + 1C>T and c.535 + 5G>A in *TMC1* (OMIM 606706) (Table 1). In 4 dominant families, four heterozygous variants associated with dominant deafness were identified, including c.534_535 in GGAGGCAGAGGAA in *PAX3* (OMIM 606597), c.1174-2A > T in *PAX3* (OMIM 606597), p.T303T in *MITF* (OMIM 156845), and p.Y113H in *PROKR2* (OMIM 607123), as well as partial co-segregating with the phenotype (Figure 1). In the HL13 proband, we detected the hemizygous deletion of *POU3F4* gene by targeted sequencing, which is consistent with the clinical phenotype of the patient. The co-separation of the reported mutations was confirmed from the hearing phenotype of the extended family members by Sanger sequencing (Figures 1, 2). Of the 19 mutations identified in this study, 10 were reported to be associated with deafness for the first time (Table 1, Figure 2).

Using targeted NGS and SNP arrays, the HL5 proband was found to replicate approximately 544 kb in chromosome region 5q14.3 [arr5q14.3 (89887683-90431463) X3] (Figure 2). Whole exon sequencing revealed a 99 kb of copy number variation in the HL6 proband at 15q15.3 (43888567-43988112), including *STRC*, *CKMT1A*, *CKMT1B,* and *CATSPER2* genes. Using MLPA, we found that the sibling in the HL6 family with the same symptoms also had the same CNV (Figure 3). In the HL7 family, the results of WES and MLPA revealed that the proband had a homozygous deletion in exon 8 and 10 of *CKMT1B* gene, and exon 19, 23–25 of *STRC* gene, heterozygous deletion of exon 1, 2, 4, 7, and 12 of *CATSPER2* gene. Using MLPA, we detected heterozygous deletion of exon 8, 10 of *CKMT1B* gene, and exon 19, 23–25 of *STRC* gene in the father of the proband; heterozygous deletion in exon 8 and 10 of *CKMT1B* gene, exon 19, 23–25 of *STRC* gene, and exon 1, 2, 4, 7, and 12 of *CATSPER2* gene in the mother of the proband (Figure 3).

Discussion

In *CDH23*, homozygous nonsense, frameshift, some missense and splice site mutations, or compound heterozygotes combined of these above USH1D alleles are considered hypomorphic alleles with no sufficient retinal, vestibular, and auditory cochlear function leading to USH1D. Conversely,

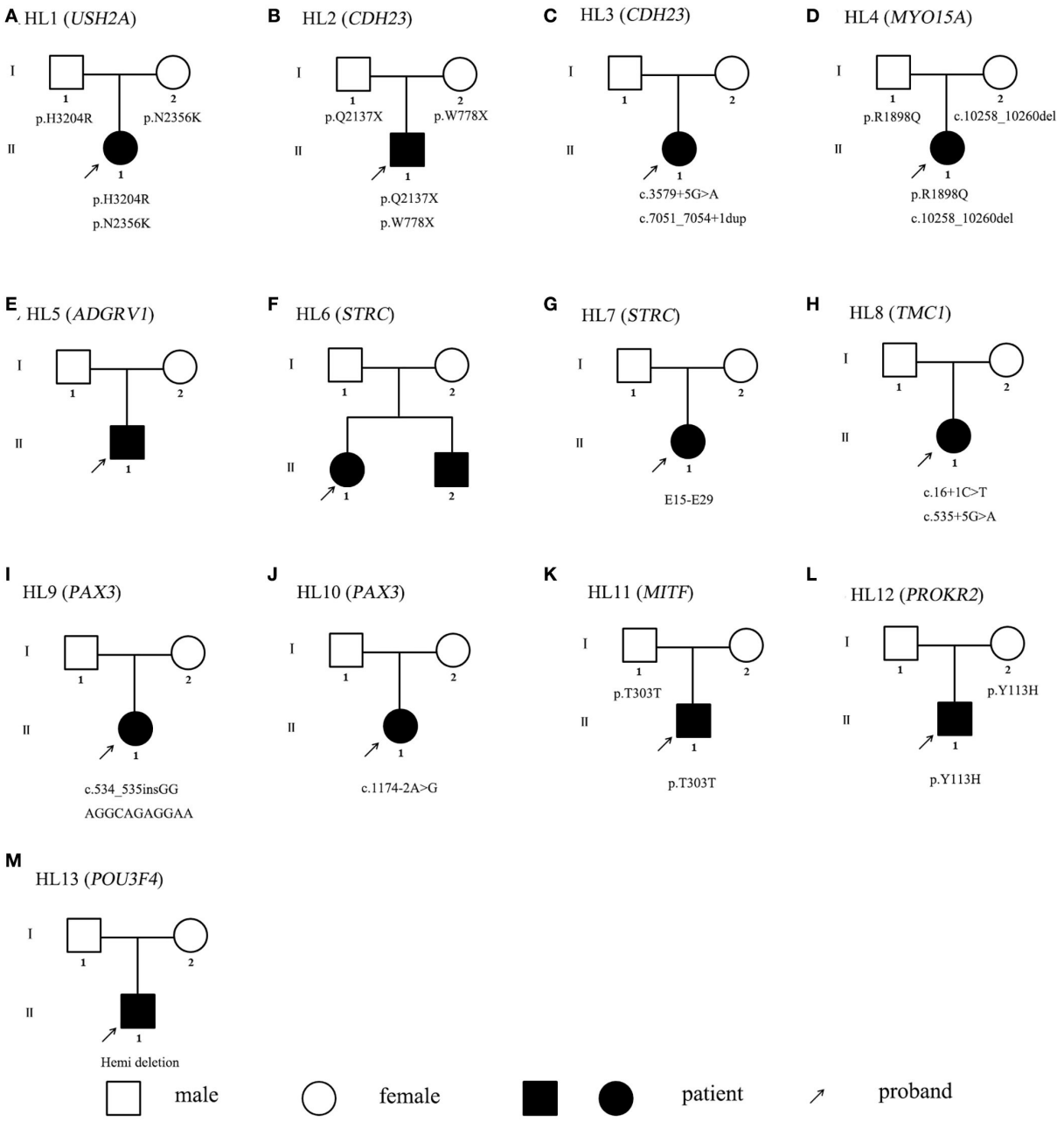

FIGURE 1
(A–M) Pedigrees of HL1-13.

missense mutations in *CDH23* are associated with non-syndromic DFNB12 deafness. The DFNB12 allele maintains normal retinal and vestibular function and is dominant to the USH1D allele phenotypically, even in the presence of the USH1D allele (6). In this study, patients were young at the time of diagnosis. While there are no obvious vestibular and retina symptoms, based on the above principles, we can make a USH1D diagnosis in this study due to the nonsense and splice site mutations of *CDH23* in the proband HL2 and HL3. *ADGRV1* is a pathogenic gene of USH2C, which is belonging to USH2. The primary clinical manifestation of USH2 is congenital moderate to severe deafness, and onset of retinitis pigmentosa within 1–20 years of life, but without vestibular impairment. Besnard et al. (7) concluded that *ADGRV1* mutations account for 6.4% and a small but significant proportion of mutations that cause USH2. Newly

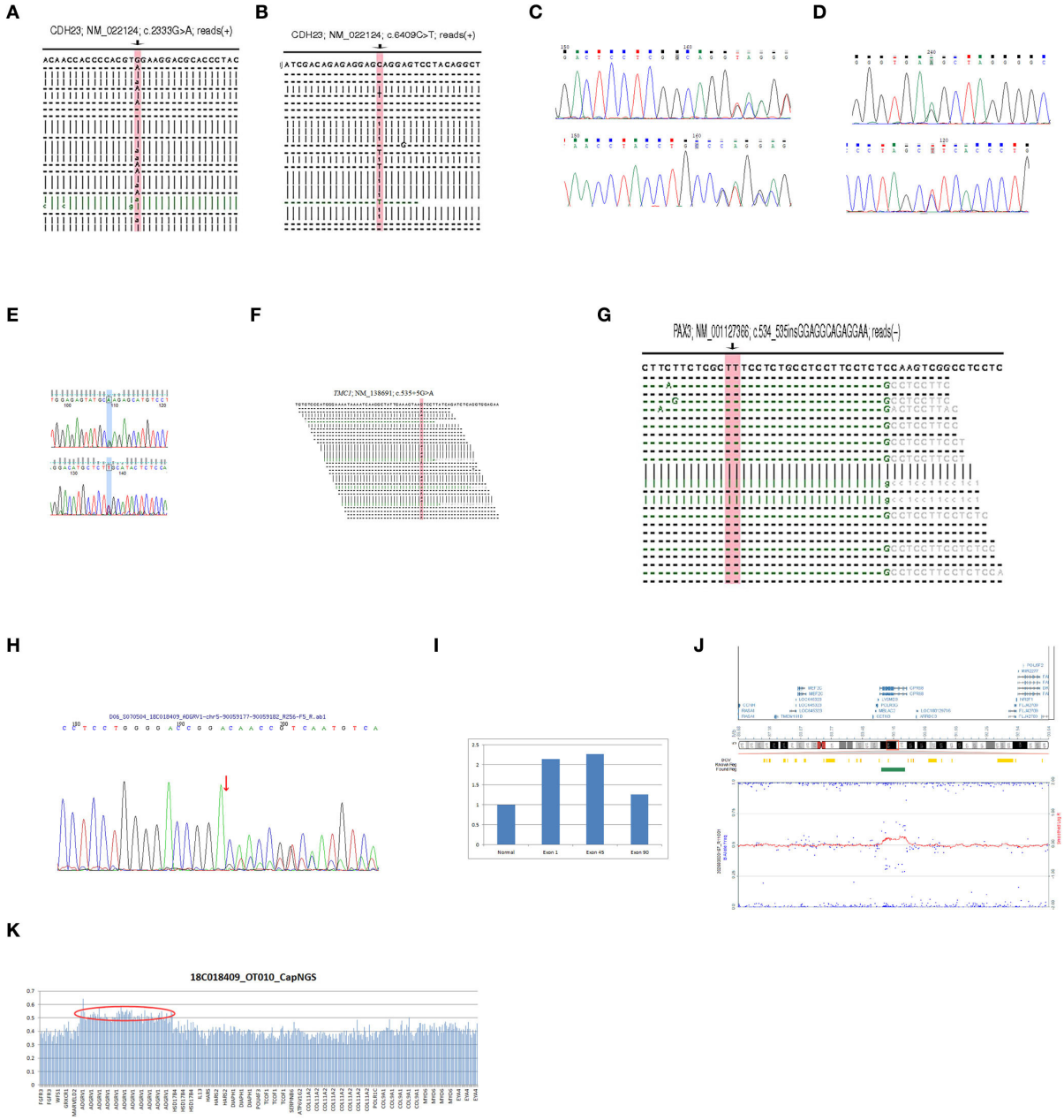

FIGURE 2
(A) The NGS result of the mutation c.2333G > A in *CDH23* of HL2 proband. **(B)** The NGS result of the mutation c.6409C > T in *CDH23* of HL2 proband. **(C)** The Sanger sequencing result of the mutation c.3579 + 5G > A in *CDH23* of HL3 proband. **(D)** The Sanger sequencing result of the mutation c.7051_7054 + 1dup in *CDH23* of HL3 proband. **(E)** The Sanger sequencing result of the mutation c.5693G > A in *MYO15A* of HL4 proband. **(F)** The NGS result of the mutation c.535 + 5G > A in *TMC1* of HL8 proband. **(G)** The NGS result of the mutation c.534_535insGGAGGCAGAGGAA in *PAX3* of HL9 proband. **(H)** The Sanger sequencing result of the mutation c.12177_12181delGGTTG in *ADGRV1* of HL5 proband. **(I)** The qPCR results of the exon 1, 45, and 90 in *ADGRV1* of the HL5 proband contrast to normal. **(J)** The SNP array result of the proband HL5. **(K)** The NGS result of the HL5 proband.

research suggests gene dysfunction associated with Usher syndrome is the second-leading genetic cause of hereditary sensorineural hearing loss after connexin dysfunction (8). In this study, because the probands of HL1, 2, and 3 were still young and only showed hearing problems, they will develop into Usher syndrome in the future. The proband HL5 was over

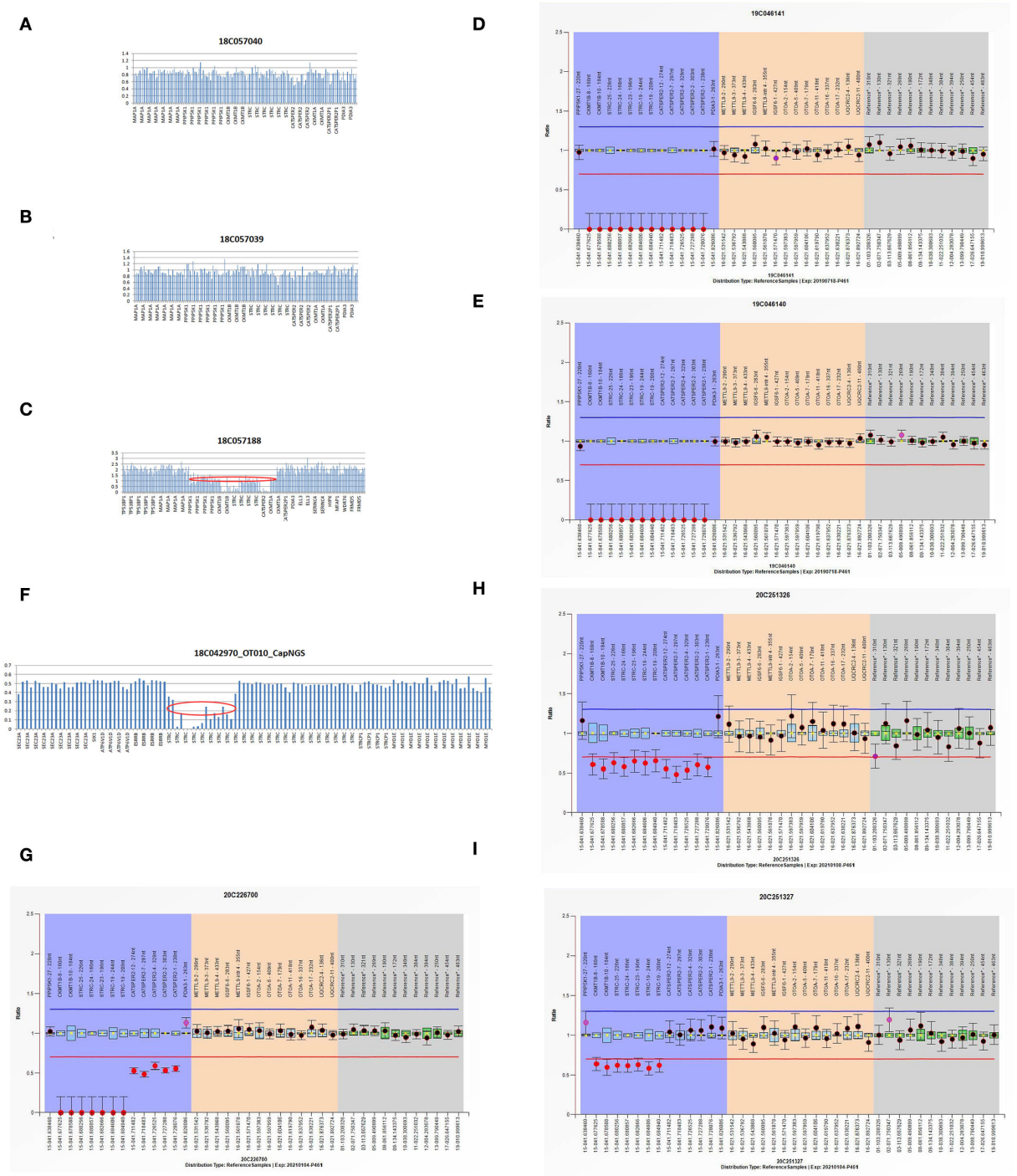

FIGURE 3
(A–C) The WES results of I:1, I:2, and II:1 in HL6 family. **(D,E)** The MLPA results of II:1 and II:2 in HL6 family. **(F)** The NGS result of HL7 proband. **(G–I)** The MLPA results of II:1, I:2, and I:1 in HL7 family.

30 years old, and he showed typical symptoms of the Usher syndrome, including hearing loss, small vision, night blindness, and amblyopia.

Of all congenital sensorineural deafness, *STRC* mutations reported for the first time in 2001 are currently estimated to account for ∼5–6% (9). However, given variable *STRC*

allele frequencies existing in different races, there may be a higher proportion, and an increasing number of cases are reporting copy number variation relevant to clinical in the *STRC* locus (10). *STRC*, with 99.6% coding sequence identity, is closely linked to the pseudogene and is a challenge for the analysis. The gene *CATSPER2*, a neighboring gene to *STRC*, is responsible for sperm motility and leads to deafness infertility syndrome in males, most commonly with sequential deletion of both *STRC* and *CATSPER2* genes. Women with this serial loss only suffer from hearing loss (11). The study indicates that, after the *GJB2* gene which is the majority of mild to moderate inherited deafness, *STRC* deletion accounts for the second most common cause (12). Due to racial differences and insufficient attention, the role of *STRC* gene mutations in the pathogenic of hereditary deafness in China is less reported. The results show that copy number variation of *STRC* gene is not uncommon in clinics. Next-generation sequencing can identify such cases. Combining with the MLPA method, patients can be accurately diagnosed with the *STRC* gene mutation, which requires us to pay more attention to its pathogenicity in the clinic.

Waardenburg syndrome is susceptible to being misdiagnosed as autosomal recessive due to *PAX3* spontaneous mutation and ignores *MITF*-related freckle phenotype. It is a *de novo* mutation c.534_535ins GGAGGCAGAGGAA of *PAX3* in the HL9 proband. C.1174-2A > T in *PAX3* of the HL10 proband and c.909G >A in *MITF* of the HL11 proband were inherited from their fathers, respectively, with heterochromia iridis or excessive freckles but no hearing loss.

DFNX2 (X-linked deafness type 2), with clinical features, typically include progressive mixed hearing loss, stapes fixation, and temporal bone anomalies, is the most common type of X-linked deafness in humans (13, 14). The *POU3F4* mutations account for approximately 50% of genetic causes of DFNX2 (15). Affected men showed mixed hearing loss or less commonly, only sensorineural hearing loss. Typical manifestations of MRI are characterized by hypoplasia of the cochlear base, thickening of the base of stapes floor, loss of the bony modiolus, expansion of internal acoustic meatus, and abnormally wide communication between the cochlear base and the auditory bone (16). In our study, we investigated the HL13 proband was characterized by structural abnormalities of inner ear, X-linked recessive inheritance, and hemizygous deletion in *POU3F4*.

Our research resulted in a limited number of sporadic family samples, and the genetic results of some families are lack of validation by other affected family members, which needs a further evaluation from other relevant studies, especially those novel mutations. Our results also further verified the pathogenicity of the reported mutation sites in the hearing loss population.

Conclusion

The results of the limited samples of this study show that hearing loss is a highly genetic heterogeneous disease. In hearing loss patients negative of *GJB2*, *SLC26A4*, and mitochondrial 12S rRNA, Usher and Waardenburg syndrome-related genes account for a major proportion in Chinese Han families, followed by *STRC* causing mild to moderate hearing loss.

Data availability statement

The datasets presented in this study can be found in online repositories. The names of the repository/repositories and accession number(s) can be found at: https://www.ncbi.nlm.nih.gov/, PRJNA876030.

Ethics statement

The studies involving human participants were reviewed and approved by the Ethics Committee of Xinhua Hospital affiliated to Shanghai Jiaotong University School of Medicine. Written informed consent to participate in this study was provided by the participants' legal guardian/next of kin.

Author contributions

LS and ZL wrote the paper. XW, JS, YL, and YH collected and analyzed the data. JY and LS designed the research. All authors contributed to the article and approved the submitted version.

Funding

This research was supported by grants from the National Natural Science Foundation of China, Grant/Award Numbers: 81873698.

Acknowledgments

The authors thank the family members for their cooperation.

Conflict of interest

The authors declare that the research was conducted in the absence of any commercial or financial relationships

that could be construed as a potential conflict of interest.

Publisher's note

All claims expressed in this article are solely those of the authors and do not necessarily represent those of their affiliated organizations, or those of the publisher, the editors and the reviewers. Any product that may be evaluated in this article, or claim that may be made by its manufacturer, is not guaranteed or endorsed by the publisher.

Supplementary material

The Supplementary Material for this article can be found online at: https://www.frontiersin.org/articles/10.3389/fneur.2022.1048218/full#supplementary-material

References

1. Morton CC, Nance WE. Newborn hearing screening–a silent revolution. *N Engl J Med.* (2006) 354:2151–64. doi: 10.1056/NEJMra050700

2. Shearer AE, Smith RJ. Genetics: advances in genetic testing for deafness. *Curr Opin Pediatr.* (2012) 24:679–86. doi: 10.1097/MOP.0b013e3283588f5e

3. Liu X, Xu L, Zhang S, Xu Y. Epidemiological and genetic studies of congenital profound deafness in the general population of Sichuan, China. *Am J Med Genet.* (1994) 53:192–5. doi: 10.1002/ajmg.1320530214

4. Koffler T, Ushakov K, Avraham KB. Genetics of hearing loss: syndromic. *Otolaryngol Clin N Am.* (2015) 48:1041–61. doi: 10.1016/j.otc.2015.07.007

5. Sun L, Wang X, Hou S, Liang M, Yang J. Identification of MYO6 copy number variation associated with cochlear aplasia by targeted sequencing. *Int J Pediatr Otorhinolaryngol.* (2020) 128:109689. doi: 10.1016/j.ijporl.2019.109689

6. Schultz JM, Bhatti R, Madeo AC, Turriff A, Muskett JA, Zalewski CK, et al. Allelic hierarchy of CDH23 mutations causing non-syndromic deafness DFNB12 or Usher syndrome USH1D in compound heterozygotes. *J Med Genet.* (2011) 48:767–75. doi: 10.1136/jmedgenet-2011-100262

7. Besnard T, Vache C, Baux D, Larrieu L, Abadie C, Blanchet C, et al. Non-USH2A mutations in USH2 patients. *Hum Mutat.* (2012) 33:504–10. doi: 10.1002/humu.22004

8. Guillaume J, Céline P, Marta S, Clémence J, Evan G, Carl A, et al. Genetics of Usher Syndrome: New Insights from a Meta-analysis. *Otol Neurotol.* (2019) 40:121–9. doi: 10.1097/MAO.0000000000002054

9. Marková SP, BroŽková DŠ, Laššuthová P, Mészárosová A, Krutová M, Neupauerová J, et al. gene mutations, mainly large deletions, are a very important cause of early-onset hereditary hearing loss in the Czech population. *Genet Test Mol Biomarkers.* (2018) 22:127–34. doi: 10.1089/gtmb.2017.0155

10. Sloan-Heggen CM, Bierer AO, Shearer AE, Kolbe DL, Nishimura CJ, Frees KL, et al. Comprehensive genetic testing in the clinical evaluation of 1119 patients with hearing loss. *Hum Genet.* (2016) 135:441–50. doi: 10.1007/s00439-016-1648-8

11. Zhang Y, Malekpour M, Al-Madani N, Kahrizi K, Zanganeh M, Lohr NJ, et al. Sensorineural deafness and male infertility: a contiguous gene deletion syndrome. *J Med Genet.* (2007) 44:233–40. doi: 10.1136/jmg.2006.045765

12. Kim BJ, Oh DY, Han JH, Oh J, Kim MY, Park HR, et al. Significant Mendelian genetic contribution to pediatric mild-to-moderate hearing loss and its comprehensive diagnostic approach. *Genet Med.* (2020) 22:1119–28. doi: 10.1038/s41436-020-0774-9

13. Cremers CW, Huygen PL. Clinical features of female heterozygotes in the X-linked mixed deafness syndrome (with perilymphatic gusher during stapes surgery). *Int J Pediatr Otorhinolaryngol.* (1983) 6:179–85. doi: 10.1016/S0165-5876(83)80118-9

14. Phelps PD, Reardon W, Pembrey M, Bellman S, Luxom L. X-linked deafness, stapes gushers and a distinctive defect of the inner ear. *Neuroradiology.* (1991) 33:326–30. doi: 10.1007/BF00587816

15. De Kok YJ, Van der Maarel SM, Bitner-Glindzicz M, Huber I, Monaco AP, Malcolm S, Pembrey ME, Ropers HH, Cremers FP. Association between X-linked mixed deafness and mutations in the POU domain gene POU3F4. *Science.* (1995) 267:685–8. doi: 10.1126/science.7839145

16. Gong WX, Gong RZ, Zhao B. HRCT and MRI findings in X-linked non-syndromic deafness patients with a POU3F4 mutation. *Int J Pediatr Otorhinolaryngol.* (2014) 78:1756–62. doi: 10.1016/j.ijporl.2014.08.013

frontiers | Frontiers in Neurology

TYPE Case Report
PUBLISHED 09 January 2023
DOI 10.3389/fneur.2022.1072220

OPEN ACCESS

EDITED BY
Michael Strupp,
Ludwig Maximilian University of Munich, Germany

REVIEWED BY
Jorge Kattah,
University of Illinois at Chicago, United States
Sun-Uk Lee,
Korea University Medical Center, Republic of Korea

*CORRESPONDENCE
Yu Geng
gengyu@hmc.edu.cn

SPECIALTY SECTION
This article was submitted to Neuro-Otology, a section of the journal Frontiers in Neurology

RECEIVED 17 October 2022
ACCEPTED 14 December 2022
PUBLISHED 09 January 2023

CITATION
Wang H, Shi T, Shang Y, Chen X, Xu J and Geng Y (2023) Case report: Spiller syndrome initially mimicking vestibular neuritis. *Front. Neurol.* 13:1072220. doi: 10.3389/fneur.2022.1072220

Case report: Spiller syndrome initially mimicking vestibular neuritis

Huiyuan Wang[1,2], Tianming Shi[2], Yafei Shang[1,2], Xinyi Chen[2], Jie Xu[2] and Yu Geng[1,2]*

[1]Department of Clinical Medicine, Bengbu Medical College, Bengbu, China, [2]Center for Rehabilitation Medicine, Department of Neurology, Zhejiang Provincial People's Hospital (Affiliated People's Hospital, Hangzhou Medical College), Hangzhou, China

Spiller syndrome is a rare subtype of medial medullary infarction (MMI). Herein, we report on a patient with progressing stroke who presented with the initial features of acute peripheral vestibulopathy and MMI (Spiller syndrome), as confirmed by magnetic resonance imaging (MRI). A 42-year-old man experienced acute persistent vertigo with nausea, vomiting, and severe gait instability for 6 h before presenting to the emergency department. He exhibited spontaneous right-beating horizontal-torsional nystagmus that intensified on rightward gaze. The patient fell to the left side during the Romberg test. Cranial computed tomography (CT) performed immediately upon admission did not provide evidence for ischemia or hemorrhage of the brainstem and cerebellum; however, the symptoms underwent exacerbation 4 h after admission, manifesting as left-sided limb weakness and dysarthria, without dysphagia. Furthermore, bedside examination revealed difficulty in extending the tongue to the right, positive left Babinski's sign, and abnormal vibration and position sense in the paralyzed limb. Head impulse test recording revealed a normal gain in the vestibulo-ocular reflex, and numerous consistent covert corrective saccades were captured upon turning the head to the left side. Cranial MRI depicted an acute infarct confined to the right side of the medial medulla, which met the diagnostic criteria for Spiller syndrome. Our study underscores the importance of considering the possibility of a nucleus prepositus hypoglossi lesion even if the signs and symptoms support the diagnosis of peripheral lesions in patients with acute vestibular syndrome exhibiting vascular risk factors.

KEYWORDS

Spiller syndrome, vestibular neuritis (VN), nucleus prepositus hypoglossal, ischemic stroke (IS), vertigo, nystagmus

1. Introduction

Spiller syndrome, a rare subtype of medial medullary infarction (MMI), is characterized by a triad of contralateral hemiparesis sparing the face, the contralateral loss of deep sensation, and ipsilateral hypoglossal paralysis (1, 2). Owing to the complexity and variability of the vascular supply to the medial medulla oblongata (3, 4), a typical triadic presentation of Spiller syndrome is uncommon (5–7).

Acute vestibular syndrome (AVS) manifests as recent-onset continuous vertigo, nausea, vomiting, motion intolerance, and gait instability lasting from days to weeks (8). Vestibular neuritis (9) is a common etiology of AVS. However, it also occurs in patients with stroke involving the cerebellum or brainstem, i.e., pseudo-vestibular neuritis (10, 11), which has rarely been reported in Spiller syndrome.

This case report describes a patient with progressing stroke who initially presented with the features of both acute peripheral vestibulopathy and MMI (Spiller syndrome), as confirmed by magnetic resonance imaging (MRI).

2. Case description

A 42-year-old man presented with acute persistent vertigo, concomitant with nausea, vomiting, and severe gait instability for 6 h prior to admission to the emergency department (ED). He denied experiencing headaches, neck pain, auditory symptoms, diplopia, dysphagia, dysarthria, and other focal neurological symptoms. He had a history of cerebral hemorrhage, hypertension for 7 years, and diabetes mellitus for 5 years. Physical examination revealed spontaneous right-beating horizontal-torsional nystagmus that became more prominent on rightward gaze (Supplementary Video 1). There were no corrective saccades on the bedside head impulse test (HIT), without head tilt or skew deviation (Supplementary Video 2). The patient fell to the left side during the Romberg test. The general physical and remaining neurological examinations yielded normal results. Cranial computed tomography (CT) performed immediately upon arrival to the ED did not provide any (imaging) evidence for ischemia or hemorrhage of the brainstem and cerebellum (Figure 1). However, CT revealed leftward conjugate ocular deviation upon closing the eyes (Figure 1B). Since the bedside HITs were normal, we considered this patient to have a "pseudo-vestibular neuritis" with central HINTS and administered pharmacotherapy for symptom relief.

Four hours following admission, the symptoms underwent exacerbation, manifesting as left-sided limb weakness and dysarthria, without dysphagia. A bedside examination revealed spontaneous right-beating nystagmus, difficulty in extending the tongue to the right, positive left Babinski's sign, and abnormal vibration and position sense in the paralyzed limb; nonetheless, the patient did not have pain and fever. Subsequently, he underwent cranial magnetic resonance imaging (MRI), which revealed an acute infarct confined to the right side of the medial medulla (Figures 2A–C). Cervical and cranial CT angiography revealed occlusion of the left vertebral artery at the V4 segment (Figure 2D). Furthermore, we recorded nystagmus using a video-oculography system (ICS Impulse, Otometrics, Denmark). The patient exhibited spontaneous right-beating nystagmus with a mean slow-phase velocity (SPV) of 7.7°/s, which decreased during visual fixation, with a mean SPV of 1.6°/s (Figure 3A). Nystagmus was identical to spontaneous nystagmus in all gaze directions but was more intense upon gazing to the right (Figure 3B). HIT recording using the ICS Impulse system revealed a normal gain in the vestibulo-ocular reflex (VOR) (0.99 for the right horizontal canal and 0.84 for the left horizontal canal; normal value >0.80), and numerous consistent covert corrective saccades were captured upon turning the head to the left side (Figure 3C). Echocardiography and electrocardiography did not provide any evidence for a cardiogenic etiology.

Following 1 week, the vestibular symptoms and nystagmus had largely disappeared, and the left limb weakness and deep sensory deficits had partially improved; however, he was still unable to walk independently.

3. Discussion

The patient presented with central unilateral paralysis of the hypoglossal nerve, contralateral limb hemiparesis, and deep sensory hemianopia; thus, the lesion was localized clinically to the sublingual nucleus, corticospinal tract, and medial tegmental tract. Moreover, cranial MRI revealed an acute cerebral infarct in the medial medulla, which met the diagnostic criteria for Spiller syndrome (1). The initial clinical symptoms and abnormal oculomotor signs presented a diagnostic challenge. This is because infarcts located at this anatomical site present only with symptoms of isolated acute vestibular damage commonly arising from the brainstem root entry zone, vestibular nucleus, or cerebellum (12), but not the medial medulla. Therefore, the functional and anatomical relationship between the signs and symptoms of vertigo and medullary infarction in this patient requires further explanation (12, 13).

Interestingly, HIT examinations of the patient demonstrated covert left corrective saccades at 4 days following onset. Furthermore, the gain in the VOR was still within the normal range at 4 days, which confirmed the presence of a clear central

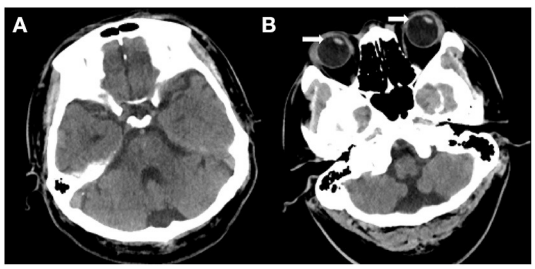

FIGURE 1
(A, B) Cranial computed tomography (CT) demonstrates no abnormality in the brain tissue. **(B)** A leftward conjugate ocular deviation is observed while the eyes are closed (white arrow).

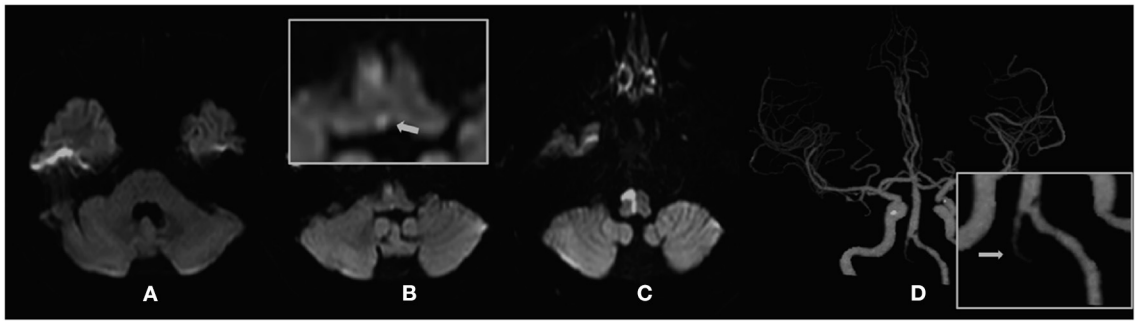

FIGURE 2
(A–C) Diffusion-weighted magnetic resonance imaging (DWI) of the patient. **(A)** No abnormal signal is observed in the vestibular nucleus of the pons. **(B)** Acute infarction in the medial medulla, which involves the nucleus prepositus hypoglossal (NPH) (white arrow). **(D)** Cranial computed tomography angiography (CTA) of the patient demonstrates total occlusion of the left intracranial vertebral artery (ICVA), which represents the offending vessel.

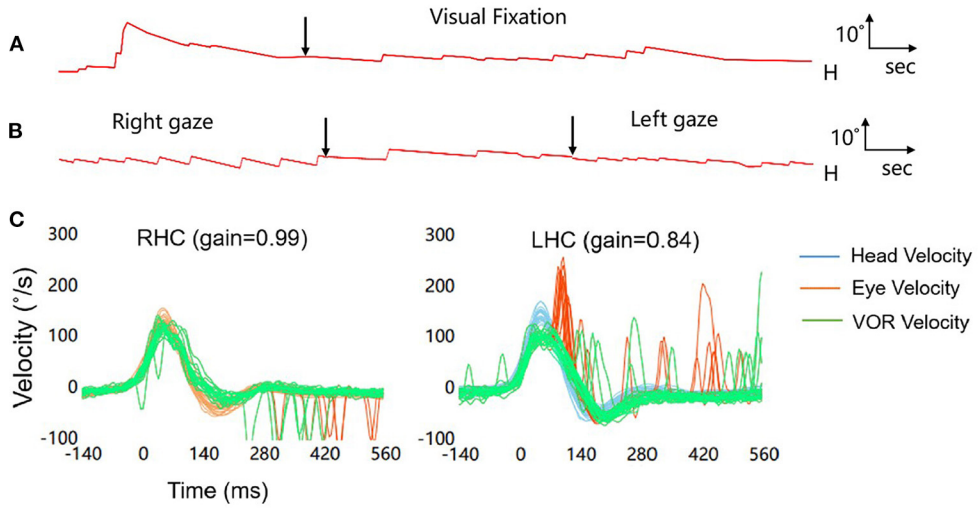

FIGURE 3
(A) Without visual fixation, the patient demonstrates spontaneous right-beating nystagmus with a linear nystagmus waveform and a mean slow-phase velocity (SPV) of 7.7°/s, which decreases during visual fixation, with a mean SPV of 1.6°/s. **(B)** Nystagmus in all gaze directions is similar with spontaneous nystagmus, and is more intense upon staring to the right. **(C)** Results of the video-oculography-based HIT (vHIT) (RHC, right horizontal semicircular canal; LHC, left horizontal semicircular canal). The vHIT results demonstrate numerous corrective saccades in the left horizontal semicircular canal, but the VOR gain is in the normal range, thereby suggesting damage in the central nervous system. vHIT examination of the bilateral anterior semicircular canal and posterior semicircular canal reveals no abnormality.

vestibular compensatory effect (13, 14), thus suggesting the symptoms of vertigo were closely related to the impairment of central vestibular function (11, 15–18). Fibers originating from the nucleus prepositus hypoglossi (NPH) near the dorsal midline of the medulla oblongata can affect contralateral vestibular function by inhibiting the pathway formed by the inferior olive–cerebellar lobule–vestibular nucleus on the contralateral side (12, 19, 20) (Figure 4). Therefore, damage to one side of the NPH leads to vestibular dysfunction on the side opposite to the lesion, vertigo symptoms resembling vestibular neuritis, spontaneous horizontal nystagmus, and vestibular ataxia (12, 20). Moreover, the fibers emanating from the NPH can affect the excitability of the contralateral paramedian pontine reticular formation (PPRF) by affecting the neural pathways between the ipsilateral cerebellar flocculus and fastigial nucleus. Damage to one side of the NPH leads to a decline in the inhibitory effect on the PPRF on the contralateral side, thus increasing excitability; furthermore, the patients may exhibit an ocular contrapulsion (Figure 1B) (21–23). Moreover, an NPH lesion reduces the inhibitory effect on the vestibular nucleus, thus contributing

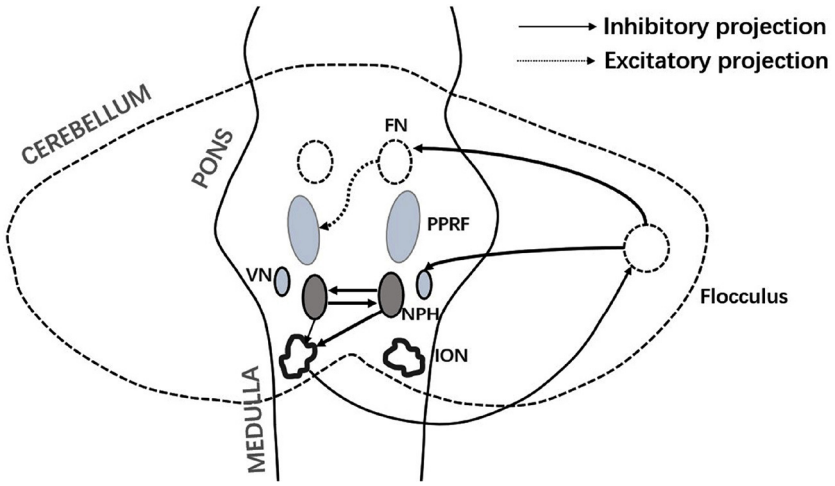

FIGURE 4
Connections between the NPH and vestibular-brainstem-cerebellar system. FN, fastigial nucleus; VN, vestibular nucleus; NPH, nucleus prepositus hypoglossal; PPRF, paramedian pontine reticular formation; and ION, inferior olivary nucleus. The ION principally accepts inhibitory fibers from the contralateral NPH. Damage to one side of the NPH excites the contralateral Purkinje fibers. The contralateral VN and cerebellar fastigial nucleus are suppressed, and the excitability of the contralateral PPRF increases.

to the establishment of central compensatory function and shortening the duration of the vestibular symptoms.

4. Conclusion

This case report described a clinically rare case of progressive classic Spiller syndrome that initially mimicked vestibular neuritis. Clinicians unfamiliar with the NPH may require clarification about the correlation between the initial presentation of contralateral pseudovestibular neuritis to the lesion of this progressive stroke. This case report explains the anatomical site of the NPH and its pathophysiological mechanism in the vestibular-ocular movement pathway such that non-nerve-otology professionals can understand the pathogenesis and clinical manifestations of NPH-mediated "pseudovestibular neuritis."

Data availability statement

The original contributions presented in the study are included in the article/Supplementary material, further inquiries can be directed to the corresponding author.

Ethics statement

Written informed consent was obtained from the individual(s) for the publication of any potentially identifiable images or data included in this article.

Author contributions

HW and YG mainly wrote this article. TS participated in the revision and provided valuable medical records and professional advice. All authors helped organize the case data and provided valuable advice. All authors contributed to the article and approved the submitted version.

Conflict of interest

The authors declare that the research was conducted in the absence of any commercial or financial relationships that could be construed as a potential conflict of interest.

Publisher's note

All claims expressed in this article are solely those of the authors and do not necessarily represent those of their affiliated organizations, or those of the publisher, the editors and the reviewers. Any product that may be evaluated in this article, or claim that may be made by its manufacturer, is not guaranteed or endorsed by the publisher.

Supplementary material

The Supplementary Material for this article can be found online at: https://www.frontiersin.org/articles/10.3389/fneur.2022.1072220/full#supplementary-material

References

1. Pergami P, Poloni TE, Imbesi F, Ceroni M, Simonetti F. Dejerine's syndrome or Spiller's syndrome? *Neurol Sci.* (2001) 22:333–6. doi: 10.1007/s10072-001-8178-3

2. Fukuoka T, Takeda H, Dembo T, Nagoya H, Kato Y, Deguchi I, et al. Clinical review of 37 patients with medullary infarction. *J Stroke Cerebrovasc Dis.* (2012) 21:594–9. doi: 10.1016/j.jstrokecerebrovasdis.2011.01.008

3. Tatu L, Moulin T, Bogousslavsky J, Duvernoy H. Arterial territories of human brain: brainstem and cerebellum. *Neurology.* (1996) 47:1125–35. doi: 10.1212/wnl.47.5.1125

4. Bassetti C, Bogousslavsky J, Mattle H, Bernasconi A. Medial medullary stroke: report of seven patients and review of the literature. *Neurology.* (1997) 48:882–90. doi: 10.1212/wnl.48.4.882

5. Pongmoragot J, Parthasarathy S, Selchen D, Saposnik G. Bilateral medial medullary infarction: a systematic review. *J Stroke Cerebrovasc Dis.* (2013) 22:775–80. doi: 10.1016/j.jstrokecerebrovasdis.2012.03.010

6. Kim JS, Han YS. Medial medullary infarction: clinical, imaging, and outcome study in 86 consecutive patients. *Stroke.* (2009) 40:3221–5. doi: 10.1161/STROKEAHA.109.559864

7. Akimoto T, Ogawa K, Morita A, Suzuki Y, Kamei S. Clinical study of 27 patients with medial medullary infarction. *J Stroke Cerebrovasc Dis.* (2017) 26:2223–31. doi: 10.1016/j.jstrokecerebrovasdis.2017.05.004

8. Hotson JR, Baloh RW. Acute vestibular syndrome. *N Engl J Med.* (1998) 339:680–5.

9. Jeong SH, Kim HJ, Kim JS. Vestibular neuritis. *Semin Neurol.* (2013) 33:185–94. doi: 10.1055/s-0033-1354598

10. Thömke F, Hopf HC. Pontine lesions mimicking acute peripheral vestibulopathy. *J Neurol Neurosurg Psychiatry.* (1999) 66:340–9. doi: 10.1136/jnnp.66.3.340

11. Tarnutzer AA, Berkowitz AL, Robinson KA, Hsieh YH, Newman-Toker DE. Does my dizzy patient have a stroke? A systematic review of bedside diagnosis in acute vestibular syndrome. *CMAJ.* (2011) 183:E571–92. doi: 10.1503/cmaj.100174

12. Seo SW, Shin HY, Kim SH, Han SW, Lee KY, Kim SM, et al. Vestibular imbalance associated with a lesion in the nucleus prepositus hypoglossi area. *Arch Neurol.* (2004) 61:1440–3. doi: 10.1001/archneur.61.9.1440

13. Tighilet B, Bordiga P, Cassel R, Chabbert C. Peripheral vestibular plasticity Vs Central compensation: evidence and questions. *J Neurol.* (2019) 266:27–32. doi: 10.1007/s00415-019-09388-9

14. Swamy Suman N, Kumar Rajasekaran A, Yuvaraj P, Pruthi N, Thennarasu K. Measure of central vestibular compensation: a review. *J Int Adv Otol.* (2022) 18:441–6. doi: 10.5152/iao.2022.21207

15. Strupp M, Bisdorff A, Furman J, Hornibrook J, Jahn K, Maire R, et al. Acute unilateral vestibulopathy/vestibular neuritis: diagnostic criteria. *J Vestib Res.* (2022) 32:389–406. doi: 10.3233/VES-220201

16. Newman-Toker DE, Kattah JC, Alvernia JE, Wang DZ. Normal head impulse test differentiates acute cerebellar strokes from vestibular neuritis. *Neurology.* (2008) 70:2378–85. doi: 10.1212/01.wnl.0000314685.01433.0d

17. Mantokoudis G, Tehrani AS, Wozniak A, Eibenberger K, Kattah JC, Guede CI, et al. Vor gain by head impulse video-oculography differentiates acute vestibular neuritis from stroke. *Otol Neurotol.* (2015) 36:457–65. doi: 10.1097/mao.0000000000000638

18. Machner B, Erber K, Choi JH, Sprenger A, Helmchen C, Trillenberg P, et al. Simple gain-based evaluation of the video head impulse test reliably detects normal Vestibulo-Ocular Reflex indicative of stroke in patients with acute vestibular syndrome. *Front Neurol.* (2021) 12:741859. doi: 10.3389/fneur.2021.741859

19. Kim JS, Choi KD, Oh SY, Park SH, Han MK, Yoon BW, et al. Medial medullary infarction: abnormal ocular motor findings. *Neurology.* (2005) 65:1294–8. doi: 10.1212/01.wnl.0000180627.80595.10

20. Cho HJ, Choi HY, Kim YD, Seo SW, Heo JH. The clinical syndrome and etiological mechanism of infarction involving the nucleus prepositus hypoglossi. *Cerebrovasc Dis.* (2008) 26:178–83. doi: 10.1159/000145325

21. Kim SH, Zee DS, du Lac S, Kim HJ, Kim JS. Nucleus Prepositus Hypoglossi lesions produce a unique ocular motor syndrome. *Neurology.* (2016) 87:2026–33. doi: 10.1212/wnl.0000000000003316

22. Choi WY, Gold DR. Ocular motor and vestibular disorders in brainstem disease. *J Clin Neurophysiol.* (2019) 36:396–404. doi: 10.1097/WNP.0000000000000593

23. Britton Z, Scott G. Ocular ipsipulsion caused by posterior inferior cerebellar artery stroke. *Stroke.* (2022) 53:037510. doi: 10.1161/strokeaha.121.037510

frontiers | Frontiers in Neurology

TYPE Case Report
PUBLISHED 26 June 2023
DOI 10.3389/fneur.2023.1222697

OPEN ACCESS

EDITED BY
Michael Strupp,
Ludwig Maximilian University of Munich, Germany

REVIEWED BY
Nicolina Goldschagg,
Ludwig Maximilian University of Munich, Germany
Bryan Kevin Ward,
Johns Hopkins University, United States

*CORRESPONDENCE
Alexander Andrea Tarnutzer
✉ alexander.tarnutzer@ksb.ch

RECEIVED 15 May 2023
ACCEPTED 31 May 2023
PUBLISHED 26 June 2023

CITATION
Spiegelberg M, Ermiş E, Raabe A and Tarnutzer AA (2023) Triggered episodic vestibular syndrome and transient loss of consciousness due to a retrostyloidal vagal schwannoma: a case report.
Front. Neurol. 14:1222697.
doi: 10.3389/fneur.2023.1222697

Triggered episodic vestibular syndrome and transient loss of consciousness due to a retrostyloidal vagal schwannoma: a case report

Maritta Spiegelberg[1], Ekin Ermiş[2], Andreas Raabe[3] and Alexander Andrea Tarnutzer[1,4]*

[1]Neurology, Cantonal Hospital of Baden, Baden, Switzerland, [2]Department of Radiation Oncology, Bern University Hospital, University of Bern, Bern, Switzerland, [3]Neurosurgery, Bern University Hospital, Bern, Switzerland, [4]Faculty of Medicine, University of Zurich, Zurich, Switzerland

Background: Various conditions may trigger episodic vertigo or dizziness, with positional changes being the most frequently identified condition. In this study, we describe a rare case of triggered episodic vestibular syndrome (EVS) accompanied by transient loss of consciousness (TLOC) linked to retrostyloidal vagal schwannoma.

Case description: A 27-year woman with known vestibular migraine presented with a 19-month history of nausea, dysphagia, and odynophagia triggered by swallowing food and followed by recurrent TLOC. These symptoms occurred independently of her body position, resulting in a weight loss of 10 kg within 1 year and in an inability to work. An extensive cardiologic diagnostic work-up undertaken before she presented to the neurologic department was normal. On the fiberoptic endoscopic evaluation of swallowing, she showed a decreased sensitivity, a slight bulging of the right lateral pharyngeal wall, and a pathological pharyngeal squeeze maneuver without any further functional deficits. Quantitative vestibular testing revealed an intact peripheral-vestibular function, and electroencephalography was read as normal. On the brain MRI, a 16 x 15 x 12 mm lesion in the right retrostyloidal space suspicious of a vagal schwannoma was detected. Radiosurgery was preferred over surgical resection, as resection of tumors in the retrostyloid space bears the risk of intraoperative complications and may result in significant morbidity. A single radiosurgical procedure (stereotactic CyberKnife radiosurgery, 1 x 13Gy) accompanied by oral steroids was performed. On follow-up, a cessation of (pre)syncopes was noted 6 months after treatment. Only residual infrequent episodes of mild nausea were triggered by swallowing solid food remained. Brain MRI after 6 months demonstrated no progression of the lesion. In contrast, migraine headaches associated with dizziness remained frequent.

Discussion: Distinguishing triggered and spontaneous EVS is important, and identifying specific triggers by structured history-taking is essential. Episodes being elicited by swallowing solid foods and accompanied by (near) TLOC should initiate a thorough search for vagal schwannoma, as symptoms are often disabling, and targeted treatment is available. In the case presented here, cessation of (pre)syncopes and significant reduction of nausea triggered by swallowing was noted with a 6-month delay, illustrating the advantages (no surgical complications) and disadvantages (delayed treatment response) of first-line radiotherapy in vagal schwannoma treatment.

KEYWORDS

case report, dysphagia, radiotherapy, transient loss of consciousness, dizziness

1. Introduction

Vagal schwannomas are rare benign nerve tumors with a low incidence that hardly undergo malignant transformation and often present as slow-growing asymptomatic neck masses (1). Definitive pre-operative diagnosis and hence deciding on optimal treatment is often challenging, especially when located in the skull base within the retrostyloid space. In this study, we describe the rare case of a young female patient with recurrent episodes of dizziness, vertigo, and nausea accompanied by (near) transient loss of consciousness (TLOC) triggered by swallowing solid food, that was diagnosed with a retrostyloid vagal schwannoma and focus on the diagnostic workup, differential diagnoses, and treatment options.

2. Case description

A 27-year-old woman presented to our dizzy clinic in February 2021 with a 19-month history of recurrent episodes of dizziness (lasting 2–3 min) accompanied by nausea and dysphagia (located to the right side of the throat by the patient) and odynophagia following swallowing solid foods. Frequently, these episodes were followed by cold sweats, pallor, palpitations, and progressive right-sided tinnitus (with the tinnitus being known for more than 12 years). At the time of presentation, TLOC for approximately 2 to 3 min was noticed at least four times per week (see Figure 1 for the timeline of events). These symptoms occurred independently of her head and body position, and she could not avoid her episodes of TLOC with typical prevention maneuvers for vasovagal syncope such as squatting and leg crossing. Cervical pain, especially during horizontal head rotations or while lying on the right side, was denied. Due to these food-intake-related episodes, the patient lost 10 kg within 12 months. The patient's history was otherwise uneventful except for episodic migraine headaches without aura and a vestibular migraine (with episodes occurring about every other month and lasting for 1 day), and she did not take any medication on a regular basis. The patient's mother suffered from episodic headaches also, and an aunt had been diagnosed with a stroke.

Before presenting to our dizzy clinic, the patient had already received an extensive diagnostic work-up including a cardiologic assessment with no signs of structural heart disease or cardiac arrhythmia (with normal results on transthoracic echocardiography, stress echocardiography, long-term electrocardiography, and heart MRI). A gastroscopy showed normal results. On detailed neurologic and neuro-otologic examination at the time of presentation to our clinic, the patient showed no Horner syndrome, postural hypotension, or paroxysmal cough. Gait and balance testing was within normal range, and no signs of peripheral-vestibular loss-of-function were found on head-impulse testing. Hearing was normal. No symptoms of neurofibromatosis 1 could be detected.

With the episodes being triggered by swallowing solid foods, a fiberoptic endoscopic evaluation of swallowing (FEES) was performed. On FEES, a slight bulging of the right lateral pharyngeal wall with decreased sensitivity to touch was noticed. Pharyngeal squeeze maneuvers revealed a diminished contraction of the right lateral pharyngeal wall, which was considered pathological in comparison to the left side. Pharyngeal squeeze maneuvers also triggered cold sweats and dizziness without progression to syncope. No further functional deficits were noted on FEES, especially no recurrent laryngeal nerve paresis.

Extensive neurologic evaluation including electroencephalography (EEG) and hemodynamic functional testing (Schellong test, 72 h-continuous electrocardiography, and 24 h blood pressure measurement), as well as quantitative vestibular testing (video head-impulse-testing (vHIT), cervical vestibular-evoked myogenic potentials (VEMPs), ocular VEMPs, and caloric irrigation), demonstrated normal results. On magnetic resonance imaging (MRI) of the brain a homogenous, contrast-enhancing lesion in the retrostyloidal space suspicious of a vagal schwannoma (dimensions = 16 x 15 x 12 mm) was detected (Figures 2A–C). On MRI of the cervical spine, no degenerative or post-infectious changes could be depicted. Subsequently, a 68-Ga-DOTA-peptite PET/CT scan was performed to better characterize the metabolic properties of this lesion. Testing showed no expression of SSTR2; hence, a paraganglioma or a glomus vagale tumor was considered unlikely.

Based on these findings, the case was presented to neuro-oncologists, neuro-radiologists, neurosurgeons, and otorhinolaryngologists at the interdisciplinary Schwannoma Board of the University Hospital of Bern, Switzerland. After evaluation, the board proposed a single radiosurgical procedure (stereotactic CyberKnife radiotherapy, 1x13Gy) accompanied by cortisone treatment (dexamethasone 4 mg per day, halving the dose every 3 days) for 10 days in order to cope with any radiation-induced edema. The patient agreed to this treatment, which was performed in March 2022 and was tolerated without any side effects. On 6 weeks of follow-up after treatment, the patient reported no reduction of the triggered episodes of (near) TLOC, dizzy spells, and exacerbated right-sided tinnitus. Weight was stable (60.7 kg). At the same time, however, longer-lasting episodes of vertigo and light-headedness were noticed, accompanied by fear of syncope, exhaustion, and transient left-sided hemisyndrome, which were interpreted as secondary functional symptoms/panic attacks due to complete restitution without treatment. Diagnostic procedures revealed a normal MRI scan of the neurocranium, a normal CT-angiogram, and EEG as well as normal cerebrospinal fluid (CSF) puncture lab and vasculitis screening lab results.

On further follow-up, the patient reported a cessation of episodes with (near) TLOC and dysphagia by October 2022, with residual infrequent episodes of mild nausea triggered by swallowing about twice per week. In contrast, migraine headaches associated with dizziness remained frequent (up to five episodes per week). On repeated brain MRIs obtained in September 2022, the vagal schwannoma was unchanged in size and morphology (Figures 2D–F). On the last follow-up in January 2023, the patient confirmed a regression of her migraine headaches accompanied by dizziness by approximately 50% of episodes and a continuing cessation of episodes with (near) TLOC.

Written informed consent was obtained by the patient for publication. Being a description of a single, clinical case, no ethics approval was required.

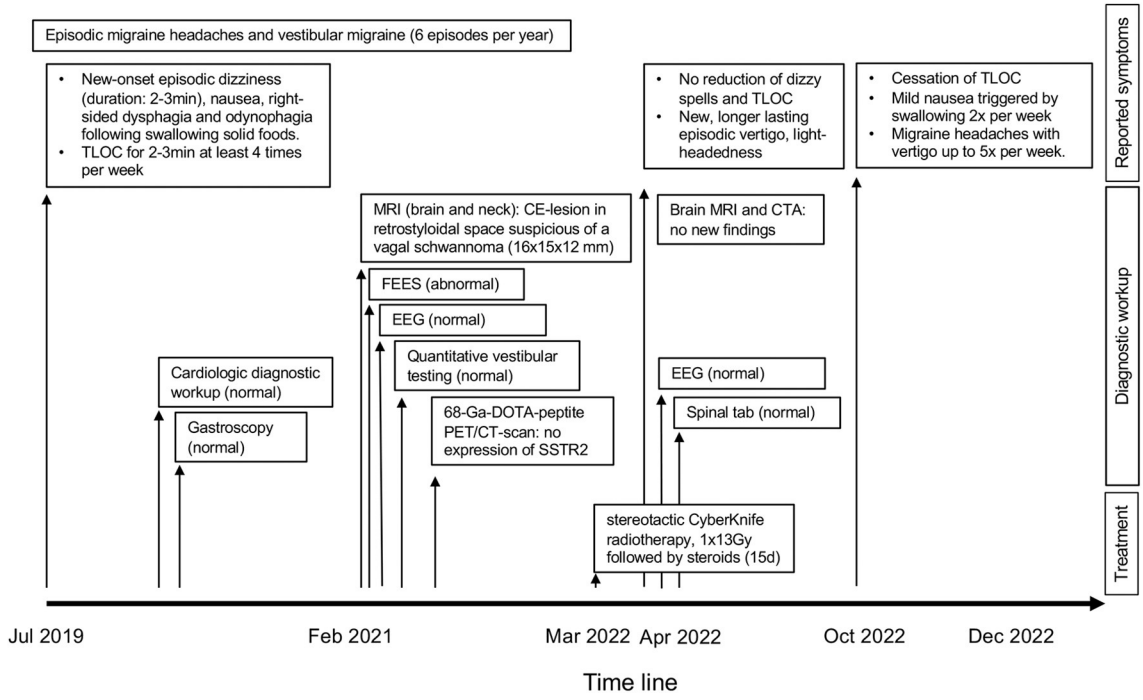

FIGURE 1
Illustration of the timeline of events, with reported complaints, diagnostic testing, and treatments is shown separately. CE, contrast-enhancing; CTA, computed tomography angiography EEG, electroencephalography; FEES, fiberoptic endoscopic evaluation of swallowing; Gy, gray; Ga-DOTA, gallium 68 labeled 1,4,7,10-tetraazacyclododecane-tetraacetic acid; MRI, magnetic resonance imaging; PET/CT, positron emission tomography/computed tomography; SSTR2, somatostatin receptor 2; TLOC, transient loss of consciousness.

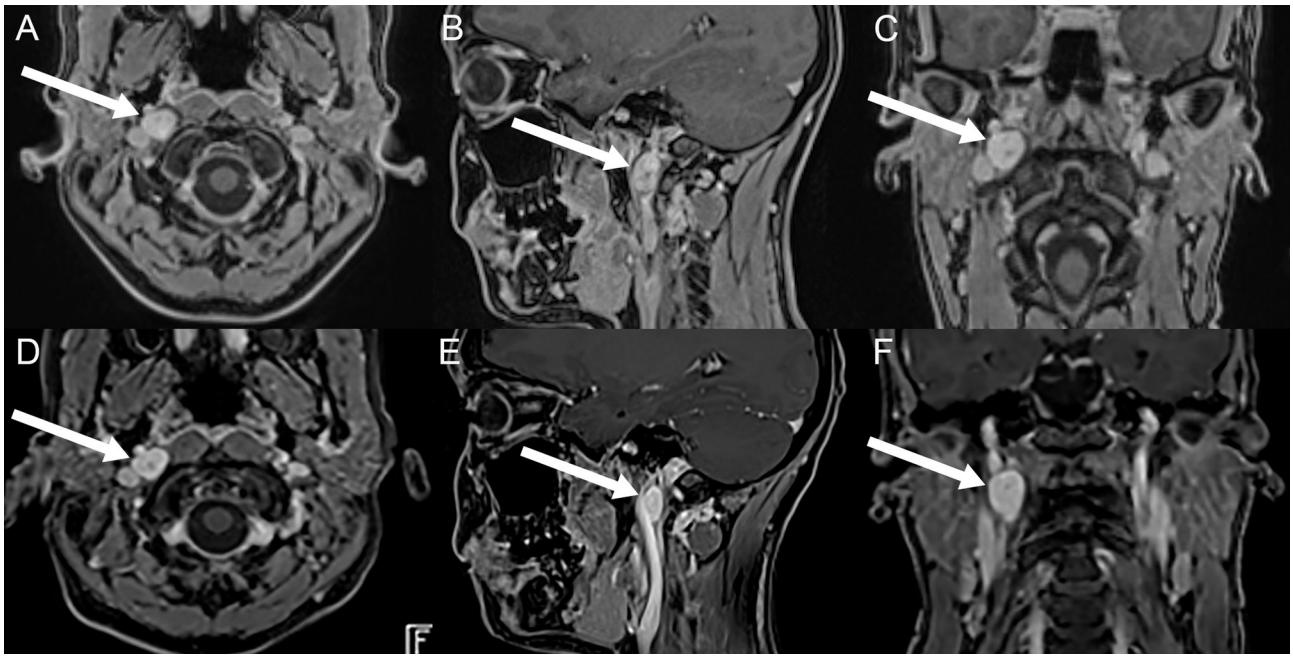

FIGURE 2
Illustration of the vagal schwannoma on brain MRI (axial, sagittal, and coronal post-contrast T1 volumetric interpolated breath-hold examination (VIBE) sequences) before treatment **(A–C)** and on follow-up, 6 months after treatment **(D–F)**. On initial imaging, a contrast-enhancing solid mass (marked with white arrows) in the right retrostyloid space in both the axial **(A)**, sagittal **(B)**, and coronal **(C)** plane can be seen. On follow-up, the solid mass is unchanged in size and morphology. Courtesy of MRI images **(A–C)**: Bilddiagnostik Basel, Switzerland.

3. Discussion

Based on her clinical presentation with recurrent triggered dizziness (2), this patient met the diagnostic criteria for a triggered episodic vestibular syndrome (tEVS) (3). While most frequently tEVS is linked to positional changes in the context of benign paroxysmal positional vertigo (BPPV) and orthostatic hypotension, visual stimuli, or head motion (in patients with chronic vestibular loss-of-function) (3), other less known causes need to be considered as well. In this context, a structured history-taking addressing the specific type of trigger(s) is essential. With swallowing solid foods as a characteristic trigger, it is important to search for rare pathologies including parapharyngeal space-occupying lesions. In our patient, the diagnosis was based on the characteristic clinical presentation and the location of the tumor on MR imaging in the retrostyloidal parapharyngeal space. Importantly, these triggered episodes need to be distinguished from the patient's known migraine headaches and the vestibular migraine.

In most of these patients, neurogenic tumors which hardly undergo malignant transformation can be diagnosed (1, 4, 5). Nevertheless, they represent a considerable diagnostic and treatment challenge: the differentiation between a prestyloid lesion and a retrostyloid lesion is important due to the fact that the majority of retrostyloid parapharyngeal lesions are peripheral nerve sheath tumors, paragangliomas, or lymph node metastases (4). In contrast, prestyloid lesions are benign in 70–80 % and mostly of salivary (pleomorphic adenomas) or rarely neurogenic origin (trigeminal schwannomas). The diagnostic approach to retrostyloid masses includes MR-imaging as well as duplex ultrasound (6) and—after the exclusion of head and neck paragangliomas (7, 8)—transoral or transcervical fine-needle aspiration cytology (9). Vagus schwannomas are well-encapsulated tumors that most often are diagnosed between the third and sixth decade of life, presenting with a cervical, slow-growing mass. When palpable, characteristic findings of parapharyngeal neurogenic tumors can be found, specifically, this mass is typically mobile transversely, but not vertically, and dislocates the carotid artery and the jugular vein anteriorly (10). Paroxysmal cough and hoarseness can be initial symptoms. Schwannomas are often located in the retrostyloid parapharyngeal space but can even extend into the posterior cranial fossa via the jugular foramen (11).

3.1. Treatment options for vagal schwannoma

Different therapeutic approaches need to be evaluated and discussed, ranging from watchful waiting to radiotherapy and microsurgical resection. Since many vagal schwannomas are asymptomatic when diagnosed, observation with serial imaging ("watchful waiting") may be a viable option depending on the size and location of the tumor as well as the age and overall health status of the patient (12). Little is known about the natural history of vagal schwannoma. As summarized by Sandler et al., most authors estimate a growth rate of 1–3 mm per year based on limited case series, anecdotal evidence, and extrapolation from the vestibular schwannoma literature (12). However, most patients on a watchful waiting strategy will eventually need targeted treatment either because of observed tumor growth or the occurrence of clinical symptoms, as in the case presented here.

Surgical excision has been considered the primary treatment option, being highly effective, however, depending on the characteristics of the tumor (location, size, and surgeon's experience) (12). Reports using intraoperative nerve monitoring have shown improved nerve preservation (12, 13). Reports on radiosurgery for vagal schwannomas are still limited (12, 14–16). Radiation therapy is a commonly employed primary treatment option for vestibular schwannomas and has been shown to be extremely effective in halting tumor growth in more than 90% of cases (17). Recently, radiosurgery has been used as a primary treatment for medium to small schwannomas and as a secondary treatment for residual or recurrent disease after microsurgery (15). On the one hand, vagal schwannomas (especially cervical vagal schwannomas) are much easier to access surgically than vestibular schwannoma and thus microsurgical removal while leaving the vagal nerve intact is feasible (12). On the other hand, surgical resection of tumors in the retrostyloid space bears the risk of intraoperative complications (including vagal nerve damage and vocal cord palsy, alterations in phonation and swallowing (including painful swallowing), emergence of a Horner syndrome, and dysfunction of the temporomandibular junction (18)) and may result in significant morbidity. Thus, radiosurgery could be considered in patients who have shown small (i.e., <30 mm in diameter) tumors with tumor growth as in our patient (from 16 mm to 20 mm diameter within 5 months) but are poor surgical candidates (18, 19). Importantly, the anticipated delay in treatment response of more than 6 months needs to be considered also when discussing different treatment options.

While the malignant transformation of vestibular schwannomas following therapeutic radiation has been reported in single cases (20), the estimated risk of a secondary malignancy or malignant transformation of a benign tumor in patients treated with radiosurgery remains low at long-term follow up [0.045% over 10 years (21)]. There are no data on the long-term outcome of vagal schwannoma after radiosurgery. For microsurgical approaches, data are very limited. Different surgical resection techniques seem to have similar recurrence rates (12, 22). Noteworthy, in a systematic review of vagal paragangliomas, the vagal nerve was functionally preserved in only 11 of 254 surgically treated patients (4.3%) (23).

Thus, with radiosurgery selected as a primary treatment strategy, the case reported here reflects a novel approach. Preference for radiosurgery over microsurgical resection was based on an acceptable low risk of neurological deterioration after treatment and the expected long-term local and functional control. To date, resection has been the mainstay treatment for patients with vagal schwannomas. Considering the difficulty in achieving tumor control by surgery alone and the high post-operative morbidity rate, radiosurgery may be an effective and safe modality and a reasonable alternative to surgical resection for small- to medium-sized schwannomas (16).

In our patient, follow-up including MRI scans 6 months after treatment demonstrated stable tumor size with no progression on

imaging and a reported complete cessation of (pre)syncopes with residual infrequent (2x per week) episodes of mild nausea. The patient could return to work by November 2022 and reported no TLOC anymore. The frequency of her vestibular migraine headaches decreased, and she felt healthy again and got pregnant. Further 1 year of follow-up after stereotactic radiosurgery will enable us to further evaluate this treatment option in this special case.

4. Conclusion

Schwannomas arising from the vagal nerve are a rare, benign pathology usually resulting in unspecific symptoms. Definitive pre-operative diagnosis and hence deciding on optimal treatment is often challenging, especially when localized in the skull base and in the retrostyloid space. The differentiation between a prestyloid lesion and a retrostyloid lesion thus is crucial for differential diagnosis. Usually, surgical excision is required, especially in cervical schwannomas, but frequently, post-operative complications can affect patients lifelong, so surgical indications should be based carefully on the balance between risks and benefits (24). Primary radiosurgery may, therefore, present a valuable alternative approach, as demonstrated in our case. Importantly, a delay in symptoms resolving of at least 6 months must be taken into account when selecting this treatment strategy.

Data availability statement

The original contributions presented in the study are included in the article/supplementary material, further inquiries can be directed to the corresponding author.

Ethics statement

Ethical review and approval was not required for the study on human participants in accordance with the local legislation and institutional requirements. The patients/participants provided their written informed consent to participate in this study. Written informed consent was obtained from the individual(s) for the publication of any potentially identifiable images or data included in this article.

Author contributions

MS: data collection, data analysis, interpretation of data for the work, drafting the manuscript, and revising the work critically for important intellectual content. AR: data analysis, interpretation, and revising the manuscript critically for important intellectual content. EE: data analysis, interpretation, and revising the manuscript critically for important intellectual content. AT: conception of the work, interpretation of data for the work, drafting the work, and revising it critically for important intellectual content. All authors approved the final version of the manuscript and agreed to be accountable for all aspects of the work in ensuring that questions related to the accuracy or integrity of any part of the work are appropriately investigated and resolved. The authors confirm that all persons designated as authors qualify for authorship, and all those who qualify for authorship are listed.

Conflict of interest

The authors declare that the research was conducted in the absence of any commercial or financial relationships that could be construed as a potential conflict of interest.

Publisher's note

References

1. Sreevatsa MR, Srinivasarao RV. Three cases of vagal nerve schwannoma and review of literature. *Indian J Otolaryngol Head Neck Surg.* (2011) 63:310–2. doi: 10.1007/s12070-011-0220-z

2. Bisdorff A, Von Brevern M, Lempert T, Newman-Toker DE. Classification of vestibular symptoms: towards an international classification of vestibular disorders. *J Vestib Res.* (2009) 19:1–13. doi: 10.3233/VES-2009-0343

3. Edlow JA, Gurley KL, Newman-Toker DE. A new diagnostic approach to the adult patient with acute dizziness. *J Emerg Med.* (2018) 54:469–83. doi: 10.1016/j.jemermed.2017.12.024

4. Varoquaux A, Fakhry N, Gabriel S, Garcia S, Ferretti A, Chondrogiannis S, et al. Retrostyloid parapharyngeal space tumors: a clinician and imaging perspective. *Eur J Radiol.* (2013) 82:773–82. doi: 10.1016/j.ejrad.2013.01.005

5. Sato Y, Imanishi Y, Tomita T, Ozawa H, Sakamoto K, Fujii R, et al. Clinical diagnosis and treatment outcomes for parapharyngeal space schwannomas: a single-institution review of 21 cases. *Head Neck.* (2018) 40:569–76. doi: 10.1002/hed.25021

6. Tomita T, Ozawa H, Sakamoto K, Ogawa K, Kameyama K, Fujii M. Diagnosis and management of cervical sympathetic chain schwannoma: a review of 9 cases. *Acta Otolaryngol.* (2009) 129:324–9. doi: 10.1080/00016480802179735

7. Olsen WL, Dillon WP, Kelly WM, Norman D, Brant-Zawadzki M, Newton TH. MR imaging of paragangliomas. *AJR Am J Roentgenol.* (1987) 148:201–4. doi: 10.2214/ajr.148.1.201

8. Janssen I, Chen CC, Millo CM, Ling A, Taieb D, Lin FI, et al. PET/CT comparing (68)Ga-DOTATATE and other radiopharmaceuticals and in comparison with CT/MRI for the localization of sporadic metastatic pheochromocytoma and paraganglioma. *Eur J Nucl Med Mol Imaging.* (2016) 43:1784–91. doi: 10.1007/s00259-016-3357-x

9. Mondal P, Basu N, Gupta SS, Bhattacharya N, Mallick MG. Fine needle aspiration cytology of parapharyngeal tumors. *J Cytol.* (2009) 26:102–4. doi: 10.4103/0970-9371.59395

10. Som PM, Sacher M, Stollman AL, Biller HF, Lawson W. Common tumors of the parapharyngeal space: refined imaging diagnosis. *Radiology.* (1988) 169:81–5. doi: 10.1148/radiology.169.1.2843942

11. Yumoto E, Nakamura K, Mori T, Yanagihara N. Parapharyngeal vagal neurilemmoma extending to the jugular foramen. *J Laryngol Otol.* (1996) 110:485–9. doi: 10.1017/S0022215100134061

12. Sandler ML, Sims JR, Sinclair C, Sharif KF, Ho R, Yue LE, et al. Vagal schwannomas of the head and neck: a comprehensive review and a novel approach to preserving vocal cord innervation and function. *Head Neck.* (2019) 41:2450–66. doi: 10.1002/hed.25758

13. Ijichi K, Kawakita D, Maseki S, Beppu S, Takano G, Murakami S. Functional nerve preservation in extracranial head and neck schwannoma surgery. *JAMA Otolaryngol Head Neck Surg.* (2016) 142:479–83. doi: 10.1001/jamaoto.2016.0113

14. Hasegawa T, Kato T, Kida Y, Sasaki A, Iwai Y, Kondoh T, et al. Gamma Knife surgery for patients with jugular foramen schwannomas: a multiinstitutional retrospective study in Japan. *J Neurosurg.* (2016) 125:822–31. doi: 10.3171/2015.8.JNS151156

15. Kano H, Meola A, Yang HC, Guo WY, Martinez-Alvarez R, Martinez-Moreno N, et al. Stereotactic radiosurgery for jugular foramen schwannomas: an international multicenter study. *J Neurosurg.* (2018) 129:928–36. doi: 10.3171/2017.5.JNS162894

16. Shinya Y, Hasegawa H, Shin M, Sugiyama T, Kawashima M, Katano A, et al. Long-term outcomes of stereotactic radiosurgery for trigeminal, facial, and jugular foramen schwannoma in comparison with vestibular schwannoma. *Cancers.* (2021) 13:1140. doi: 10.3390/cancers13051140

17. Albano L, Deng H, Wei Z, Vodovotz L, Niranjan A, Lunsford LD. The longitudinal volumetric response of vestibular schwannomas after Gamma Knife radiosurgery. *J Neurosurg.* (2022) 1–8. doi: 10.3171/2022.7.JNS22812

18. Lopez F, Suarez C, Vander Poorten V, Makitie A, Nixon IJ, Strojan P, et al. Contemporary management of primary parapharyngeal space tumors. *Head Neck.* (2019) 41:522–35. doi: 10.1002/hed.25439

19. Mendenhall WM, Strojan P, Beitler JJ, Langendijk JA, Suarez C, Lee AW, et al. Radiotherapy for parapharyngeal space tumors. *Am J Otolaryngol.* (2019) 40:289–91. doi: 10.1016/j.amjoto.2018.12.010

20. Demetriades AK, Saunders N, Rose P, Fisher C, Rowe J, Tranter R, et al. Malignant transformation of acoustic neuroma/vestibular schwannoma 10 years after gamma knife stereotactic radiosurgery. *Skull Base.* (2010) 20:381–7. doi: 10.1055/s-0030-1253576

21. Wolf A, Naylor K, Tam M, Habibi A, Novotny J, Liscak R, et al. Risk of radiation-associated intracranial malignancy after stereotactic radiosurgery: a retrospective, multicentre, cohort study. *Lancet Oncol.* (2019) 20:159–64. doi: 10.1016/S1470-2045(18)30659-4

22. De Araujo CE, Ramos DM, Moyses RA, Durazzo MD, Cernea CR, Ferraz AR. Neck nerve trunks schwannomas: clinical features and postoperative neurologic outcome. *Laryngoscope.* (2008) 118:1579–82. doi: 10.1097/MLG.0b013e3181 7b0702

23. Suarez C, Rodrigo JP, Bodeker CC, Llorente JL, Silver CE, Jansen JC, et al. Jugular and vagal paragangliomas: systematic study of management with surgery and radiotherapy. *Head Neck.* (2013) 35:1195–204. doi: 10.1002/hed.22976

24. Cavallaro G, Pattaro G, Iorio O, Avallone M, Silecchia G. A literature review on surgery for cervical vagal schwannomas. *World J Surg Oncol.* (2015) 13:130. doi: 10.1186/s12957-015-0541-6

frontiers | Frontiers in Neurology

TYPE Case Report
PUBLISHED 27 July 2023
DOI 10.3389/fneur.2023.1222475

OPEN ACCESS

EDITED BY
Michael Strupp,
Ludwig Maximilian University of Munich, Germany

REVIEWED BY
Sun-Uk Lee,
Korea University Medical Center, Republic of Korea
Doreen Huppert,
Ludwig Maximilian University of Munich, Germany
Filipp Maximilian Filippopulos,
LMU Munich University Hospital, Germany
Michael C. Schubert,
Johns Hopkins University, United States

*CORRESPONDENCE
Vincent G. Wettstein
✉ vgwettstein@gmail.com

RECEIVED 14 May 2023
ACCEPTED 29 June 2023
PUBLISHED 27 July 2023

CITATION
Wettstein VG, Feil B and Mono ML (2023) Case report: A disconjugate pattern in video head impulse testing hints toward a central cause of acute vertigo. *Front. Neurol.* 14:1222475. doi: 10.3389/fneur.2023.1222475

Case report: A disconjugate pattern in video head impulse testing hints toward a central cause of acute vertigo

Vincent G. Wettstein[1]*, Bertram Feil[2] and Marie-Luise Mono[3]

[1]Department of Otolaryngology, Rautipraxis, Zurich, Switzerland, [2]Department of Radiology, Stadtspital Zürich Triemli, Zurich, Switzerland, [3]Department of Neurology, Stadtspital Zürich Triemli, Zurich, Switzerland

When acute vertigo occurs, the challenge for the medical practitioner lies in the focused assessment to find the cause of its symptoms. Especially in the case of central pathology, a fast diagnosis is essential for therapy. The **h**ead impulse, **n**ystagmus, **t**est of **s**kew (HINTS) protocol and the additional video head impulse test (VHIT) can distinguish between central and peripheral vestibular causes in the acute setting and thus help to set the right path for further evaluation and treatment. In this case, a patient with acute onset of vertigo presented with an unusual pattern in the VHIT. Binocular eye tracking showed a disconjugate horizontal vestibulo-ocular reflex (VOR) with severe loss or gain for the adducting eye yet with a lack of corrective saccades. The abducting eye produced a pattern of mild VOR gain loss yet with pronounced corrective saccades. Together with clinical findings that were compatible with internuclear ophthalmoplegia, a probable central lesion in the medial longitudinal fasciculus (MLF) region was suspected. The patient was sent to a tertiary hospital, where the initial MRI was negative, but due to additional neurological symptoms occurring later, multiple lesions in the cervical spine and cerebellum were detected. The hypothesis of an inflammatory demyelinating disease of the central nervous system (CNS) was made. A further workup led to the final diagnosis of neurosarcoidosis. In a retrospective neuroradiologic assessment, an alteration compatible with a non-active demyelinating lesion in the MLF was detected on secondary imaging as a probable cause of the initial pathophysiologic finding. In this report, we aimed to highlight the unusual case of a disconjugate VOR as a distinctive VHIT pattern hinting toward a central cause of acute vertigo that clinicians should be aware of.

KEYWORDS

binocular, INO, neurosarcoidosis, disconjugate, internuclear ophthalmoplegia, video head impulse test (VHIT)

1. Introduction

The assessment of a patient with acute vertigo in order to come to appropriate conclusions for treatment is challenging. A variety of causes can lead to dizziness and vertigo. While peripheral-vestibular disorders account for the majority of cases (1), acute neurologic pathologies, such as stroke, can also present with dizziness without any other leading symptoms (2). Over the last few years, focused clinical examination guidelines were established in order to quickly reach a conclusive diagnosis for further treatment. The **h**ead impulse, **n**ystagmus, **t**est of **s**kew (HINTS) protocol enables clinicians to distinguish between central and peripheral disorders with high precision (3). Additionally, the video

head impulse test (VHIT) serves as a fast tool to measure semicircular canal function (4–6) and can therefore contribute to the first assessment.

However, in some cases, we are unable to achieve diagnosis in the acute setting due to challenging clinical examination when symptoms are severe and cooperation is reduced or due to unclear or unexpected clinical findings.

In this report, we present a case where we were challenged by an unusual VHIT finding not yet described in a patient with acute vertigo. A subsequent workup led to the diagnosis of a rare neurological disease.

2. Case description

A 55-year-old patient presented with acute vertigo. He complained about aggravated symptoms with movements of the head and an unstable gait, as well as nausea and vomiting. Apart from treatment for hypertension and hypercholesterinemia, the patient was healthy.

Clinical findings were as follows: predominantly down beating nystagmus in eccentric gaze positions, with and without fixation. With attempted right gaze, an adduction paresis of the left eye and an abduction nystagmus of the right eye were documented, consistent with the clinical phenotype of left internuclear ophthalmoplegia. With left gaze, no gaze palsy or abduction nystagmus was seen. Vertical eye movements were normal. The test of skew showed no ocular tilt reaction. The clinical head impulse test was inconclusive; therefore, binocular video head impulse testing [Synapsys VHIT Ulmer 2.0, Marseille (7)] was performed (Figure 1).

Horizontal semicircular canal testing with binocular eye tracking showed a reduced gain on both sides (0.65 on the right and 0.63 on the left, normal value = >0.8) and an asymmetry ratio of 1%.

The cumulative impulse graph on the right side was congruent with a mild loss of horizontal semicircular canal function, showing slightly reduced gain and both covert and overt saccades (8). Individual gain analysis revealed a higher gain (0.67) for the left (abducting) eye than for the right (adducting) eye (0.48), yet covert and overt corrective saccades were detected for both eyes in a similar pattern.

Head impulses to the left side, however, showed a disconjugate pattern of the abducting and adducting eye. Measurement of the

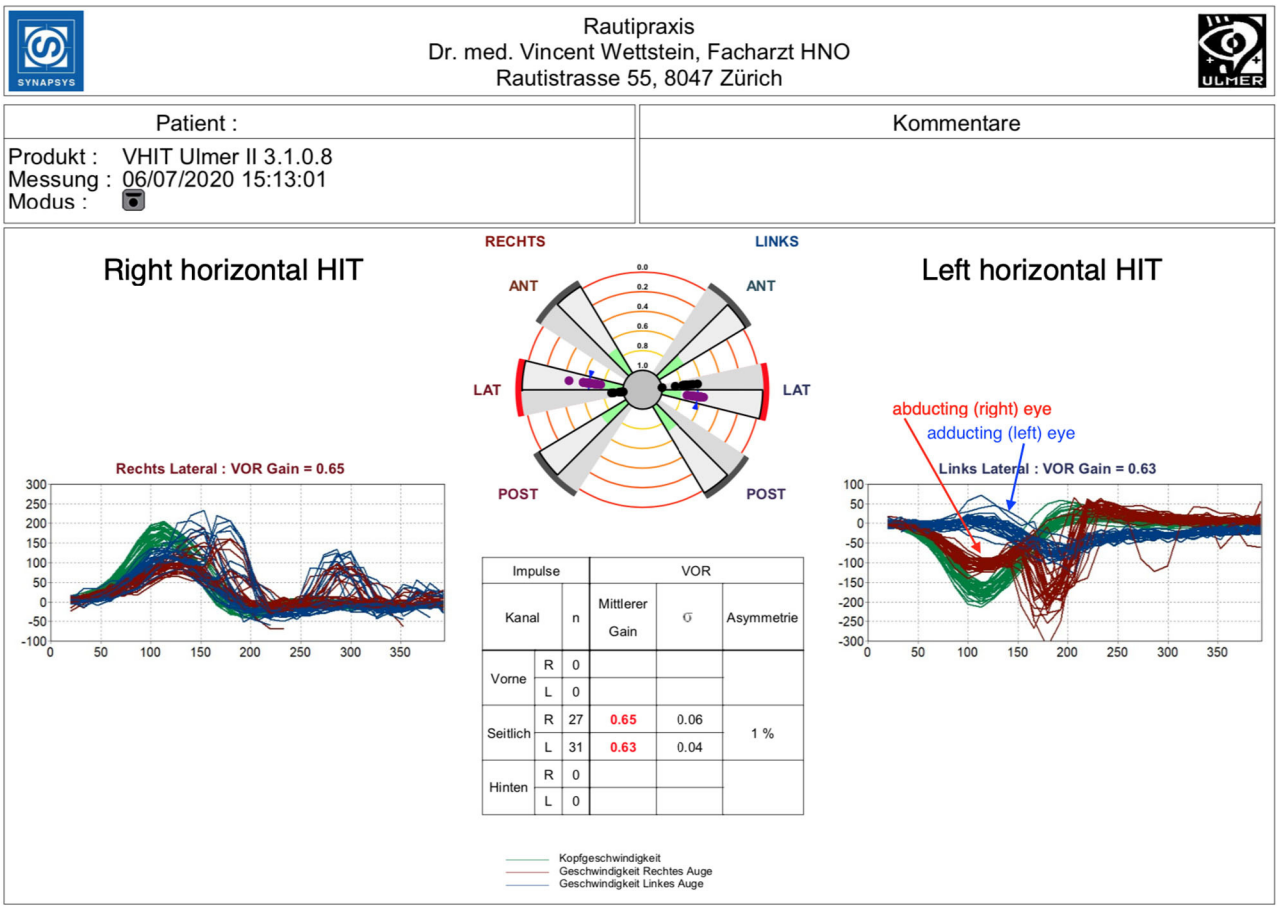

FIGURE 1
Right horizontal HIT: mild hypofunction with a reduced gain of 0.65 (normal value = >0.8) and both covert and overt saccades. Left horizontal HIT: disconjugate pattern. Mild to moderate gain reduction of 0.61 with a robust covert saccade bundle of the right abducting eye (red). Left adducting eye analysis (blue) shows a severe gain reduction of 0.09 yet no correction saccades.

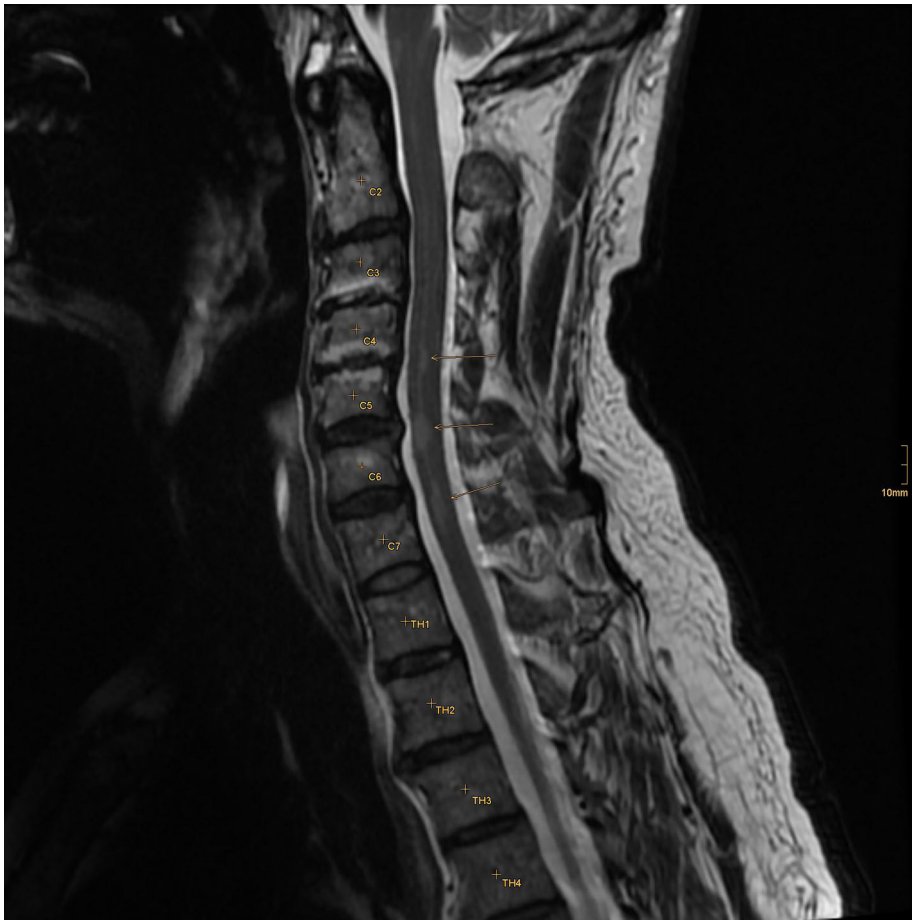

FIGURE 2
Three T2W hyperintense lesions in the cervical myelon.

right (abducting) eye revealed a mild to moderate gain reduction of 0.61 with a robust saccade bundle starting ~150–200 ms after the initiation of the head impulse. Left (adducting) eye analysis showed a severe gain reduction of 0.09 and a slight elevation of eye velocity toward the end of the head movement, yet there were no correction saccades following the head impulse in spite of the severe loss of gain.

Applying the HINTS protocol to these findings, VOR gain reduction and corrective saccades should suggest a loss of canal function and therefore a peripheral cause, while downbeating gaze nystagmus, as well as gaze palsy, hint toward central disorders. The disconjugate VHIT pattern of the right and left eye could not be attributed to a peripheral-vestibular disorder but was rather associated with a probable central lesion in the medial longitudinal fasciculus (MLF) region, as described in a scleral search coil study by Aw et al. (9).

3. Diagnostic assessment, treatment, follow-up, and outcomes

The patient was immediately admitted to the neurologic department of a tertiary hospital for further diagnosis and treatment. An MRI of the brain showed no recent ischemic or inflammatory lesion but some non-specific white matter lesions. An MRI-negative stroke due to small vessel disease was suspected, and treatment with aspirin and clopidogrel was started. A further stroke workup showed no other etiology, and the patient was discharged to home. A few days later, the patient was re-admitted due to progressive dizziness and paresis of the right leg. Extended MR imaging revealed three inflammatory lesions in the cervical spine and a hyperintense lesion in the right cerebellar hemisphere showing contrast enhancement (Figures 2, 3).

The cerebrospinal fluid (CSF) on the lumbar puncture showed pleocytosis in 86 cells and slightly elevated protein and lactate levels. There was an intrathecal IgG synthesis combined with a systemic immune reaction. There were no signs of an infective disease or systemic vasculitis. A chronic remitting inflammatory demyelinating disease of the central nervous system (CNS), e.g., multiple sclerosis, was suspected.

The patient was treated with high-dose intravenous (IV) prednisolone for 5 days and transferred to a rehabilitation clinic where his condition initially improved.

Because of a prolonged stay at the rehabilitation clinic, the follow-up examination at the tertiary hospital was several weeks later than initially planned. The patient, then, reported progressive

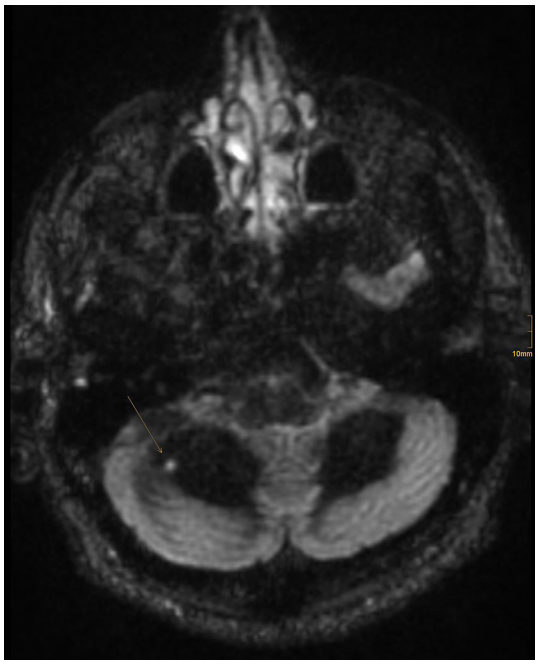

FIGURE 3
One FLAIR hyperintense lesion in the right cerebellar hemisphere showing contrast enhancement.

weakness in the right leg and paresthesia in both legs. Clinical examination revealed an impaired monoparesis of the right leg, a severe disturbance of proprioception of the leg left, and a sensitive disturbance below the eighth thoracic vertebra (T8) on both sides due to new inflammatory lesions in the cervical and thoracic spinal cord. CSF puncture revealed a mononuclear pleocytosis of 62 cells and elevated protein levels. The aquaporin and myelin oligodendrocyte glycoprotein (MOG) antibodies in serum and CSF were negative. There were also no clinical or laboratory signs of an underlying systemic disease such as systemic lupus erythematosus (SLE) or any systemic vasculitis. The sIL2 receptor in the CSF was elevated (365.1). Together with the intrathecal IgG synthesis, combined with signs of a systemic immune reaction and pleocytosis > 50, without evidence for any infective or any other autoimmune disease, this indicated the diagnosis of neurosarcoidosis.

The patient was again treated with high-dose IV prednisolone followed by oral tapering and rituximab (initially 2 × 1,000 mg). He continued to receive this treatment every 6 months with 1,000 mg. Since then, his medical condition has been stable without any evidence of disease activity or affection of the lung.

4. Discussion

To the best of our knowledge, this is the first description of a VHIT finding with disconjugate horizontal VOR in patients with acute vertigo. We report this case to highlight the correlation between the clinical finding of acute INO and a distinctive, disconjugate VHIT pattern. It reveals severe VOR gain reduction yet missing corrective saccades in the head impulse analysis of the adducting eye, whereas the results for the abducting eye display a pattern consistent with mild semicircular canal hypofunction and corrective saccades.

Disconjugate VOR deficits have been shown in multiple sclerosis patients with internuclear ophthalmoplegia (INO) by Aw et al. (9) using the binocular scleral search coil technique. In this study, the same distinctive pattern of VOR disconjugacy was found for both unilateral and bilateral INO. The adducting eye revealed a more severe loss of VOR, but no corrective saccades, whereas the abducting eye had larger VOR gains and corrective saccades. Since the same pattern was found in our case, a central-vestibular disorder was suspected and ultimately diagnosed in the form of a chronic remitting inflammatory demyelinating disease. We can, therefore, confirm a disconjugate VOR deficit originating from a CNS disease by using the binocular VHIT technique. Recently, Grove et al. were able to show that multiple sclerosis (MS) patients with low VOR gain have reduced or absent compensatory saccades (CSs) (10, 11). They further postulated that the lack of CS in correlation with reduced VOR in VHIT may be pathognomonic for INO. Using binocular VHIT assessment, we were able to specify this pattern to the adducting eye in INO. Together with the higher gain of the abducting eye in combination with present CS, we argue that this pattern could be a pathognomonic (binocular) VHIT sign for INO.

Another study using monocular VHIT on patients with INO found a deficit of the contralateral posterior canal (12). Since only one eye was tracked, this finding is of importance for clinicians using monocular VHIT systems. However, we argue that by using monocular VHIT equipment, VOR disconjugacy in correlation with clinical INO would have been missed, and therefore, the diagnosis could not have been made.

The MRI following the first and second assessments revealed remitting inflammatory lesions in the spinal cord and the cerebellum, with additional neurological workup finally leading to the diagnosis of neurosarcoidosis. With the initial clinical findings described above, we suspected a lesion in the medial longitudinal fasciculus (MLF). However, primary imaging did not reveal pathology in this region. In a retrospective neuroradiological assessment, we were able to discover a small lesion in probable correlation with the patient's neurologic visual disorder in the secondary MRI imaging. At the level of the inferior colliculi, the MLF showed an enhanced signal in the FLAIR protocol (Figure 4).

The small finding had no correlation in the diffusion-weighted sequences and no enhancement with contrast agents. Nevertheless, it is compatible with a non-active demyelinating lesion that could have caused the initial pathophysiological alteration. Why this MLF lesion was not detected at the time of primary imaging remains unclear. An explanation could be the short-time interval between the onset of the clinical finding and the first MRI. Small lesions are known to be missed in acute dizzy patients (3, 13). Inadequate slice thickness could have also led to a missed lesion in the MLF region.

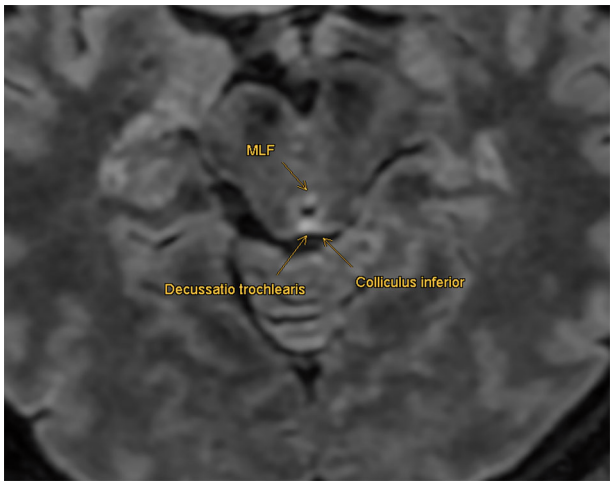

FIGURE 4
Retrospective imaging analysis: MLF shows an enhanced signal in the FLAIR protocol at the level of the inferior colliculi, compatible with a non-active demyelinating lesion. No correlation in the diffusion-weighted sequences and no enhancement with contrast agents were found retrospectively.

5. Patient perspective

In conclusion, our case supports the use of VHIT assessment in patients with acute dizziness or vertigo. By using bilateral eye tracking, ocular disconjugate VOR deficits can be revealed, leading to an accelerated and focused investigation of central pathologies. In this case, we report a distinctive VHIT pattern in correlation with the clinical finding of acute internuclear ophthalmoplegia. In the case of this patient, the origin of the pathological finding was only discovered in the further course of the disease. With our report, we hope to facilitate vestibular assessment for clinicians dealing with similar cases with a specific diagnostic feature. This might be especially helpful in patients with clinically occult INO or reduced cooperation. Further reports of acute cases with analogical binocular VHIT findings may support our hypothesis. Since new VHIT studies using binocular eye tracking emerge (14) and novel devices enter the VHIT market, we are confident that our findings will be of value in future diagnostics. We, therefore, encourage and recommend the use of VHIT in the emergency setting, while highlighting a distinctive finding that clinicians should be aware of.

Data availability statement

The original contributions presented in the study are included in the article/supplementary material, further inquiries can be directed to the corresponding author.

Ethics statement

Ethical review and approval was not required for the study on human participants in accordance with the local legislation and institutional requirements. Written informed consent from the patients/participants or patients/participants legal guardian/next of kin was not required to participate in this study in accordance with the national legislation and the institutional requirements. Written informed consent was obtained from the patient for the publication of any potentially identifiable images or data included in this article.

Author contributions

VGW carried out the first assessment of the patient including the VHIT. He is responsible for the idea, the concept, and the design of the article. MLM led the patient's further follow up and treatment. She contributed substantially to the content of the manuscript. BF investigated on and reviewed the radiologic findings and critically revised the manuscript. All authors contributed to the article and approved the submitted version.

Conflict of interest

The authors declare that the research was conducted in the absence of any commercial or financial relationships that could be construed as a potential conflict of interest.

Publisher's note

All claims expressed in this article are solely those of the authors and do not necessarily represent those of their affiliated organizations, or those of the publisher, the editors and the reviewers. Any product that may be evaluated in this article, or claim that may be made by its manufacturer, is not guaranteed or endorsed by the publisher.

References

1. Newman-Toker DE, Hsieh YH, Camargo CA Jr, Pelletier AJ, Butchy GT, Edlow JA. Spectrum of dizziness visits to US emergency departments: cross-sectional analysis from a nationally representative sample. *Mayo Clin Proc.* (2008) 83:765–75. doi: 10.4065/83.7.765

2. Tarnutzer AA, Berkowitz AL, Robinson KA, Hsieh YH, Newman-Toker DE. Does my dizzy patient have a stroke? A systematic review of bedside diagnosis in acute vestibular syndrome. *CMAJ.* (2011) 183:E571–92. doi: 10.1503/cmaj.100174

3. Kattah JC, Talkad AV, Wang DZ, Hsieh YH, Newman-Toker DE. HINTS to diagnose stroke in the acute vestibular syndrome: three-step bedside oculomotor examination more sensitive than early MRI diffusion-weighted imaging. *Stroke.* (2009) 40:3504–10. doi: 10.1161/STROKEAHA.109.551234

4. MacDougall HG, Weber KP, McGarvie LA, Halmagyi GM, Curthoys IS. The video head impulse test: diagnostic accuracy in peripheral vestibulopathy. *Neurology.* (2009) 73:1134–41. doi: 10.1212/WNL.0b013e3181bacf85

5. Mantokoudis G, Tehrani AS, Wozniak A, et al. VOR gain by head impulse video-oculography differentiates acute vestibular neuritis from stroke. *Otol Neurotol.* (2015) 36:457–65. doi: 10.1097/MAO.0000000000000638

6. Newman-Toker DE, Saber Tehrani AS, Mantokoudis G, Pula JH, Guede CI, Kerber KA, et al. Quantitative video-oculography to help diagnose stroke in acute vertigo and dizziness: toward an ECG for the eyes. *Stroke.* (2013) 44:1158–61. doi: 10.1161/STROKEAHA.111.000033

7. Murnane O, Mabrey H, Pearson A, Byrd S, Akin F. Normative data and test-retest reliability of the SYNAPSYS video head impulse test. *J Am Acad Audiol.* (2014) 25:244–52. doi: 10.3766/jaaa.25.3.3

8. Weber KP, Aw ST, Todd MJ, McGarvie LA, Curthoys IS, Halmagyi GM. Head impulse test in unilateral vestibular loss: vestibulo-ocular reflex and catch-up saccades. *Neurology.* (2008) 70:454–63. doi: 10.1212/01.wnl.0000299117.48935.2e

9. Aw ST, Chen L, Todd MJ, Barnett MH, Halmagyi GM. Vestibulo-ocular reflex deficits with medial longitudinal fasciculus lesions. *J Neurol.* (2017) 264:2119–29. doi: 10.1007/s00415-017-8607-8

10. Grove CR, Wagner A, Loyd BJ, Dibble LE, Schubert MC. Unique compensatory oculomotor behavior in people living with multiple sclerosis. *J Neurol Sci.* (2022) 442:120411. doi: 10.1016/j.jns.2022.120411

11. Grove CR, Wagner A, Yang VB, Loyd BJ, Dibble LE, Schubert MC. Greater disability is associated with worse vestibular and compensatory oculomotor functions in people living with multiple sclerosis. *Brain Sci.* (2022) 12:1519. doi: 10.3390/brainsci12111519

12. Lee SH, Kim SH, Kim SS, Kang KW, Tarnutzer AA. Preferential impairment of the contralesional posterior semicircular canal in internuclear ophthalmoplegia. *Front Neurol.* (2017) 8:502. doi: 10.3389/fneur.2017.00502

13. Saber Tehrani AS, Kattah JC, Mantokoudis G, Pula JH, Nair D, Blitz A, et al. Small strokes causing severe vertigo: frequency of false-negative MRIs and nonlacunar mechanisms. *Neurology.* (2014) 83:169–73. doi: 10.1212/WNL.0000000000000573

14. Striteska M, Chovanec M, Steinmetzer T, Chrobok V, Profant O, Schneider E, et al. Binocular video head impulse test: Normative data study. *Front Neurol.* (2023) 14:1153102. doi: 10.3389/fneur.2023.1153102

Frontiers in Neurology

Explores neurological illness to improve patient care

The third most-cited clinical neurology journal explores the diagnosis, causes, treatment, and public health aspects of neurological illnesses. Its ultimate aim is to inform improvements in patient care.

Discover the latest Research Topics

See more →

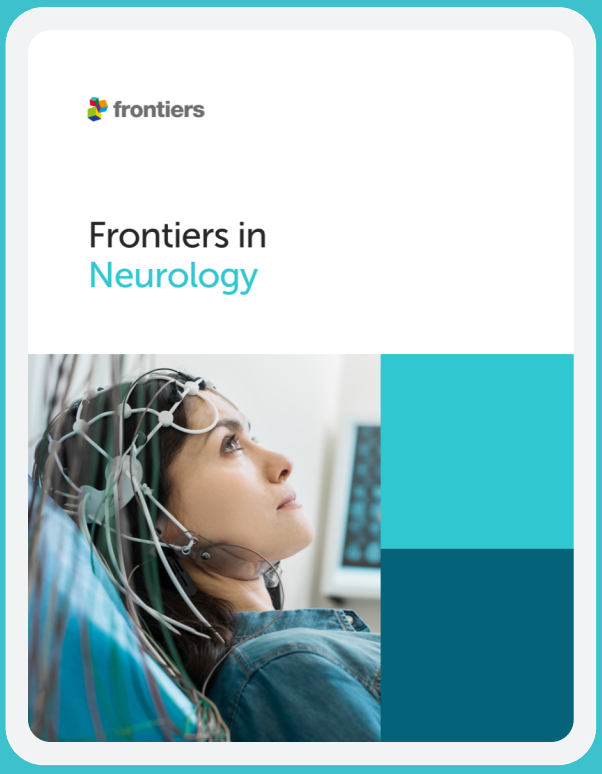

Frontiers

Avenue du Tribunal-Fédéral 34
1005 Lausanne, Switzerland
frontiersin.org

Contact us

+41 (0)21 510 17 00
frontiersin.org/about/contact